

**FINITE ELEMENT MODELLING OF MULTILAYER METALLIC FOAM CLADDING
SYSTEMS FOR RETROFITTING REINFORCED CONCRETE WALLS TO MITIGATE THE
EFFECTS OF EXPLOSIONS**

By

Jasiel Y. Ramos Delgado

A thesis submitted in partial fulfillment of the requirements for the degree of

MASTER OF SCIENCE
IN
CIVIL ENGINEERING

UNIVERSITY OF PUERTO RICO
MAYAGÜEZ CAMPUS
MAYAGÜEZ, PUERTO RICO
2016

Approved by:

Luis E. Suárez Colche, Ph.D.
President, Graduate Committee

Date

Basir Shafiq, Ph.D.
Member, Graduate Committee

Date

Felipe J. Acosta, Ph.D.
Member, Graduate Committee

Date

Luis F. Cáceres, Ph.D.
Representative of the Graduate School

Date

Ismael Pagán Trinidad, M.S.C.E.
Department Chairperson

Date

ABSTRACT

In the last decade's blast loads caused by intentional explosions had acquired great importance. The analysis of structures subjected to this type of loads and its design to mitigate their effects have been and still is the subject of numerous investigations, especially in the United States and Europe. This research investigates the feasibility of applying a method to reduce the response of reinforced concrete (RC) walls exposed to dynamic loads generated by explosives. For its validation, a numerical model was created with the program Abaqus. The idea is to adhere several layers of metallic foam to the exposed side of the RC Wall. The system, which consists of metallic foams made of aluminum in a sandwich configuration with metal plates, is referred to as *Metallic Foam Multilayer Protection System* (MFMPS). Keeping a constant thickness and varying its density and yield properties to determine the most effective type. First, a linear dynamic analysis was carried out for a preliminary design. Next, a full nonlinear dynamic analysis is performed to evaluate its efficiency under realistic conditions. The dynamic pressures due to explosions with several intensities and standoff distances were computed with a subroutine inside Abaqus called CONWEP (Conventional Weapons Effects) developed by the US Army Corp of Engineers. Due to the computational time involved, only the case of a rectangular wall fixed in all borders was considered for the analyses. The results showed that the MFMPS is able to reduce the displacements and stresses on the wall.

RESUMEN

Unas cargas extraordinarias que han adquirido importancia en las últimas décadas son aquellas producidas por explosiones intencionales. El análisis de estructuras bajo estas fuerzas y su diseño para mitigar sus efectos ha sido y sigue siendo objeto de muchas investigaciones, especialmente en Estados Unidos y Europa. En este trabajo se presenta un método novedoso para reducir la respuesta de paredes de hormigón sometidas a presiones dinámicas causadas por explosiones a distintas distancias. Para verificar el concepto se implementó una simulación mediante elementos finitos usando el programa Abaqus. La idea es adherir varias capas de un material conocido como gomaespuma metálica (“metallic foam” en inglés) a la superficie de la pared que está expuesta a la explosión. Para este trabajo se adoptaron capas de gomaespuma metálica de aluminio. Los espesores y densidades de las capas se seleccionan a base de la teoría de propagación de ondas en medios viscoelásticos estratificados. El diseño se hace mediante un análisis dinámico lineal. Posteriormente se comprueba la efectividad teniendo en cuenta el comportamiento no lineal. Las presiones debido a la explosión se generan usando el programa CONWEP (“Conventional Weapons effects”) del Cuerpo de Ingenieros de EE. UU. Debido al tiempo computacional que demanda este tipo de análisis, solo se ha considerado una pared de hormigón rectangular empotrada en sus cuatro lados. Los resultados muestran que el sistema propuesto es capaz de disminuir la respuesta (desplazamientos, tensiones) de la pared de hormigón. El siguiente curso de acción es verificar los resultados mediante experimentos físicos en el campo.

*To the Engineering Research and Development Center
(ERDC) of the U. S. Army Corps of Engineers, in
particular the Impact and Explosive Effect Branch (IEEB)
for the opportunity to work with the effects of explosive to
developed innovating ways of protecting structures and
people against it.*

ACKNOWLEDGMENTS

The achievement of this research would not be possible without the collaboration of the great people who surrounds me. Their help and support was vital for making this possible and these few lines express my gratitude towards each one of them.

To GOD, to whom belong all things and who created every visible and invisible, and gave me the strength and health to achieve this goal.

To my parents, Raúl Ramos and Madeline Delgado, that gave me life and their unconditional love and support to go forward without.

To my advisor, mentor, and friend, Dr. Luis E. Suárez, for the copious amount of knowledge and constant education to become a better professional and a better person.

To the members of my committee, Dr. Basir Shafiq, and Dr. Felipe J. Acosta, for their collaboration with the research.

To Ernesto G. Cruz, for his friendship and constant support throughout the whole master's degree courses and process.

To the Civil Engineering Department Chairman, Prof. Ismael Pagán Trinidad, for numerous of summer internship opportunities working for IEEB at the headquarters of ERDC where my passion for the effects of explosives and how to reduce them began.

Table of Contents

Abstract	i
Resumen	ii
Acknowledgements	iv
List of Figures and Tables	vii
Chapter 1 – Introduction and Literature Review	1
1.1 – Justification and scope.....	1
1.2 – Objective	3
1.3 - Methodology	3
1.4 - Aluminum alloy foam properties and manufacturing process	6
1.4.1 – Introduction	6
1.4.2– Manufacturing process	6
1.5 – Literature review	7
Chapter 2 –Development and Validation of the Finite Element Model	12
2.1 – Introduction	12
2.1.1 – General description of Abaqus 6.14 version.....	12
2.1.2 – Step by step procedure for an analysis with Abaqus	13
2.2 – Properties of the materials and geometry of the structural system.....	16
2.2.1 – Concrete property	16
2.2.2 – Metallic foams properties	17
2.2.3 – Selection of elements in Abaqus 6.14	18
2.3 – Validation of the finite element model	24
2.3.1 – Validation Specifications and Simplification	24
2.3.2 – Boundary conditions.....	25
2.3.3 – Maximum displacements calculated with the analytical formulation	28
2.4 – The damping properties.....	31
Chapter 3 – Linear Static and Dynamic Analysis of the Wall with the Metallic Foam Multilayer Protection System (MFMPs).....	34
3.1 – Introduction	34
3.2 – Metallic Foam Multilayer Protection System (MFMPs) modeling parameters.....	35
3.2.1 – MFMPs definition.....	35
3.2.2 – MFMPs and concrete wall assembly	36
3.2.3 – Loads and boundary conditions	37
3.3 – Static pressure load analysis and results.....	40
3.4 – Dynamic pressure load analysis and results	46

3.5 – CONWEP analysis and results	52
3.5.1 – Explosive standoff distance considerations	53
3.5.2 – CONWEP results	55
Chapter 4 – Nonlinear Static and Dynamic Analysis of the Wall with the Metallic Foam Multilayer Protection System (MFMPs)	68
4.1 – Introduction	68
4.2– Numerical validation of the concrete wall nonlinear behavior	69
4.2.1 –Stresses and strains for constitutive relations used in Abaqus.....	70
4.2.2 – Pushover analysis to validate the constitutive relations	76
4.2.3 – Concrete wall with and without explicit modeling of the reinforcement	78
4.3 – Nonlinear response due to a static pressure.....	82
Table 4.3: Displacements and stresses in the wall with and without MFMPs for the nonlinear static load case. ...	86
4.4 – Nonlinear response due to the impulsive pressure	86
4.5 – Nonlinear response due to the CONWEP generated load	92
Chapter 5 – Results Summary, Conclusions and Recommendations	105
5.1- Summary	105
5.2 – Final results	108
5.3 – Conclusions	110
5.4 – Recommendations for future work	110
Reference.....	113

List of Figures and Tables

Figure 1.1: Powder Metallurgical (PM) method for manufacturing metal foams	7
Figure 1.2: Illustration of: (a) Blast mitigation procedure; (b) Idealized blast pressure and transmitted pressure (Wu and Sheikh, 2012b).....	8
Figure 1.3: Single degree of freedom of cladding structure interaction model (Wu et al.,2012a).	8
Figure 1.4: CFRP design layouts (Orton et al., 2014)	10
Figure 1.5: Effect of changing the τ and κ factor in the efficiency (η) of the foam cladding system (Ye and Ma, 2007).....	11
Figure 2.1.1: Example of types of steps that can be assigned in Abaqus ver. 6.14.	15
Figure 2.2.1: Metallic Foam Multilayer Protective System (MFMPs) configuration (Not to Scale).	17
Table 2.2.1: Geometry and properties of the materials for the numerical models.	18
Figure 2.2.2: Nodes and location of the integration point for a C3D8R element.	21
Figure 2.2.3: Nodes and location of the integration point for a S4R element.	22
Figure 2.2.4: Meshing and boundary conditions of the concrete wall and MFMPs in Abaqus.	23
Figure 2.3.1a: First boundary condition: Pinned at all sides (a. Wall, b. Shell).	26
Figure 2.3.1b: Second boundary condition: Fixed -Pinned -Pinned-Pinned (a. Wall, b. Shell).	26
Figure 2.3.1c: Third boundary condition: Fixed-Fixed-Fixed-Pin (a. Wall, b. Shell).....	27
Figure 2.3.1d: Fourth boundary condition: Fixed on all sides (a. Wall, b. Shell).	27
Table 2.3.1: Comparison of maximum displacements obtained with the FE model in Abaqus and with the analytical model.....	30
Table 2.4.1: Material damping parameters used in the Abaqus models	33
Figure 2.4.1: Damping parameters input window in Abaqus ver. 6.14-4.	33
Figure 3.1: Idealized blast pressure and transmitted pressure due to the presence of an aluminum foam plate (Wu et al. 2011).....	34
Figure 3.2.1: Composite Section input window and distribution on the MFMPs model.....	35
Figure 3.2.2: Isometric and profile view of the assembly for the MFMPs and the wall.....	37

Figure 3.2.3: Idealized explosive pressure behavior, from Abaqus 6.13 Analysis User’s Guide	38
Figure 3.2.4: Static pressure load application curve.....	39
Figure 3.2.5: Dynamic pressure load application curve	39
Figure 3.2.6: Boundary conditions of the model and pressure loads directions	40
Figure 3.3.1a: Static stress evaluation of the wall against MFMPS 1	41
Figure 3.3.1b: Static stress wvaluation of the wall against MFMPS 2.....	42
Figure 3.3.1c: Static stress evaluation of the wall against MFMPS 3	42
Figure 3.3.2a: Static change in displacement evaluation of the wall vs MFMPS 1	43
Figure 3.3.2b: Static change in displacement evaluation of the wall vs MFMPS 2	43
Figure 3.3.2c: Static change in displacement evaluation of the wall vs MFMPS 3	44
Table 3.3.1: Reduction in displacements and stresses achieved by the MFMPS for the static pressure load	44
Figure 3.3.3: Isometric and profile view from Abaqus 6.14-4 of the displacements in the wall due to the static loading.....	45
Figure 3.3.4: Isometric and profile view from Abaqus 6.14-4 of the normal stresses in the wall due to the static loading.....	46
Figure 3.4.1a: Dynamic stress evaluation of the wall with MFMPS 1	47
Figure 3.4.1b: Dynamic stress evaluation of the wall against MFMPS 2	48
Figure 3.4.1c – Dynamic stress evaluation of the wall against MFMPS 3.....	48
Figure 3.4.2a: Dynamic change in displacement of the wall with MFMPS 1	49
Figure 3.4.2b: Dynamic change in displacement evaluation of the wall vs MFMPS 2.....	49
Figure 3.4.2c: Dynamic change in displacement evaluation of the wall vs MFMPS 3.....	50
Table 3.4.1: Reduction in displacements and stresses achieved by the MFMPS for the impulsive pressure load...51	51
Figure 3.4.3: Isometric and profile view from Abaqus 6.14-4 of the normal stresses in the wall due to the dynamic loading.....	51
Figure 3.4.4: Isometric and profile view from Abaqus 6.14-4 of the displacements in the wall due to the dynamic loading.....	52
Figure 3.5.1: Typical definition and parameters required by CONWEP.....	53

Figure 3.5.1: Parking and roadway control for existing buildings with no perimeter control, Source (UFC 4-010-01, 2012).....54

Figure 3.5.2: Standoff distance setup for CONWEP analysis in Abaqus 6.14-455

Figure 3.5.3a : Time response of the bare wall and wall with MFMPS 1 due to CONWEP load for a standoff distance of 10 ft and 100 lb of TNT: (a) stress; (b) displacement.56

Figure 3.5.3b: Time response of the bare wall and wall with MFMPS 2 due to CONWEP load for a standoff distance of 10 ft and 100 lb of TNT: (a) stress; (b) displacement.57

Figure 3.5.3c: Time response of the bare wall and wall with MFMPS 3 due to CONWEP load for a standoff distance of 10 ft and 100 lb of TNT: (a) stress; (b) displacement.58

Table 3.5.1: Standoff distances for new and existing buildings (UFC 4-010-01, 2012)59

Figure 3.5.4a: Time response of the bare wall and wall with MFMPS 1 due to CONWEP load for a standoff distance of 20 ft and 200 lb of TNT: (a) stress; (b) displacement.60

Figure 3.5.4b: Time response of the bare wall and wall with MFMPS 2 due to CONWEP load for a standoff distance of 20 ft and 200 lb of TNT: (a) stress; (b) displacement.61

Figure 3.5.4c: Time response of the bare wall and wall with MFMPS 3 due to CONWEP load for a standoff distance of 20 ft and 200 lb of TNT: (a) stress; (b) displacement.62

Figure 3.5.5a: Time response of the bare wall and wall with MFMPS 1 due to CONWEP load for a standoff distance of 30 ft and 300 lb of TNT: (a) stress; (b) displacement.63

Figure 3.5.5b: Time response of the bare wall and wall with MFMPS 2 due to CONWEP load for a standoff distance of 30 ft and 300 lb of TNT: (a) stress; (b) displacement.64

Figure 3.5.5c: Time response of the bare wall and wall with MFMPS 3 due to CONWEP load for a standoff distance of 30 ft and 300 lb of TNT: (a) stress; (b) displacement.65

Table 3.5.2: Reduction in displacements and stresses achieved by the MFMPS due to the CONWEP load for a standoff distance of 10 ft and 100 lb of TNT.66

Table 3.5.3: Reduction in displacements and stresses achieved by the MFMPS due to the CONWEP load for a standoff distance of 20 ft and 200 lb of TNT.66

Table 3.5.4: Reduction in displacements and stresses achieved by the MFMPS due to the CONWEP load for a standoff distance of 30 ft and 300 lb of TNT.66

Figure 4.1 : Stress-strain curve for concrete with a capacity of 4000 psi, taken from SAP2000.70

Table 4.1: Values of the stress-strain curve for concrete with $f_c' = 4000$ psi.....	70
Table 4.2: True stresses and strains calculated from the engineering values.	73
Figure 4.2a : Abaqus 6.14-4 input window for concrete damage plasticity parameters.....	75
Figure 4.2b: Information about compressive and tensile behavior of the concrete material in Abaqus 6.14-4.	76
Figure 4.3: Pushover load of 1 kip/inch applied to the wall in Abaqus.....	77
Figure 4.4: Comparison of stress-strain curves obtained from the pushover simulation and engineering data from SAP2000.....	78
Figure 4.5a: Configuration of the A36 #4@6” reinforcement grid.	79
Figure 4.5b: Steel reinforcement mesh embedded on the concrete wall	80
Figure 4.6: Stress-strain curves obtained from the pushover analyses for the models of the wall with and without reinforcement grids.....	81
Figure 4.7: Static pressure application.	83
Figure 4.8a: Nonlinear static stresses in the wall with MFMPS 1 and bare wall.	83
Figure 4.8b: Nonlinear static stresses in the wall with MFMPS 2 and bare wall.	84
Figure 4.8c: Nonlinear static stresses in the wall with MFMPS 3 and bare wall.	84
Figure 4.9a: Nonlinear static displacement in the wall with MFMPS 1 and bare wall.	85
Figure 4.9b: Nonlinear static displacement in the wall with MFMPS 2 and bare wall.	85
Figure 4.9c: Nonlinear static displacement in the wall with MFMPS 3 and bare wall.	86
Figure 4.10: Dynamic pressure load for nonlinear analyses.....	88
Figure 4.11a: Nonlinear stress time histories in the RC wall with and without the MFMPS 1.....	89
Figure 4.11b: Nonlinear stress time histories in the RC wall with and without the MFMPS 2.	89
Figure 4.11c: Nonlinear stress time histories in the RC wall with and without the MFMPS 3.....	90
Figure 4.12a: Nonlinear displacement time histories in the RC wall with and without the MFMPS 1.	90
Figure 4.12b: Nonlinear displacement time histories in the RC wall with and without the MFMPS 2.	91
Figure 4.12c: Nonlinear displacement time histories in the RC wall with and without the MFMPS 3.	91
Table 4.4: Peak displacements and stresses for the triangular load case and nonlinear analysis.	92

Figure 4.13a: Nonlinear stress and displacement time histories for the wall-MFMPS 1 system for a standoff distance of 10 ft and a 100 lb equivalent TNT : (a) stress; (b) displacement.	94
.....	95
Figure 4.13b: Nonlinear stress and displacement time histories for the wall-MFMPS 2 system for a standoff distance of 10 ft and a 100 lb equivalent TNT : (a) stress; (b) displacement.	95
Figure 4.13c: Nonlinear stress and displacement time histories for the wall-MFMPS 3 system for a standoff distance of 10 ft and a 100 lb equivalent TNT: (a) stress; (b) displacement.	96
Figure 4.14a: Nonlinear stress and displacement time histories for the wall-MFMPS 1 system for a standoff distance of 20 ft and a 200 lb equivalent TNT : (a) stress; (b) displacement.	97
Figure 4.14b: Nonlinear stress and displacement time histories for the wall-MFMPS 2 system for a standoff distance of 20 ft and a 200 lb equivalent TNT : (a) stress; (b) displacement.	98
Figure 4.14c: Nonlinear stress and displacement time histories for the wall-MFMPS 3 system for a standoff distance of 20 ft and a 200 lb equivalent TNT : (a) stress; (b) displacement.	99
Figure 4.15a: Nonlinear stress and displacement time histories for the wall-MFMPS 1 system for a standoff distance of 30 ft and a 300 lb equivalent TNT : (a) stress; (b) displacement.	100
Figure 4.15b: Nonlinear stress and displacement time histories for the wall-MFMPS 2 system for a standoff distance of 30 ft and a 300 lb equivalent TNT : (a) stress; (b) displacement.	101
Figure 4.15c: Nonlinear stress and displacement time histories for the wall-MFMPS 3 system for a standoff distance of 30 ft and a 300 lb equivalent TNT : (a) stress; (b) displacement.	102
Table 4.5: Nonlinear peak displacements and stresses in the MFMPS 1 + Wall system due to a CONWEP generated load for 100 lb of explosives at a 10 ft standoff distance.....	103
Table 4.6: Nonlinear peak displacements and stresses in the MFMPS + Wall systems due to a CONWEP generated load for 200 lb of explosives at a 20 ft standoff distance.....	103
Table 4.7: Nonlinear peak displacements and stresses in the MFMPS + Wall systems due to a CONWEP generated load for 300 lb of explosives at a 30 ft standoff distance.....	103
Figure 5.1: Metallic Foam Multilayer Protective System (MFMPS) configuration.....	106
Table 5.1: Geometry of the structure and mechanical properties of the materials.	106
Table 5.2: Response reduction achieved for the static pressure and for linear and nonlinear analyses (140 psi) .	108

Table 5.3: Response reduction achieved for the triangular dynamic pressure and for linear and nonlinear analyses (140 psi).....	108
Table 5.4: Response reduction achieved for the CONWEP loading and for linear and nonlinear analyses (100 lb of TNT and a 10 ft standoff distance).....	109
Table 5.5: Response reduction achieved for the CONWEP loading and for linear and nonlinear analyses (200 lb of TNT and a 20 ft standoff distance).....	109
Table 5.6: Response reduction achieved for the CONWEP loading and for linear and nonlinear analyses (300 lb of TNT and a 30 ft standoff distance).....	109

Chapter 1 – Introduction and Literature Review

1.1 – Justification and scope

The analysis and design of structures are governed by codes written over the years by experts in the field. Organizations such as the American Society of Civil Engineers (ASCE), the American Concrete Institute (ACI), the American Institute of Steel Construction (AISC), the Federal Emergency Management Agency (FEMA) and the Earthquake Engineering Research Institute (EERI) are examples of entities that publish manuals and standards that help civil engineers to design and build safe structures. In addition to the standard service loads, i.e. dead loads and live load, these professional organizations have developed methodologies to determine the so called environmental loads such as earthquakes, high winds, water ponding, snow, or their combination. These codes are updated every number of years based on more experience gained from experimental or analytical research work, or from observations gathered after a natural disaster event. Even though there still room for improvement, the codes specifications can be used with confidence to design safe structures, even under extreme natural loads.

Unfortunately, these are not the only loads that can affect a structure and there are loading conditions that are so severe that it is difficult to design structures to withstand them. In recent years due to terrorist activities such as the September 11, 2001, event as well as the bombing of train stations, embassies and military facilities, the need for more accurate prediction of explosive effects and better blast mitigation technology has increased drastically. The explosives discharge generate a high-pressure wave that impacts a structure in fractions of seconds and disappears in a similar length of time. This poses a problem because the current common standards do not take into account this kind of extremely impulsive and high-intensity loads. The dynamic loads that are considered in the codes, for example,

those arising from strong earthquakes, are cyclic, have a much longer duration, and are not localized as those from an explosive event. There are, however, specialized publications that deal with blast analysis and mitigation but for special facilities that due to their function have a higher chance of being involved in an explosive event (i.e. petrochemical plants). These facilities have in many cases their own specific design procedure to make them blast-resistant. In principle, the procedures in manuals such as ASCE's Design of Blast-Resistant Buildings in Petrochemical Facilities (ASCE, 2010) could be adopted to develop guidelines for new structures. On the other hand, there is still the issue of how to strengthen pre-existing structures. The differences between the explosions from an industrial process gone wrong and those planned by terrorists to inflict maximum damage also need to be considered.

One way to address the dangers posed by intentionally created explosions, at least partially, is to properly retrofit vital structures such as hospitals, schools, and government buildings to make them blast-resistant. There have been numerous research works involving a large variety of methods and materials to achieve this goal. Among them, there a few methods that stand out and look promising for further studies. For example, the use of composite laminates such as fiber-reinforced polymers (FRP) can help to strengthen the structure while at the same time can successfully prevent flying debris (Orton et al., 2014). Another method involves the use of spray-on elastomeric polymers such as polyurea and polyurethane which have strengthening attributes and they can also provide additional debris protection (Raman et al., 2012). Although both of these techniques have shown promising results, the first one requires higher construction time and more intrusive approach while the other needs very sophisticated and expensive application tools (Wu and Sheikh, 2012b). Recent research at the University of Adelaide in Australia examined the application of mobile and lightweight materials like metallic foams (i.e. aluminum foam). Metallic foams consist of a matrix of metal (i.e. aluminum) that is impregnated with air pockets (Wu et al., 2011). These materials have shown promising results to mitigate and redistribute

the pressure wave generated by explosives events (Wu et al., 2011). An extension of this idea forms the basis of this thesis. It is proposed to investigate the use of a multilayered system of metallic foams with different properties: the appropriate selection of the properties of the different layers might reduce the pressure wave generated by an explosion propagating through the stratum.

More specifically, the goal of this project was to evaluate the applicability of a multilayer metallic foam system for retrofitting reinforced concrete (RC) walls against explosions using a finite element model simulation. Due to its availability and powerful capabilities, the computer program ABAQUS was selected to create the numerical models and to analyze them. The properties of the different metallic foam layers were chosen to minimize the pressure wave that propagates through refraction at each interface. The ultimate goal was to reduce the impulsive pressure that reaches the RC wall and to redistribute its effects over a larger surface, compared to the results achieved with a single layer (or without any protection system at all).

1.2 – Objective

The primary purpose of this research work is to ascertain using numerical simulation with finite elements the capabilities of layers of metallic foams with selected properties to reduce the stresses and displacements due to explosions on RC walls.

1.3 - Methodology

Predicting the effects of explosions in structures and assessing the potential benefits of blast mitigation techniques are very complicated tasks. This is due to the complexity caused by the high intensity of the loads involved that can drive the structures into the nonlinear range, compounded by their very short duration. Contrary to blast loading, most of the more conventional loads that are

considered in the structural analysis and design process are static or dynamic forces with a relatively long duration and smaller rate of application. Nowadays there are powerful finite element codes that can handle the simulation of blast loads acting on flexible structures, albeit at a high computational cost. Therefore, to reduce the analysis time the structure to be considered for the study is a single reinforced concrete wall modeled as a 3D body. To validate the numerical model created in Abaqus, the static displacements obtained with the program are compared with those obtained from closed form solutions from the Theory of Plates using different support conditions when subjected to a uniform distributed load. Once the validation is done, the properties of the metallic foams that will be used for the multilayer mitigation system are defined using information gathered by the Fraunhofer Institute for Manufacturing and Advanced Materials (IFAM, 2010). Three Metallic Foam Multilayer Protective System (from here on referred to as MFMPs) are considered using the properties provided by IFAM. Three load cases are considered: static pressure, dynamic with triangular shape and a CONWEP generated pressure wave. The last one is a set of algorithms programmed in a subroutine inside Abaqus that simulates an explosive event. CONWEP takes into consideration the weight of the explosive defined as equivalent pounds of TNT and the standoff distance (the distance between the point of the explosion and the structure). Three amounts of explosives, 100 lb, 200 lb and 300 lb of TNT, are used and each is associated with an increasing standoff distance: 10 ft, 20 ft, and 30 ft. In the first set of analysis it is assumed that the wall and MFMPs have a linear elastic behavior. Next a more realistic but also much more time consuming nonlinear analyses are carried out. To carry out the nonlinear analyses, a stress-strain curve for the concrete wall with steel reinforcement is obtained and input into Abaqus. For each loading condition the maximum stresses and displacements are retrieved and compared to draw a conclusion as to whether the MFMPs is a viable solution for blast mitigation. In addition, the best

performing Metallic Foam Multilayer Protective System is selected. Finally some recommendations for future works are suggested.

A summary of the specific tasks to achieve the objective of this study are:

- Select three metallic foam materials and obtain their properties (linear and nonlinear) using information in the technical literature.
- Choose a number of layers and thickness for each one that will form the Metallic Foam Multilayer Protective System as well as for the restraining metal plates.
- Develop in Abaqus numerical models of the reinforced concrete wall with each of the three MFMPS configuration.
- Carry out a linear elastic analysis of the numerical models subjected to a static pressure and to an impulsive dynamic pressure that simulates the effects of an explosion.
- Use the set of subroutines called CONWEP available in Abaqus to simulate more accurately the pressure wave caused an explosive charge hitting the wall.
- Repeat the two dynamic analyses (with the impulsive pressure and the CONWEP generated load) but allowing nonlinear behavior of the materials.

- Based on the results of all the analyses, determine which one of the three MFMP configurations is able to better reduce the effects of the blast generated stresses and displacements.

1.4 - Aluminum alloy foam properties and manufacturing process

1.4.1 – Introduction

In recent years the use of a wide variety of high deformation and energy absorption materials have been use for blast mitigation. Among these relatively new materials, closed-cell metal foams such as aluminum alloy (Al-allow) have a vast potential thanks to its lightweight and when transportation is consider. Even though there are several manufacturing methods, the more current ones allows an effective control over its density, but none of them have appropriate control in the cellular structure (Duarte and Oliveira, 2012). This section will show the manufacturing process of the metallic foam and the consideration taken in the development of this particular material.

1.4.2– Manufacturing process

Metallic Foam can be manufactured by two distinct method, direct and indirect. For the direct foaming some of the methods include but are not limited to, molted metal with uniform dispersed ceramic particles to which gas bubble are inserted directly or throughout chemical method by decomposition of a blowing agent (Duarte and Oliveira, 2012). Meanwhile the indirect foaming consist of having a foamable precursor that is subsequently foamed by heating. These precursors consists of a dense compacted powders that have a uniform distribution of a blowing agent in the metallic matrix (Duarte and Oliveira, 2012). *Figure 1.1* shows a diagram of the typical manufacturing process for Al-alloys using the Powder Metallurgical Method (PM) which is an indirect foaming method.

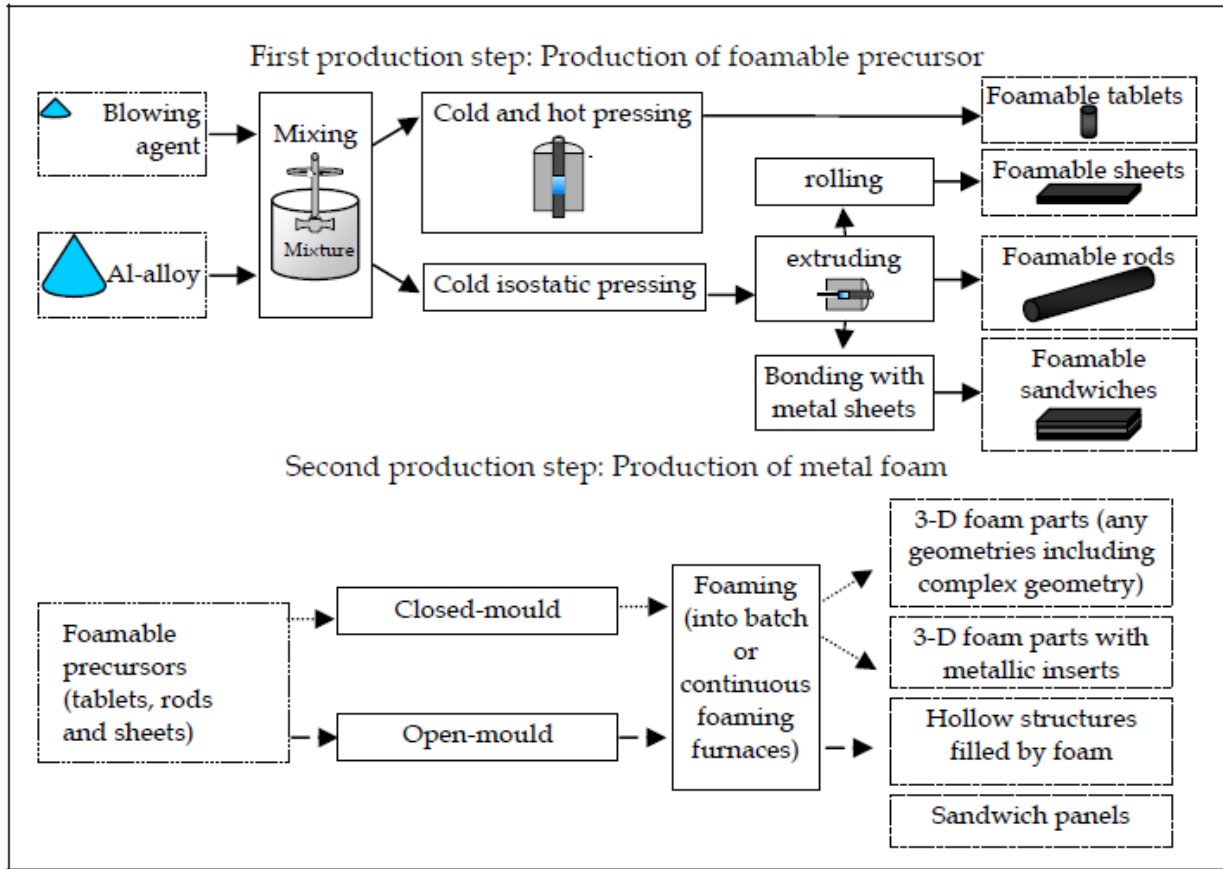


Figure 1.1: Powder Metallurgical (PM) method for manufacturing metal foams.

1.5 – Literature review

Wu et al. (2011, 2012a, 2012b) investigated the use of lightweight retrofitting systems such as metallic foams. They analyzed the properties and behavior of the aluminum foam (i.e., thickness, compressibility) and performed real field-testing to study its performance against standoff explosives (Wu et al., 2011). Wu also compared the protection capabilities of foam materials with those of ultra-high performance concrete (UHPC) which has higher strength, deformation capacity and toughness than typical concrete. They used finite element (FE) models to investigate the mitigation of blast effects that can be achieved by applying foam cladding over concrete. In addition, the researchers created FE models of UHPC and masonry walls with FRP to evaluate their behavior against explosive events (Wu,

2012a). Figure 1.2 (a) shows the blast mitigation procedure and Figure 1.2 (b) displays the idealized blast pressure and the transmitted pressure. Based upon the behavior observed, they developed a single degree of freedom (SDF) shown in Figure 1.3 to model the interaction of the foam and the RC (Wu and Sheikh, 2012b).

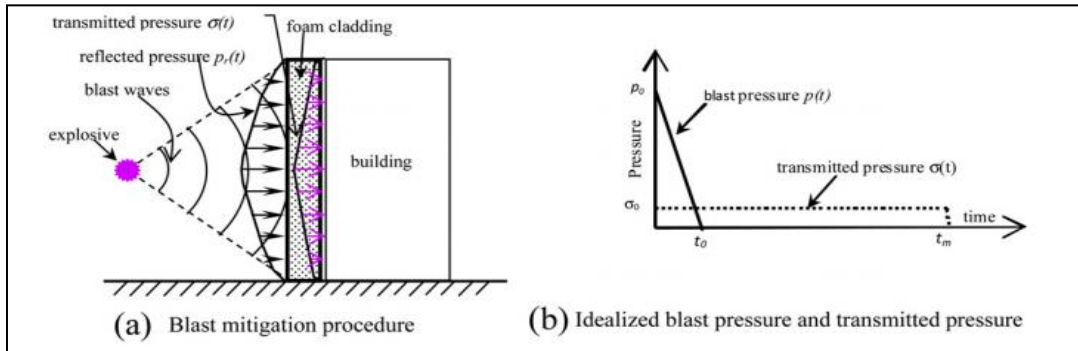


Figure 1.2: Illustration of: (a) Blast mitigation procedure; (b) Idealized blast pressure and transmitted pressure (Wu and Sheikh, 2012b).

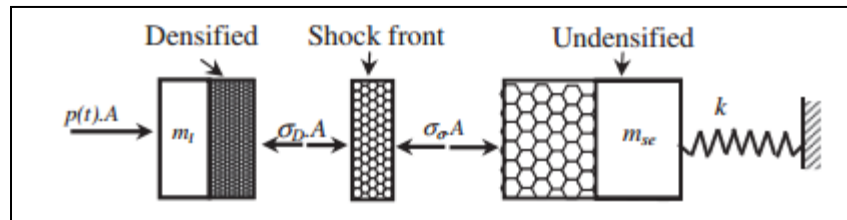


Figure 1.3: Single degree of freedom of cladding structure interaction model (Wu et al., 2012a).

Raman et al. (2012) also examined the use of elastomeric polymers to protect RC structures from the effects of blast loading. In this research they worked with particular elastomers such as polyurea and polyurethane to increase the strength and elasticity of the RC taking advantage of the high strain capacity, high ductility and strength of the polymers. As part of the project, they determined the optimal thickness of the polymer coating and the side of the RC wall that should be coated. They

concluded that coating with polyurethane both sides of the RC wall drastically increased its deformation capacity. They also discovered that covering the inner side (i.e. the one not exposed to the blast directly) was better than coating the outer side. This allowed controlling the amount of debris generated by the RC walls and it also made possible to achieve better strength than covering the opposite side (Raman et al., 2012).

Orton et al. (2014) in collaboration with researchers from the US Army Engineer Research and Development Center (ERDC) in Vicksburg, MS, implemented a series of experimental tests dealing with the applications of carbon fiber reinforced polymers (CFRP) for retrofitting RC slab elements for close-in blasts. After differentiating the two primordial blast cases (far-field and close-in) and their particular behavior, they carried out extensive research on the CFRP failures, such as delamination and debonding, developing two types of designs for the CFRP layer system as shown in Figure 1.4. Using a scale range of $0.6 \text{ m/kg}^{1/3}$ and $0.4 \text{ m/kg}^{1/3}$ and comparing each of the designs against a control test (unstrengthened slab), an overall displacement reduction of 60% was achieved by applying the CFRP. The scale range was the parameter established to determine a more appropriate standoff distance of the explosive charge. Moreover, the CFRP was also able to retain flying debris for the 0.6 scale range. For the $0.4 \text{ m/kg}^{1/3}$ scale range, the CFRP did not prevent the breach of the RC element, but it did reduce the residual displacements and velocities of the back of the slab by 75% (Orton et al., 2014).

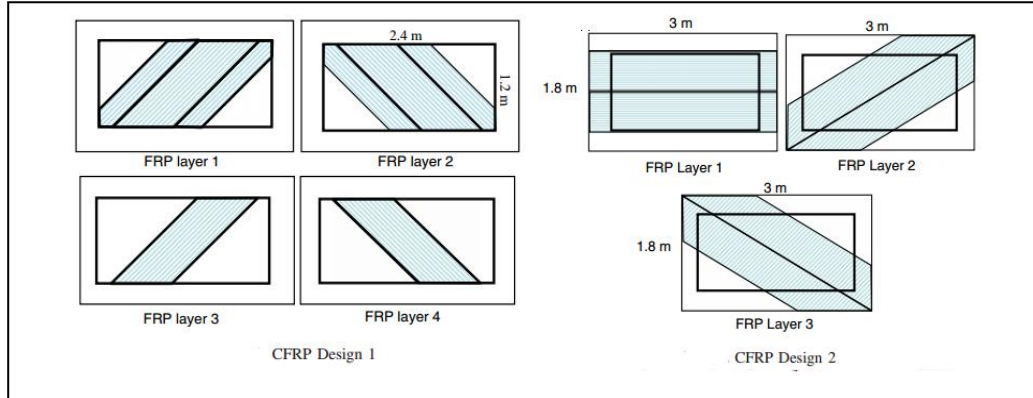


Figure 1.4: CFRP design layouts (Orton et al., 2014)

Ye et al. (2007) also studied the effects of using foam cladding systems as a retrofitting method against blast loads. They observed that the compressive deformation behavior of the metallic foam consisted of three regions: linear-elastic, a plateau of constant stress and finally a densification region. They found that the maximum allowable external blast load does not depend only on the foam capacity, the structure or the blast load, but actually it is a combination of these three components. It was determined that in order for the cladding system to work, it was necessary to establish a relationship between the blast load and the resistant capacity of the foam and structure. When the blast load is lower than the foam resistant capacity and less than the structure, the foam cladding will compress so fast that it will be as if no protective system was implemented. On the other hand, if the blast load is higher than the resistant capacity of the foam, the pressure transmitted to the structure may become larger. The authors determined blast load equations as well as equations of motion for an elastic equivalent system. In order to simplify some of the calculations, two non-dimensional parameters, τ and κ , were defined. The parameter κ describes the relation between the plateau stress of the foam and the resistance of the structure. The parameter τ is the ratio between the maximum duration of the transmitted rectangular pressure and the time for maximum deflection of the structure. Ye and Ma (2007) prepared graphs to relate the efficiency, measured by a parameter n that relate the impulse result with foam and without it, to the two previously mentioned non-dimensional parameters. After performing a parametric study by

changing the values of τ and κ and comparing the system without cladding and with cladding with the foam fully compacted, they concluded that a more efficient foam cladding may be achieved by keeping $\kappa \leq 1$ and τ as large as possible (Ye & Ma, 2007). The curves in Figure 1.5 show how the variation of the parameters τ and κ affect the performance of the cladding system (Ye and Ma, 2007).

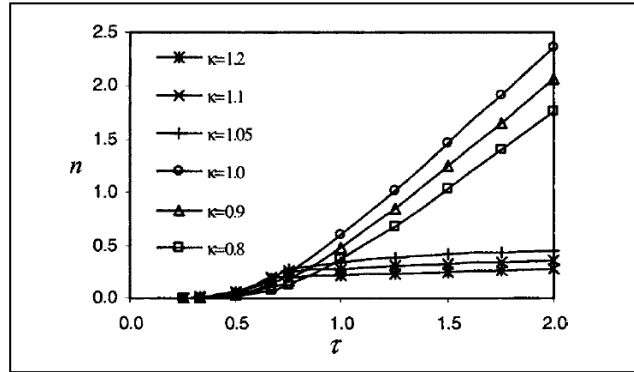


Figure 1.5: Effect of changing the τ and κ factor in the efficiency (n) of the foam cladding system (Ye and Ma, 2007)

Duarte and Oliveira (2012) from the University of Aveiro in Portugal presented a detailed overview of the methods, equipment and industrial procedures for manufacturing metallic foams of good quality. In their work they gave detailed information related to the types of materials used for the metallic foams as well as the production techniques for foaming methods. A direct foaming method starts from a molten metal which contains a uniformly dispersed ceramic particles to which gas bubbles are directly injected to it. On the other hand, an indirect foaming method uses a foamable precursor that is foamed by heating it. The precursors are a powder mixture of the metal and some blowing agent like titanium hydride (TiH_2). Metallic foam products can be tablets, sheets, rods and sandwich-like structures. Contrary to the direct method, the indirect approach allows for shape variety during production.

Chapter 2 –Development and Validation of the Finite Element Model

2.1 – Introduction

Finite element numerical models are becoming increasingly popular due to their effectiveness in determining the behavior of different structures and materials under a wide variety of loading scenarios. Thanks to the advancement in the numerical modeling techniques and the software and hardware available, the experimental cost and time associated with the development, design and verification of a commercial product or a structural system have been significantly reduced. Still, some validation is always needed to ensure that the response predicted by the numerical model is within acceptable parameters. These validations are performed by comparing with experimental results or by using time-tested analytical techniques that can approximate the physical behavior under investigation. This chapter presents the development as well as the validation of the finite element numerical model created in the program Abaqus version 6.14.

2.1.1 – General description of Abaqus 6.14 version.

Due to the increasing interest in carrying out finite element analysis for mechanical, aerospace and civil engineering structural systems, a plethora of software that can perform this type of numerical simulation was released in the last decades. Nevertheless, there are a few of them that stand out as more powerful or more reliable, although each particular software is better tailored for a specific kind of analysis. Among them, Abaqus, Ansys, Nastran and LS-Dyna are one of the general-purpose commercial finite element analysis programs most used by the engineering community around the world.

Abaqus is a finite element analysis and computer-aided engineering software suite originally release in 1973, and currently owned and developed by Dassault Systemes. It was previously the property of Hibbitt, Karlsson & Sorensen, Inc., until its acquisition in 2005 by the European engineering simulation company (Dassault/Systemes, 2016). The Abaqus suite, now called Abaqus Unified FEA, consists of four programs. Abaqus/CAE is a complete environment that delivers a consistent interface for creating, submitting, monitoring, and evaluating result from three types of analysis modules. Abaqus/Standard is the first of them which works as a general-purpose finite element program, the second one is Abaqus/Explicit whichs is a special-purpose finite element program suited for dynamic nonlinear problems and Abaqus/CFD is a software that deals with computational fluid dynamics (Abaqus: User'sGuide, 2013). Abaqus/Explicit is the program used through this project for all the analysis cases: static, dynamic, and CONWEP (a blast simulation routine described in a following chapter).

2.1.2 – Step by step procedure for an analysis with Abaqus

Before running any model in Abaqus, there are a series of steps that must be followed in a particular order for a successful analysis. Part, Properties, Assembly, Step, Interaction, Load, Mesh and Job are the steps of the general module that must be followed in that order when doing an analysis using Abaqus.

The *Part* module allows the user to draw in specific dimensions all the model components and select what type of general element behavior it will be, e.g. beam, wire, shell or point in 2D or 3D. This particular module is the starting point of the analysis because it determines if it is going to be deformable or rigid body (discrete or analytical). It also takes into consideration the dimensional characteristics of the part, whether it is a three-dimensional (3D), planar or axisymmetric body. *Table*

2.2.1 shows in columns 2, 3 and 4 from the left side the information required by this module, namely the geometry of the model.

After defining all the part parameters, the material properties, section properties and orientation are define in the module **Properties**. The mechanical behavior described by its elasticity, plasticity, and density are a few of the properties obtained through material testing or from typical values that one can input to the software to provide an accurate representation of the real material and its capacity.

Once all the model components properties and parameters are assigned, it must be assembled using the **Assembly** module. With this module, all the element parts come together to create the full model. For the structural system of the present study, there are only two part items, the concrete wall and the Metallic Foam Multilayer Protection System (MFMPs). In the **Assembly** module, position constraints can be defined. Which means that the components will have a restriction or relation in the way they can move relatively to each other (i.e., parallel to a surface).

After the assembling, the next module **Step** permits to choose the kind of analysis to perform, the time increments that will be used for the analysis, the amount of output variable and frequency of output as well as assigning an interaction or a load to a particular step or time interval. *Figure 2.1.1* illustrates the window from the **Step** module as well as some examples of the types of analysis to perform for some steps.

If the model contains contact surface, rigid bodies, special surface or object, they are define in the **Interaction** module. Tie constraints, as well as any interaction (i.e., general contact, surface-to-surface contact, incident wave) that are related to the analysis.

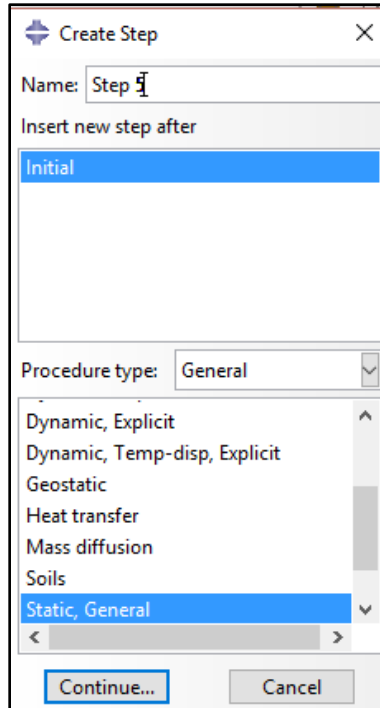


Figure 2.1.1: Example of types of steps that can be assigned in Abaqus ver. 6.14.

Once all interactions have established, the kind of loading such as concentrated, pressure, hydrostatic loads, and others, and all the boundary conditions are assigned in the **Load** module. This module, as well as any other after the Step module depends on in the type of step, was define controlling the load types in particular. In the Load module, any category of the load is applied in the model can be determined by the user in the form of amplitude with the characteristics decided by the user.

Once the model has all the internal and external qualities, assignments (properties, loads, constraints, and others.), each part of the model can be seed and mesh with the **Mesh** module. This module is the one that deals with the finite element part of the analysis where the user can assign element types and other properties.

After all the properties, characteristics and conditions of the model are determined by the modules described before, the analysis is executed in the *Job* module. This module is where the analysis process is established by the number of the processor of the computer are going to use and what data is going to be selected and evaluated.

Finally, results in a visual representation of the analysis can be shown with the *Visualization* module as well as all the results for the parameters that were define in the *Step* module such as stresses, strains, displacements and energy outcomes for the load conditions that were applied to the model. Also, graphical data and tabular data of the analysis can be obtain from this module and exported to other data analysis software (i.e., Excel). The *Visualization* module can also let the user observe an animation of how the model was affected by the loads and boundary conditions step by step, depending on the values of time intervals assigned in the *Step* module. The process describe before is a simple explanation of the step using Abaqus, its capacity and a wide range of data and information that can be obtain from it goes farther that the one explain in this section.

2.2 – Properties of the materials and geometry of the structural system

2.2.1 – Concrete property

The compressive strength of concrete is its most important material property. The particular values depend on the particular application and can vary starting as low as 2,500 pounds per square inch (psi). For this study the most common value of 4,000 psi, as recommended in Chapter 9 section 9.3.2 of the “Report for the Design of Concrete Structures for Blast Effects - ACI 370R-14” (ACI Committee 370, 2014) was adopted. Since the proposed protective system to be studied is intended for existing concrete structures, it is reasonable to assume that most of them will have this typical strength capacity.

2.2.2 – Metallic foams properties

To put to the test the capabilities of the Metallic Foam Multilayer Protection System (MFMPs) as a mean to mitigate the effects of blast loadings, four numerical models were developed in Abaqus. Three of these models consisted of two-part assemblies: a reinforced concrete wall and the MFMPs. The fourth model, which was used as a control specimen, involved a single part assembly, i.e. the bare reinforced concrete wall. Figure 2.2.1 shows the different layers that comprise the protective system of the three models. The dimensions and mechanical properties used in these models are presented in Table 2.2.1. The input data includes the Young's modulus (E), the Poisson's ratio (ν), the mass density (ρ) as well as the yield strength (σ_y). The basic mechanical properties for the three types of metallic foams were obtained from the information provided in the report FOAMINAL (IFAM, 2010) prepared by the German research agency Fraunhofer Institute for Manufacturing Technology and Advanced Materials - IFAM.

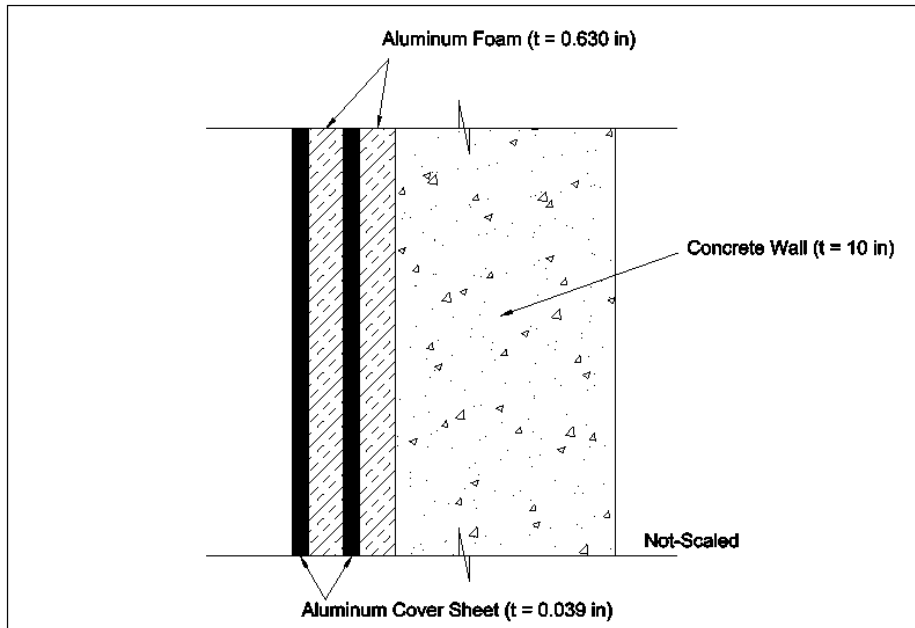


Figure 2.2.1: Metallic Foam Multilayer Protective System (MFMPs) configuration (Not to Scale).

Table 2.2.1: Geometry and properties of the materials for the numerical models.

Material	Width (in)	Height (in)	Thickness (in)	Mass Density (lb.s ² /in ⁴)	E (psi)	Poisson Ratio	Compressive Yield Strength (psi)
Concrete	180.00	120.000	10.000	2.15E-04	3604996	0.180	4000
Aluminum	180.00	120.000	0.630	4.67E-05	507632	0.334	2016
Foam (FoamA)							
Aluminum	180.00	120.000	0.630	5.61E-05	710684	0.334	2726
Foam (FoamB)							
Aluminum	180.00	120.000	0.630	6.54E-05	957249	0.334	3524
Foam (FoamC)							
Metallic Sheet (Al)	180.00	120.000	0.039	2.51E-04	10200000	0.334	40000

Abaqus is a program that works without any particular unit system. Therefore it is important to keep a consistent throughout the modeling and analysis to avoid any discrepancy or errors. The values presented in *Table 2.2.1* for the aluminum metallic sheet and the concrete are typical values for the selected materials.

2.2.3 – Selection of elements in Abaqus 6.14

The selection of elements in Abaqus depends first on whether the Abaqus/Explicit or Abaqus/Standard version of the program will be used. Abaqus/Standard has a larger variety of elements and more variation within a same element than Abaqus/Explicit. For example, in addition to those elements used for stress analysis, it has elements for heat transfer, acoustics, fluid mechanics, etc. However, as explained in the next chapter, the Abaqus/Explicit version was used throughout this thesis because it is tailored to the type of nonlinear dynamic problems that are the objective of this work. With

some exceptions (i.e., for beam elements) the library of Abaqus/Explicit is composed mostly of first-order (linear) interpolation elements.

To model the concrete wall the elements known as C3D8R were selected from the Abaqus/Explicit library. The name stands for Continuum 3-Dimensional, 8-Nodes, Reduced integration. Because hexahedral elements such as the C3D8R are geometrically versatile, they can be used in automatic meshing algorithms. These are general purpose linear three-dimensional elements (also known as “brick” elements). To decrease the time of analysis, a reduced integration (one point) is used. *Figure 2.2.2* shows the configuration of a typical C3D8R element. There is no occurrence of the phenomenon known as “locking” (explained later in this section).

One of the shortcomings of the C3D8R element is that the stresses and strains are calculated more accurately at the integration points and because in this element this point is located at the centroid, smaller elements are required to calculate accurately stress concentration at the borders thus increasing the number of elements to achieve precise results in these situations. Moreover, the C3D8R element is not very useful if the numerical problem known as “hourglassing” (explained below) is not controlled. However, in the newer versions of Abaqus hourglass control is automatically activated for this element, thus alleviating this issue.

Reduced integration: An essential part of a finite element program is the computation of the element stiffness matrix. When complicated or higher order elements are used, it becomes necessary to resort to numerical integration to calculate the stiffness matrix. Usually in finite element calculations the integration procedure known as Gaussian Quadrature is used because it requires less function evaluations due to the fact that it is not restricted to using fixed intervals (as the well-known Simpson’s rule). To integrate a function with the Gaussian Quadrature method a number of points are calculated;

their position are known as Gaussian coordinates. In the reduced integration schemes a smaller number of Gaussian coordinates are used to solve the integrals, as opposed to a full integration. Using less integration points reduces the computation costs of running an analysis but at the price of producing a less accurate answer. Nevertheless, in the displacement-based FE formulations such as those commonly used to solve solid mechanics problems, the stiffness matrix is always overestimated and the use of reduced integration points produces a less stiff element thus compensating the loss of accuracy.

The hourglass modes: Hourglassing is a numerical problem in a finite element mesh associated with a spurious deformation mode of the elements. Among others, it can happen in hexahedral 3-D solid elements with reduced integration such as the C3D8R element of Abaqus. The phenomenon can be seen by optically inspecting the deformed mesh and searching for elements with a deformed shape in the form of an hourglass (i.e. with the form of a trapezoid with two inclined sides and two horizontal parallel sides). The normal and shear stresses at the integration point are zero and hence the strain energy of this deformed shape is also zero. Therefore, it is referred to as a zero-energy mode (it should not be confused with a vibration mode since they are not related at all). The hourglassing phenomenon has to be numerically controlled; otherwise it can lead to meaningless results. Each finite element software, including of course Abaqus, has its own way to internally control the occurrence of hourglassing.

The layers of MFMPs were modeled by shell elements. Among the three standard large-strain shell elements available in the Abaqus library, the four-node doubly-curved element identified as S4R was selected. Abaqus describes the S4R element as a robust, general purpose shell element that is suitable for a wide range of applications and it recommends its use. The element is based on the Mindlin-Reissner flexural theory which includes the effect of transverse shear.

The S4R uses a reduced integration rule with a single integration point and hourglass control. *Figure 2.2.3* displays its configuration along with the reduced integration point location. The S4R elements help to avoid a numerical phenomenon known as “shear locking” in which an element becomes overly stiff (“locked”) when subjected to bending moments.

Shear locking: This is another numerical error that occurs in finite element analysis due to the linear nature of fully integrated quadrilateral elements. The first order (i.e., linear) elements do not accurately model the actual curvature present in the material under bending and an artificial shear stress, called parasitic shear, is introduced. The additional shear stress in the element (which does not occur in the actual structural member) causes the element to reach equilibrium with smaller displacements, In other words, this condition makes the element appear to be stiffer than it actually is, thus predicting smaller displacements than the real ones. The reduced integration used in the S4R elements helps to avoid the shear locking problem.

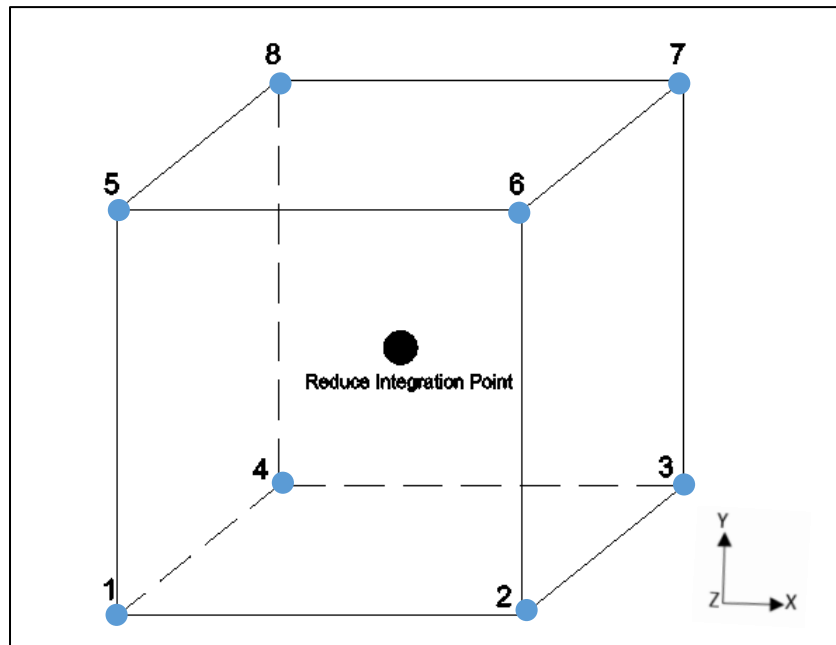


Figure 2.2.2: Nodes and location of the integration point for a C3D8R element.

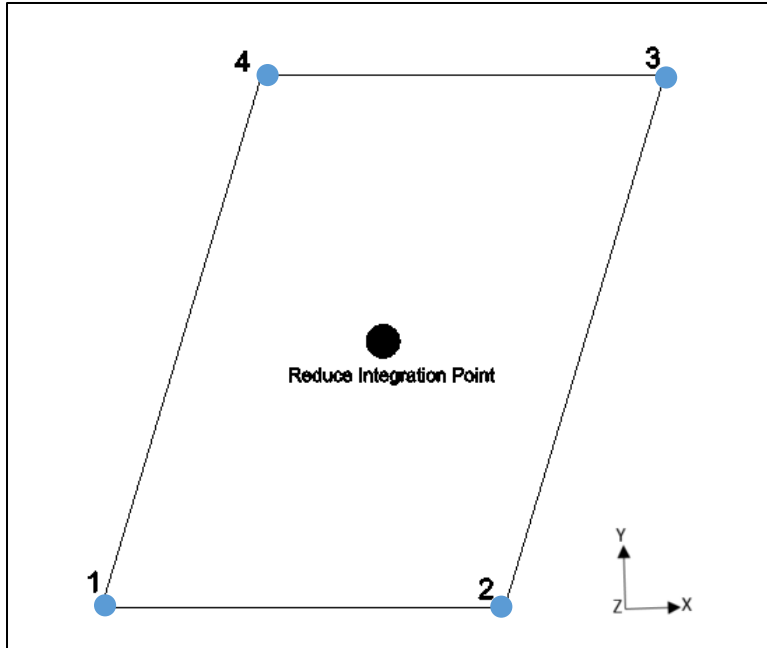


Figure 2.2.3: Nodes and location of the integration point for a S4R element.

The metallic foam multilayer protective system (MFMPs) was modeled in Abaqus as a composite shell to minimize potential problems, such as the wrong contact between the parts and missing values in the analysis. All model materials and properties were considered homogeneous which eliminated any fracture or failure due to any manufacturing process.

It is well-known that the accuracy of the results of a finite element analysis depends on the type of elements, their sizes and numbers. Obviously, the more refined the mesh is, the better the results but unfortunately, and in particular for nonlinear dynamic problems, it has associated a significant increase in the analysis time. The models used in the present work consisted of 925 nodes and 864 elements for the MFMPs part and 2775 nodes and 1728 elements for the concrete wall part. Once both parts are assembled, the total number of nodes is 3700 and the number of elements is 2592. Even though this is a significant number of nodes and elements, the computational time was relatively fast (3-10 minutes for

linear and nonlinear analyses, respectively, in a laptop with microprocessor Intel i7 with 4 cores running at 3.2 GHz with 8 Gb RAM).

Figure 2.2.4 displays a typical fine mesh used in the analyses, as well as the boundary conditions. The boundary condition used in all the cases (except in the validation process presented in a following section) was clamped (or built-in condition: no displacements nor rotations) in the four edges. This support condition was selected to simulate in the simplest way the presence of columns, beams and the surrounding structural elements.

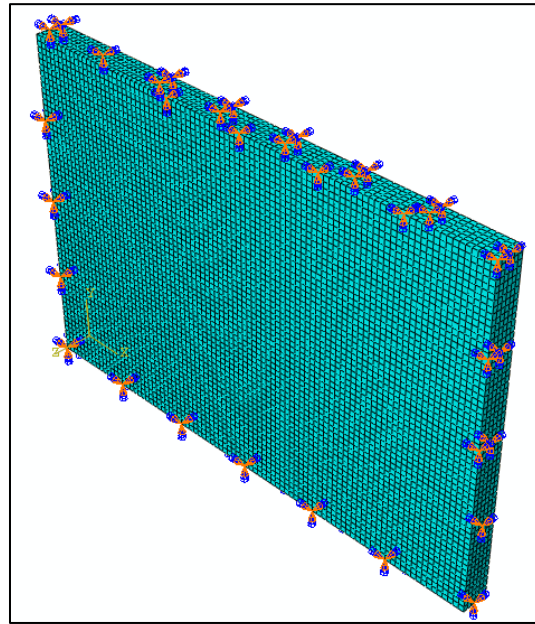


Figure 2.2.4: Meshing and boundary conditions of the concrete wall and MFMPs in Abaqus.

For the assembly of the MFMPs and the concrete wall, all the restrictions pertained to position constraints, surface – surface and edge – edge, etc. This position constraint allows for a simpler and complete assembly, making it continuous between wall and MFMPs allowing more accurate results. All load cases, static and dynamic, used to determine the efficiency of the different MFMPs against each other and the control model (the concrete wall without MFMPs).

2.3 – Validation of the finite element model

Before proceeding with the dynamic analyses, a numerical validation of the finite element model created in Abaqus was carried out. The behavior of the 3-D finite element model of the reinforced concrete wall can be approximated to that of a thin plate in bending. Therefore, the closed form expressions for the deflections of flat plates with different boundary conditions available in the classic book “Theory of Plates and Shells” (Timoshenko and Woinowsky-Krieger, 1987) were adopted to validate the FE model. The analytical results were compared with those from the model of the concrete wall in Abaqus. In such comparison, some difference is always expected. Taking this into consideration, a new model for the wall with the same properties but changing the FE to a shell structure to determine a consistency in the analysis was created.

2.3.1 – Validation Specifications and Simplification

Most of the formulas available in the book by Timoshenko & Woinowsky-Krieger (1987) to calculate the deflection of plates with different boundary conditions use a Poisson’s ratio equal to 0.3. Even though the contribution of the Poisson’s ratio to the deflection formulas is not important, for consistency the same Poisson’s ratio was assigned in Abaqus to the concrete wall model. For the posterior dynamic analyses, another value more appropriate for concrete was used.

The other modification with respect to the analyses carried out in the following chapters was the load applied to the wall. A 25 pound per square inch static pressure was applied uniformly throughout the outer surface of the model. The same load was used for the wall with different boundary conditions. To compare the results of the finite element model and the formulas, the maximum displacement was

used. The point where it occurs depends on the constraints that were applied in each of the four cases. In other to verify the consistency in the model the same analysis was run for the wall but model as a shell.

2.3.2 – Boundary conditions

Four boundary conditions were selected for the validation of the finite element model. They are:

- Pinned - Pinned - Pinned – Pinned (i.e., a simply supported plate).
- Pinned - Fixed - Pinned - Pinned
- Fixed - Fixed - Fixed - Pinned
- Fixed – Fixed - Fixed – Fixed (i.e., a plate clamped at all sides)

The order used to describe the type of support conditions is the following: it begins at the left side when viewing the plate from the positive Z axis direction and then ones moves counterclockwise. *Figure 2.3.1a* through *2.3.1d* show the Abaqus model with the four support conditions cases. To better appreciate the support, the finite element mesh is not shown.

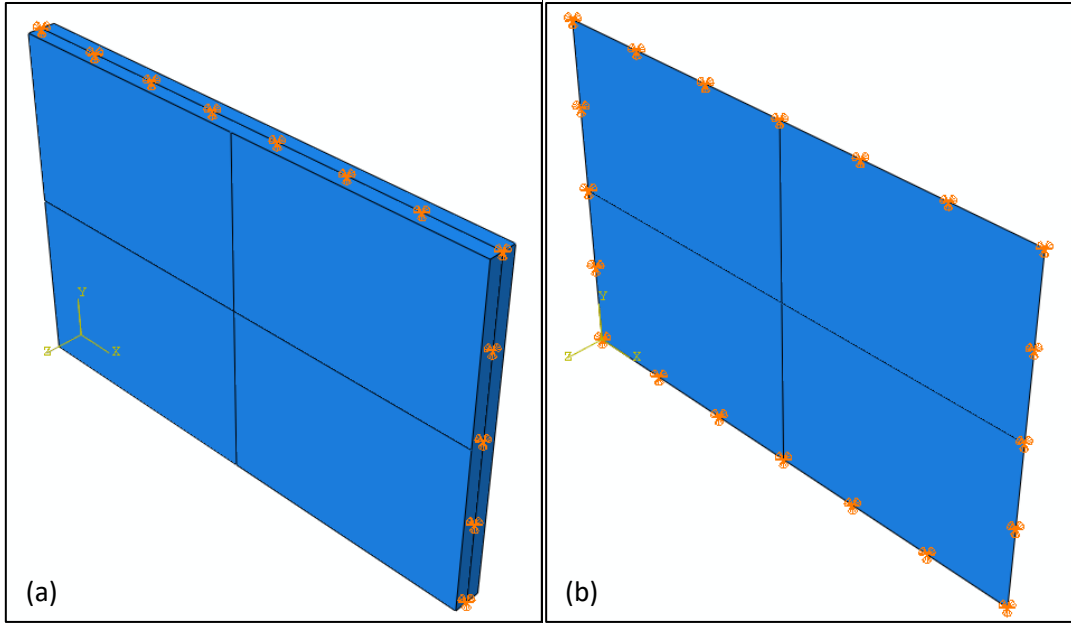


Figure 2.3.1a: First boundary condition: Pinned at all sides (a. Wall, b. Shell).

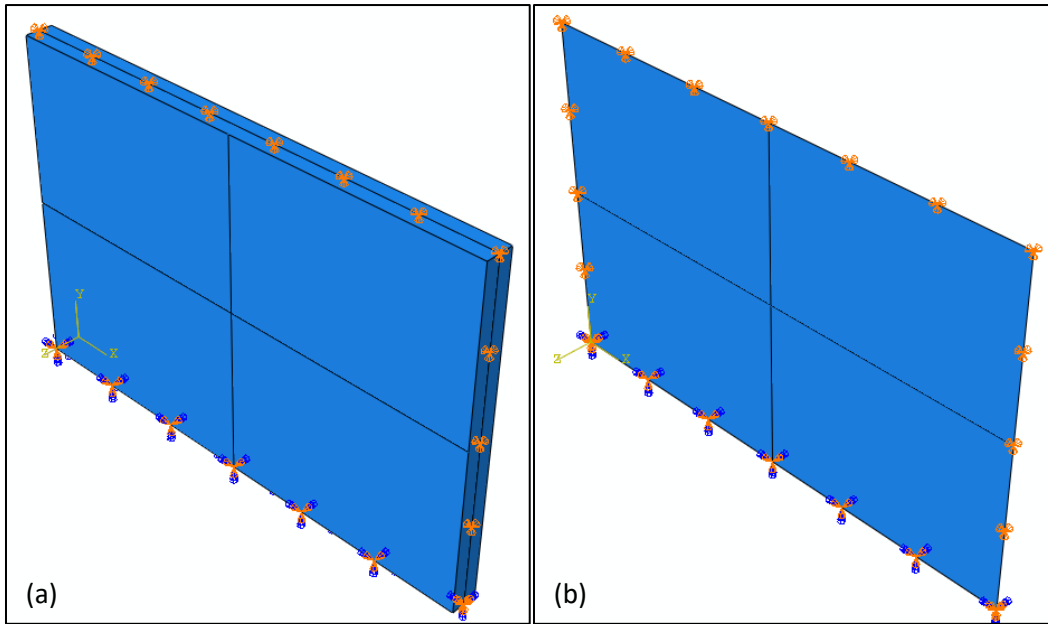


Figure 2.3.1b: Second boundary condition: Fixed -Pinned -Pinned-Pinned (a. Wall, b. Shell).

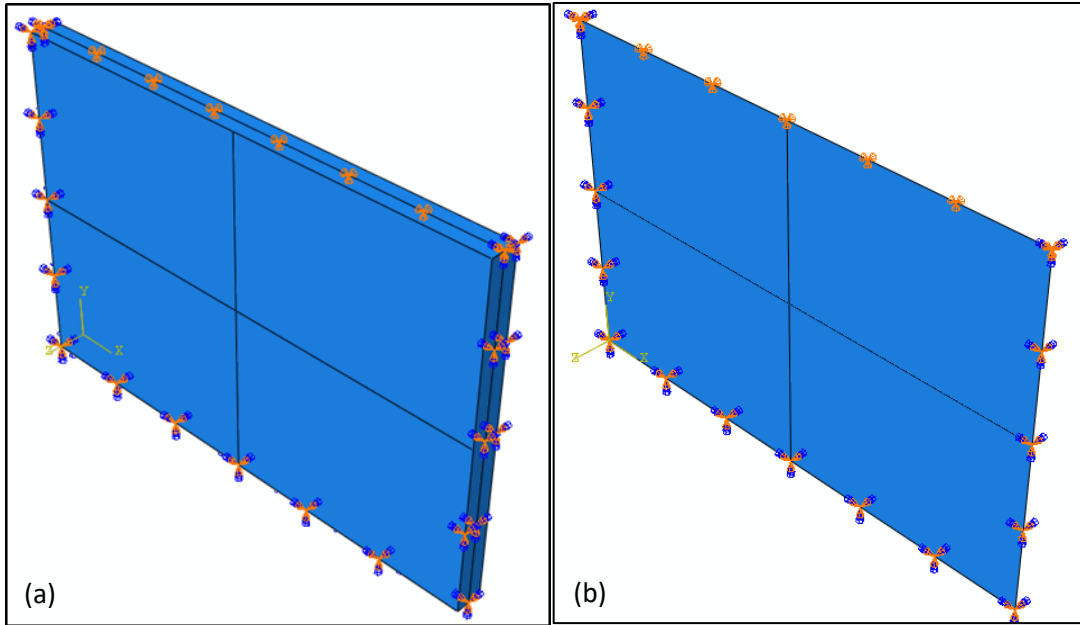


Figure 2.3.1c: Third boundary condition: Fixed-Fixed-Fixed-Pin (a. Wall, b. Shell).

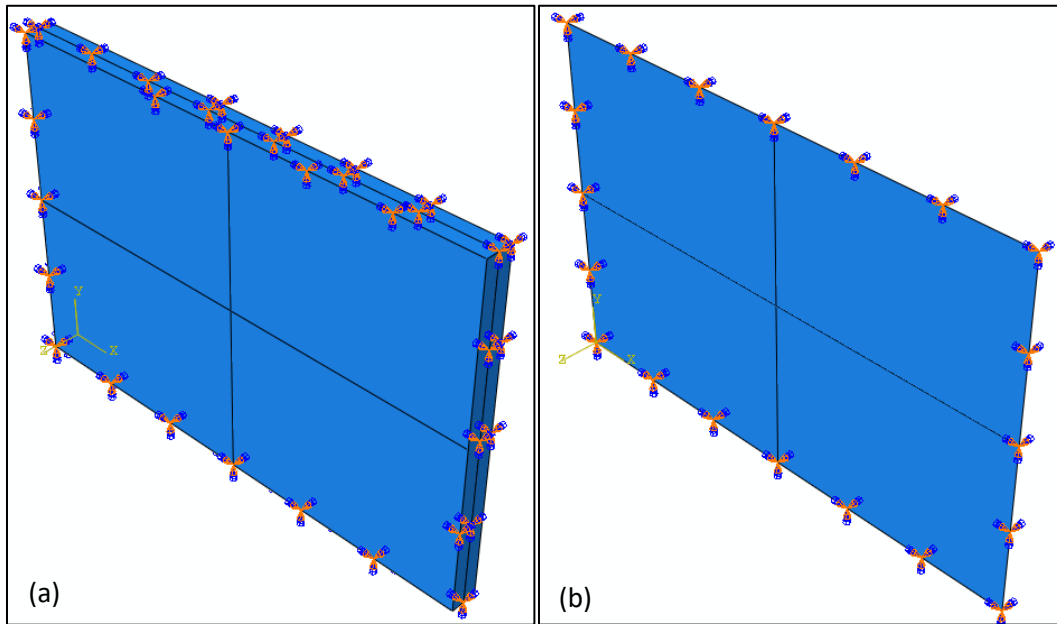


Figure 2.3.1d: Fourth boundary condition: Fixed on all sides (a. Wall, b. Shell).

2.3.3 – Maximum displacements calculated with the analytical formulation

As mentioned before, to validate the numerical model only the displacement equations from the classic book Theory of Plates and Shells were used. The geometry of the plate as well as the material properties presented in *Table 2.2.1* were considered, with the only difference that the Poisson's ratio the concrete was changed from 0.18 to 0.3. A uniform pressure q of 25 pounds per square inch (psi) was employed in the formulas and in the Abaqus models.

The displacements of the elastic uniform plates derived following the concepts of the Theory of Elasticity are expressed as sums of infinite number of terms. However, these series converge rapidly and an accurate value can be obtained with adding just the first few terms. According to Timoshenko and Woinowsky-Krieger (1987), regardless of the supports at the four boundaries, the maximum deflections of rectangular plates can be expressed as:

$$w_{\max} = \alpha \frac{q a^4}{D} \quad (2.1)$$

where α is numerical factor that depends on the ratio a/b between the two dimensions a and b of the plate. It is assumed that $a > b$. The parameter D is known as the flexural stiffness of a plate and it is defined as in terms of the elastic modulus E , the thickness of the plate t , and the Poisson's ratio ν :

$$D = \frac{Et^3}{12(1-\nu^2)} \quad (2.2)$$

For all the cases considered in this section, the flexural stiffness is constant. Using a Young's modulus $E = 3600 \text{ ksi}$, a thickness $t = 10 \text{ in}$, and $\nu = 0.3$, the constant D becomes:

$$D = \frac{Et^3}{12(1-\nu^2)} = \frac{3600 \times 10^3}{12(1-0.3^2)} = 329,670 \text{ kip.in} \quad (2.3)$$

The coefficient α to calculate the maximum deflection for the case of a rectangular plate simply supported on all sides is obtained from Table 8, p. 120 of the book by Timoshenko & Woinowsky-Krieger for $b/a = 0.6667$:

$$\omega = 0.00143 * \frac{q*a^4}{D} = 0.114 \text{ in} \quad (2.4)$$

The second support condition, Three edge pinned and the other fix, is considered in Table 32, p. 194 of the “Theory of Plates and Shells” book. Entering the table with b/a ratio of 2/3 one obtains:

$$\omega = 0.00458 * \frac{q*b^4}{D} = 0.0721 \text{ in} \quad (2.5)$$

For the third case, one edge simply supported and the other three edges clamped, Table 38 in p. 207 of the reference cited provides the coefficient α . The length ratio $b/a = 2/3$ is not in the table and thus the value of α was interpolated. The maximum deflection is:

$$\omega = 0.00340 * \frac{q*b^4}{D} = 0.0535 \text{ in} \quad (2.6)$$

In the final case studied, the plate clamped on all sides, the coefficient α is provided in Table 35 in p. 202 of Timoshenko and Woinowsky-Krieger (1987). For a ratio $b/a = 0.6667$ α is 0.00220 and thus,

$$\omega = 0.00046 * \frac{q*a^4}{D} = 0.0366 \text{ in} \quad (2.7)$$

Table 2.3.1 presents a comparison of the maximum displacements of the concrete plate with the four different boundary conditions and subjected to the uniform pressure. The results obtained with the

finite element models (FEM) created in Abaqus and shown in *Figures 2.3.1 a, b, c, d* are compared with those from EQ (2.4) through (2.7) based on the Theory of Elasticity. The difference in percent was calculated as follows:

$$\text{Difference in \%} = \frac{|FEM \text{ value} - Th \text{ of } E \text{ value}|}{FEM \text{ value}} \times 100 \quad (2.8)$$

The last column in *Table 2.3.1* is a string (text) output produced by an Excel file that shows if the finite element model was validated or not. The FEM 1 are the result for the wall as a 3D element and the FEM 2 are for the walls as a 2D shell element. In can be seen that the difference between the two models was less than 7% and the difference between the models and the theoretical values were less than 16%.

Table 2.3.1: Comparison of maximum displacements obtained with the FE model in Abaqus and with the analytical model.

Displacement (in)									
Condition	Analytical Value (AV)	FEM 1	FEM 2	Difference FEM 1- AV	Difference FEM 2- AV	Difference FEM 1- FEM 2	error % (AV & FEM 1)	error % (AV & FEM 2)	error % (FEM1 & FEM 2)
Pin-Pin-Pin-Pin	0.1136	0.1306	0.1350	0.0170	0.0214	0.0044	13.0383	15.8726	3.2593
Fix-Pin-Pin-pin	0.0721	0.0748	0.0704	0.0027	0.0017	0.0044	3.562	2.4697	6.2544
Fix-Fix-Fix-Pin	0.0535	0.0599	0.0613	0.0064	0.0078	0.0014	10.6268	12.6971	2.3165
Encastre	0.0366	0.0381	0.0388	0.0015	0.0022	0.0007	3.9625	5.6209	1.7268

Some words of caution regarding the differences between the displacements calculated with the two approaches. Usually the results obtained from analytical formulations based on continuum models, such as those presented by Timoshenko and Woinowsky-Krieger, are regarded as exact. However, it must be pointed out that the formulas were obtained employing a series of assumptions, for instance that the thickness of the plate is thin, that the shear deformations can be neglected, etcetera. On the other hand, the results obtained from the numerical models such as the finite elements approach are

considered to be approximate. However, in the models created in Abaqus the concrete plate was discretized with a large number of degrees of freedom using 3-D finite elements that account for the shear deformations, among other features. Therefore, it is not evident which one of the two results can be considered as the most accurate one and hence the term “error” was not used to describe the differences. By “validating” the FE model, we mean that if the models created in Abaqus gives reasonable results between each other and against the analytical value for Timoshenko, means that the proper support conditions were used, and the loading was correctly applied, that there are no meshing issues, that the material properties were correctly assigned in the program, etcetera.

2.4 – The damping properties

There are two ways to account for the energy dissipation (i.e. the damping characteristics) of the structure and materials in a linear elastic dynamic analysis. The first method, known as the classical damping assumption, consists of assigning a damping ratio ζ_j to each mode of vibration of the model: usually the same value is assumed for all the modes. This is a very convenient and easy to apply method but it has the limitation that it is only valid when the structure behaves in a linear elastic fashion. The other approach, which is valid for either linear or nonlinear analysis, is known as the *Rayleigh damping model*, sometimes also referred to as the *proportional damping* assumption.

In the Rayleigh damping model the damping matrix [C] is generated as a linear combination of the mass matrix [M] and stiffness matrix [K] through two coefficients α and β :

$$[C] = \alpha [M] + \beta [K] \quad (2.9)$$

The values of the coefficients α and β are determined using the condition that two predetermined modes of the system, say the m^{th} and p^{th} modes, have preselected damping ratios, i.e. ζ_m and ζ_p ,

respectively. It can be shown that the constants α and β can be defined with the following expressions (Suárez, 2008):

$$\alpha = \frac{2\omega_m\omega_p}{\omega_p^2 - \omega_m^2} (\omega_p\xi_m - \omega_m\xi_p) \quad (2.10)$$

$$\beta = \frac{2\omega_m\omega_p}{\omega_p^2 - \omega_m^2} \left(\frac{\xi_p}{\omega_m} - \frac{\xi_m}{\omega_p} \right) \quad (2.11)$$

In these equations ω_m and ω_p are the natural frequencies of the m^{th} and p^{th} modes, respectively.

Usually it is sought that the two modes that most contribute to the dynamic response have damping ratios chosen in advance by the user. For the present investigation the first and second modes are selected, i.e. $m = 1$ and $p = 2$ in EQ (2.10) and (2.11). Moreover, in most cases there is not enough information to select different damping ratios for the two modes and thus for the present study $\check{\zeta}_m$ and $\check{\zeta}_p$ are taken as equal.

Table 2.4.1 shows the values of all the parameters required to define the Rayleigh damping in Abaqus for the finite element model of the concrete wall with the metallic foam layers and constraining sheets. According to the information available in the technical literature (Ashby et al., 2000), metallic foams have a damping capacity typically between five and ten times that of the metal they are made from. An average value of 7.5 times the damping capacity of aluminum was assumed for the dynamic analyses in this thesis. The damping ratios for the aluminum sheet and for the concrete wall were taken equal to 0.04 and 0.02, respectively.

Table 2.4.1: Material damping parameters used in the Abaqus models

Material	Damping parameters						
	ξ	ω_m (Hz)	ω_p (Hz)	ω_m (rad/s)	ω_p (rad/s)	α	β
Concrete	0.020	89.753	135.840	563.936	853.510	15.723	0.00002
Aluminum foam (FoamA)	0.300	89.753	135.840	563.936	853.510	203.743	0.00042
Aluminum foam (FoamB)	0.300	89.753	135.840	563.936	853.510	203.743	0.00042
Aluminum foam (FoamC)	0.300	89.753	135.840	563.936	853.510	203.743	0.00042
Metallic sheet (Al)	0.040	89.753	135.840	563.936	853.510	27.166	0.00006

Figure 2.4.1 illustrates an example of how the values of the constants α and β were input into the Abaqus software.

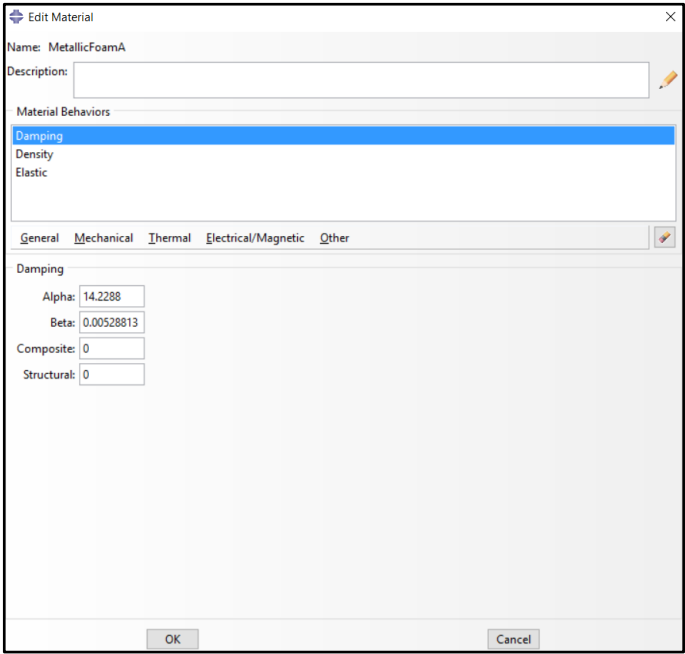


Figure 2.4.1: Damping parameters input window in Abaqus ver. 6.14-4.

Chapter 3 – Linear Static and Dynamic Analysis of the Wall with the Metallic Foam Multilayer Protection System (MFMPs)

3.1 – Introduction

Metallic foams are very promising materials for use in civil engineering structures for explosive blast mitigation. The reasons are its high energy absorption and a suitable modification of the high-intensity short-duration applied pressure due to the explosion. Aluminum foams, due to their pockets of air and its absorption capacity, are able to create a virtually constant stress level as shown in *Figure 3.1*, allowing to reduce the magnitude of the blast load by distributing for a longer time interval (Wu et al., 2011). Nevertheless, due to the mechanical material properties of these metallic foam creating a numerical model of this material is not an easy task.

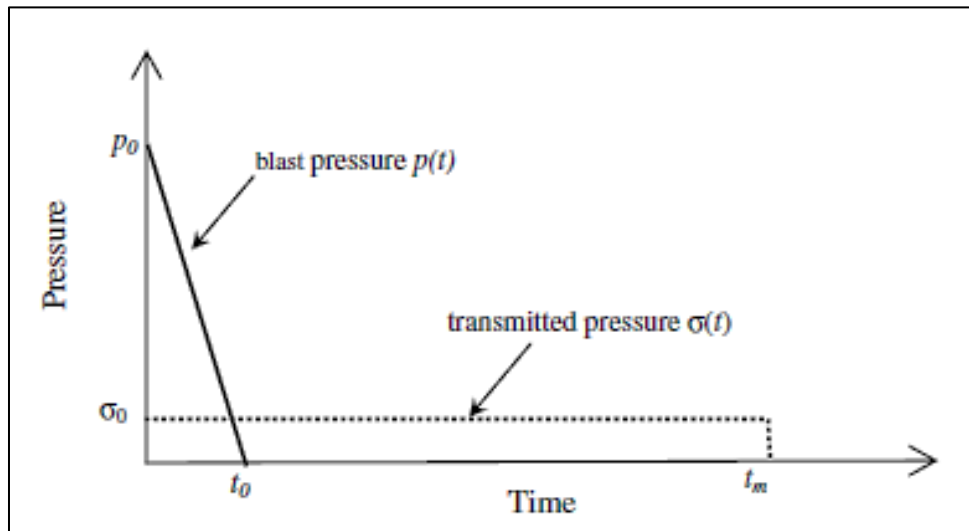


Figure 3.1: Idealized blast pressure and transmitted pressure due to the presence of an aluminum foam plate (Wu et al. 2011).

This chapter presents a numerical simulation of the response of a reinforced concrete wall retrofitted with three different Metallic Foam Multilayer Protection System (identified as MFMPs). The finite element model will be created with the program Abaqus and the assembly will be subjected to

three types of loads: a static pressure and two dynamic pressures. One of the dynamic pressures is a user-defined short duration pulse and the other is a pressure wave generated with a set of special algorithms called CONWEP and available in Abaqus. In this chapter it will be assumed that the wall and MFMPs display a linear elastic behavior regardless of the intensity of the loading. In all cases the responses of the original wall will be compared with those obtained from the wall covered by one of the proposed MFMPs.

3.2 – Metallic Foam Multilayer Protection System (MFMPs) modeling parameters

3.2.1 – MFMPs definition

As it was mentioned in Chapter 2, the MFMPs were defined using shell elements S4R which are four nodes shell elements with one point reduced integration. In order to secure a consistent behavior of the MFMPs, it was a model with a composite section for the layers, two aluminum sheets that work as dividers and two metallic foam layers between them. Although it is a composite, each layer is isotropic, thus the orientation angles are all zeros. *Figure 3.2.1* displays the input value window on Abaqus for one configuration of the MFMPs as well as a distribution of the layers in the software.

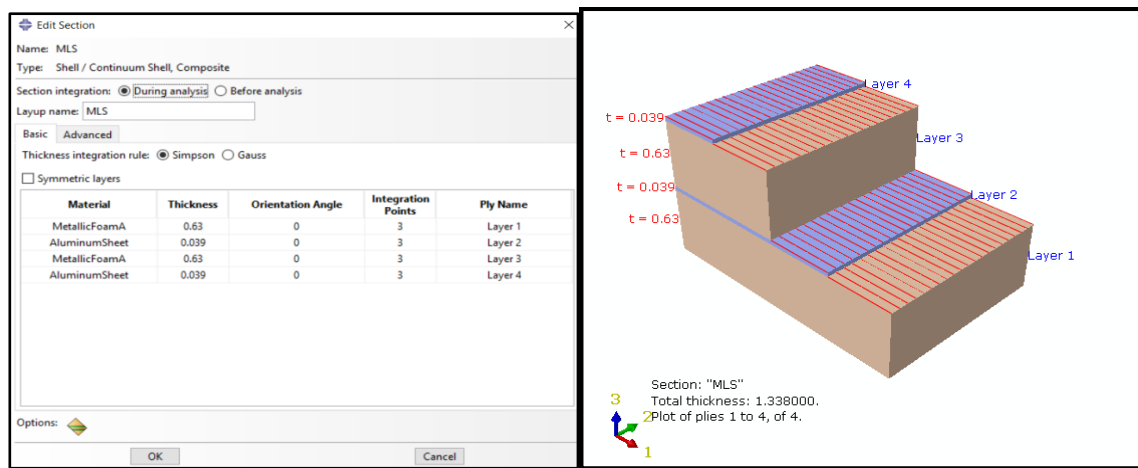


Figure 3.2.1: Composite Section input window and distribution on the MFMPs model

The use of this composite section feature allows for a simplification of the model reducing analysis time, minimizing ensemble errors and easy editing of the values field in case of future analysis such as increasing the number of layers or a change in the thickness. The Simpson's integration rule is used as a default for this composite section. According to the Abaqus Analysis, User's Guide, the Simpson's integration should be used if the results output is the shear stress are required at the interface of each layer and must be used in cases of a heat transfer or coupled temperature – displacement shell elements. On the other hand, the Gauss quadrature is more limited therefore for these numerical experiments the default input of Simpson's integration rule was considered.

3.2.2 – MFMPs and concrete wall assembly

To simplify the modelling process, the different layers of metallic foam and aluminum sheet that form the MFMPs system were represented as a composite structure. As it was mentioned before, the RC wall was modeled using 3D elements, Therefore, to join these two bodies it is necessary to apply a so called “position constraint”. The constraints are used in Abaqus whenever it is necessary to eliminate a group of nodes and to couple their motions to those of user-defined master nodes. For instance, this is useful when a 3-D solid model which has no rotation stiffness at its nodes needs to be coupled with a shell element. In this study this feature is used to enforce contact between the two surfaces: the back face of the MFMPs and the front face of the wall. A surface constraint avoids any embedment of the MFMPs into the wall allowing the continuity and the transfer of the forces, stresses, strains, and displacements from one object to the other.

Another position constraint was applied to the MFMPs: it is known as edge constraint. In the case of the edge constraints, contrary to the surface constraint, they restrain the motion of the MFMPs

from sliding, in either direction of the wall, functioning as a glue or epoxy among the instances. This Assembly is shown in *Figure 3.2.2*.

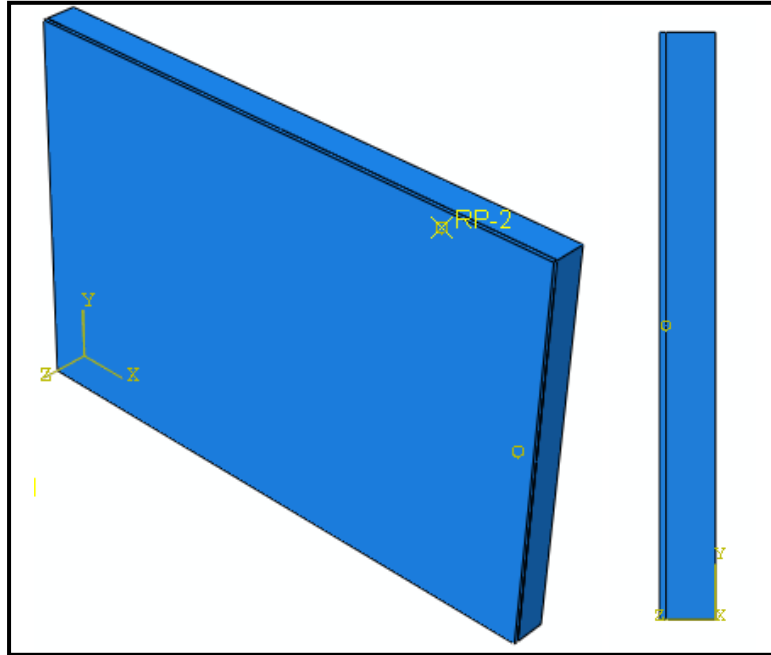


Figure 3.2.2: Isometric and profile view of the assembly for the MFMPS and the wall.

3.2.3 – Loads and boundary conditions

Two type of pressure loads acting at the front of the MFMPS were considered for the linear elastic analysis. The first one is a static pressure with an intensity of 140 psi; this is applied in such a way that slowly increases its magnitude until it reaches the final value as shown in *Figure 3.2.4*. The final application time needs to be much higher than the fundamental period of the structure to avoid dynamic effects. The second loading condition is a dynamic pressure, also with a peak magnitude of 140 psi, but with a triangular variation in time. *Figure 3.2.5* illustrates the variation in time of this pressure. The shape of this dynamic pressure represents a further simplification of the idealized loading caused by an explosive event. According to the technical literature, the time variation of the explosive pressure obtained from experimental observations has the approximate shape shown in *Figure 3.2.3*; in this case

this was taken from section 34.4.6 of the Online Abaqus Analysis User's Guide. This pressure representation takes into consideration the time of detonation of the explosive and the arrival time of the pressure wave. It is divided into two phases: a positive and a negative one. In the dynamic analysis the negative phase is usually disregarded because its effects are not significant compared to the positive phase, therefore a simplified model of the dynamic pressure can be defined with two time points. These are those presented in *Figure 3.2.5*: the time t_0 in which the load reaches its peak and the total duration of the load t_d .

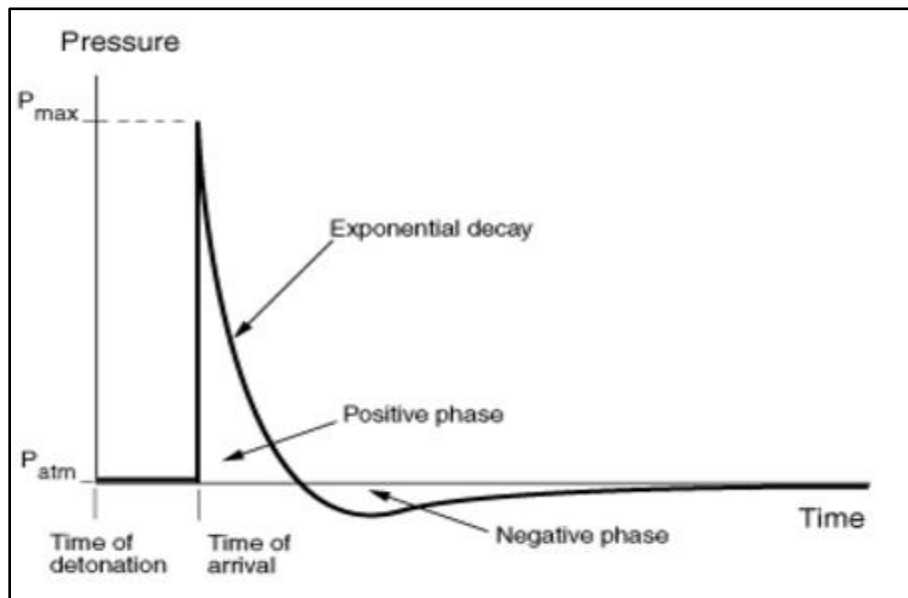


Figure 3.2.3: Idealized explosive pressure behavior, from Abaqus 6.13 Analysis User's Guide

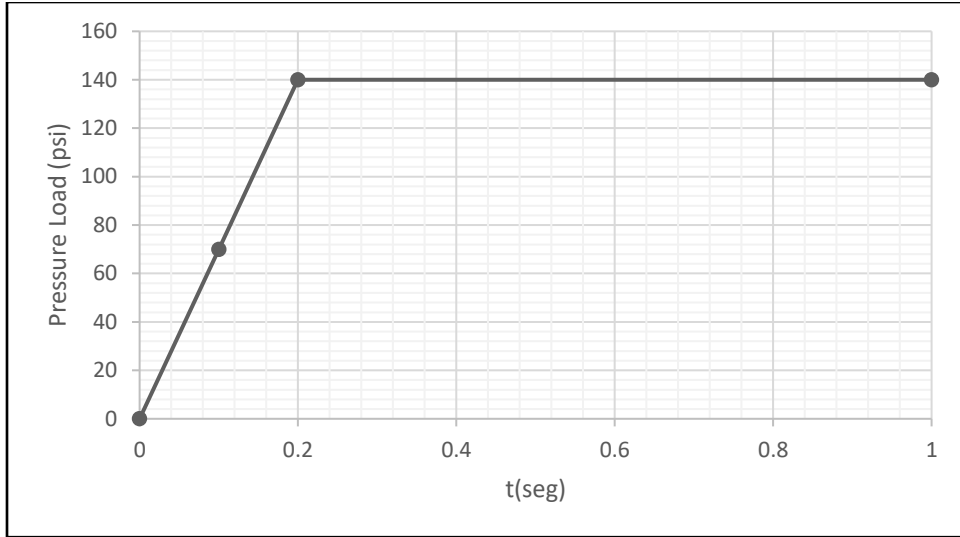


Figure 3.2.4: Static pressure load application curve

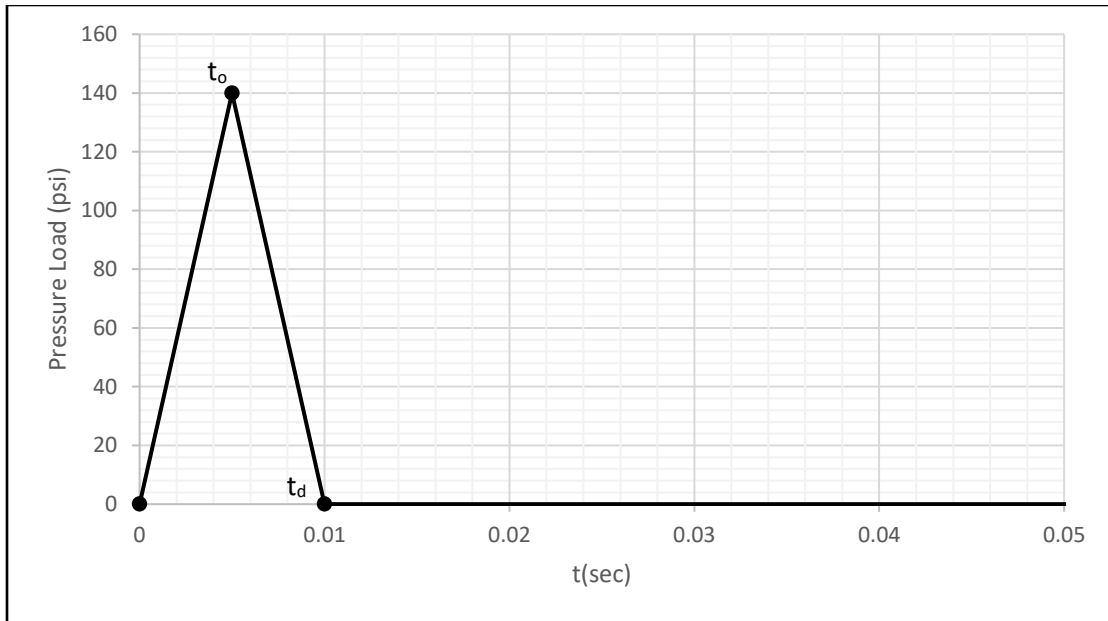


Figure 3.2.5: Dynamic pressure load application curve

Boundary conditions base on the continuity on the wall on both sides as well as the connection between the roof slab and next upper floor wall with the wall that's been a model. These connections restrict the movement and rotation of the model, therefore, a fix/encase conditions were established. This means that there are not going to be any displacement nor rotation along the connection of the wall been a model with the nearby wall segment. The boundary conditions can be appreciated in *Figure*

3.2.6. Were the blue cone symbolize restriction of displacement in any XYZ direction and the orange cone symbolize the restraint of rotation about any axis. The *Figure 3.2.6* also show the way both pressure loads, static and dynamic, apply on the MFMPs and the wall.

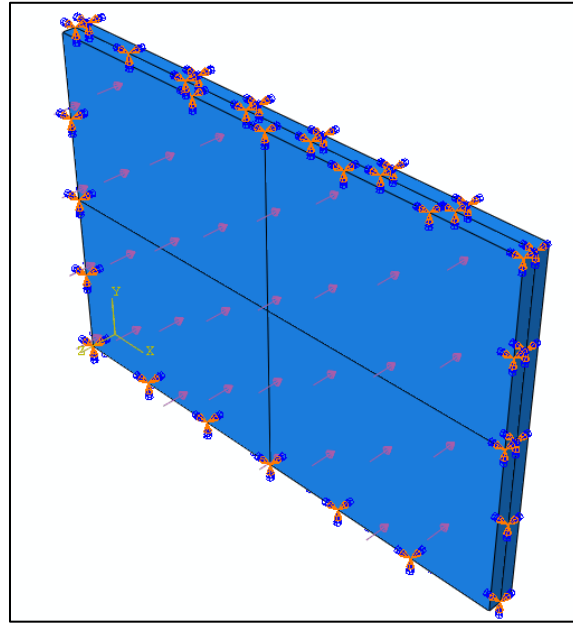


Figure 3.2.6: Boundary conditions of the model and pressure loads directions

3.3 – Static pressure load analysis and results

As shown in *Figure 3.2.4*, the static pressure load was applied in small increments following a ramp distribution until it reached the desired load of 140 psi and keeping it constant after the peak value was reached. The value of 140 psi was chosen in order to amplify the displacements and so that the concrete wall would undergo inelastic excursions. This in turn permits to observe the differences between a lineal-elastic behavior and a non-linear behavior response (Chapter 4) and the effect of the MFMPs in these two cases. The response quantities to be monitored are the displacements at the middle of the wall and the normal stress at the point at the center of the top end of the wall. Since the main objective of this project is to evaluate the behavior of the wall with and without the three different

MFMPs, the same nodes in the wall will be used to examine the reduction in the response achieved. As a result of the static load analysis, four response curves were generated for the wall with each of the three MFMPs configurations and the bare wall. *Figures 3.3.1a*, through *3.3.1c* display the principal stress at the selected point of the wall without the protective sheets and with each of the configurations. The figures show the variation with time because, as it was mentioned before, the pressure was applied slowly increasing its magnitude. *Figures 3.3.2a*, through *3.3.2c* present the displacements at the point at the geometric center of the wall for the three cases.

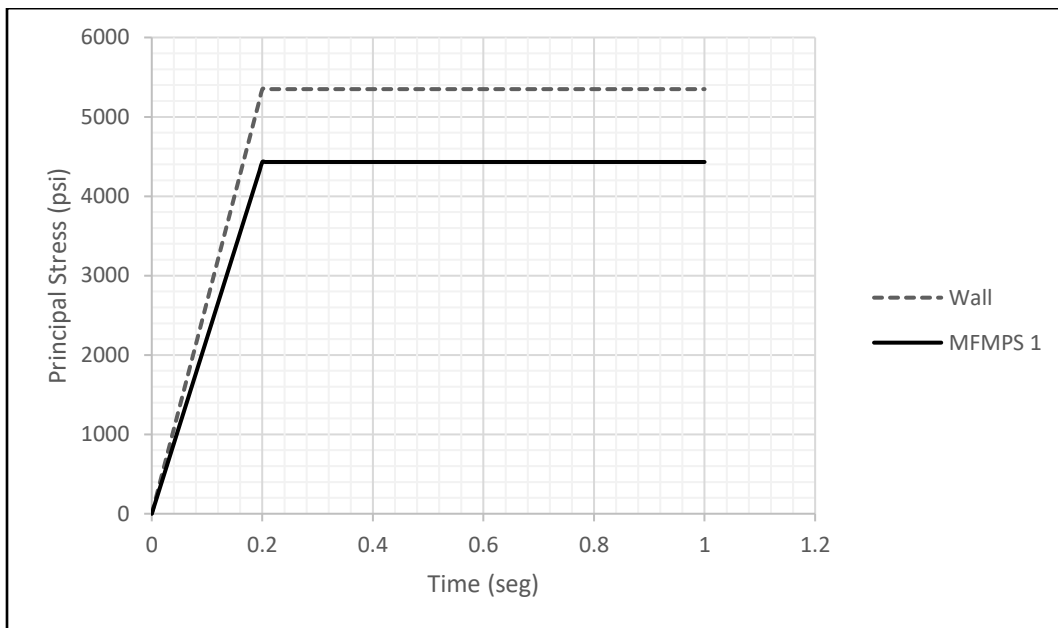


Figure 3.3.1a: Static stress evaluation of the wall against MFMPs 1

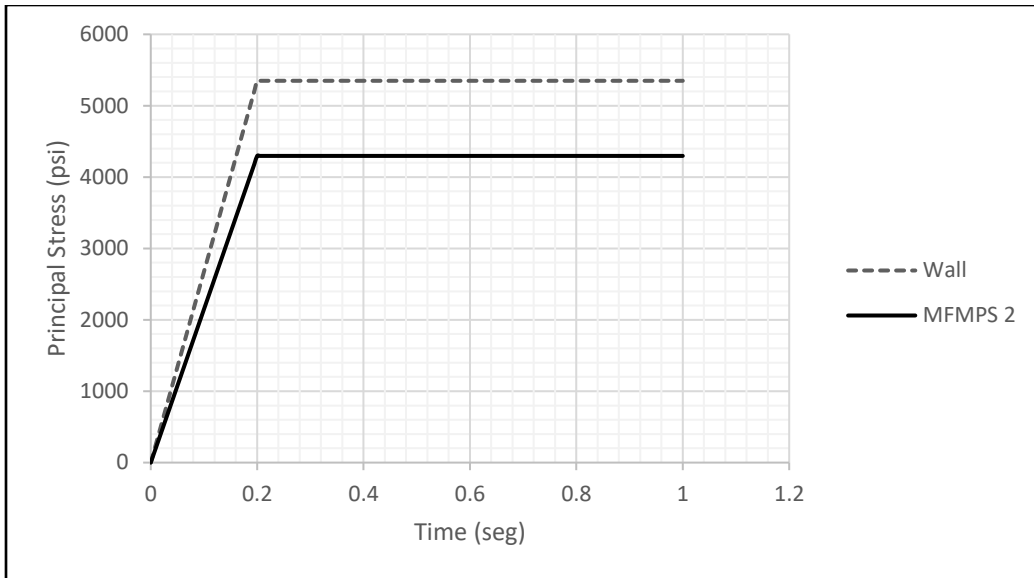


Figure 3.3.1b: Static stress wvaluation of the wall against MFMPs 2

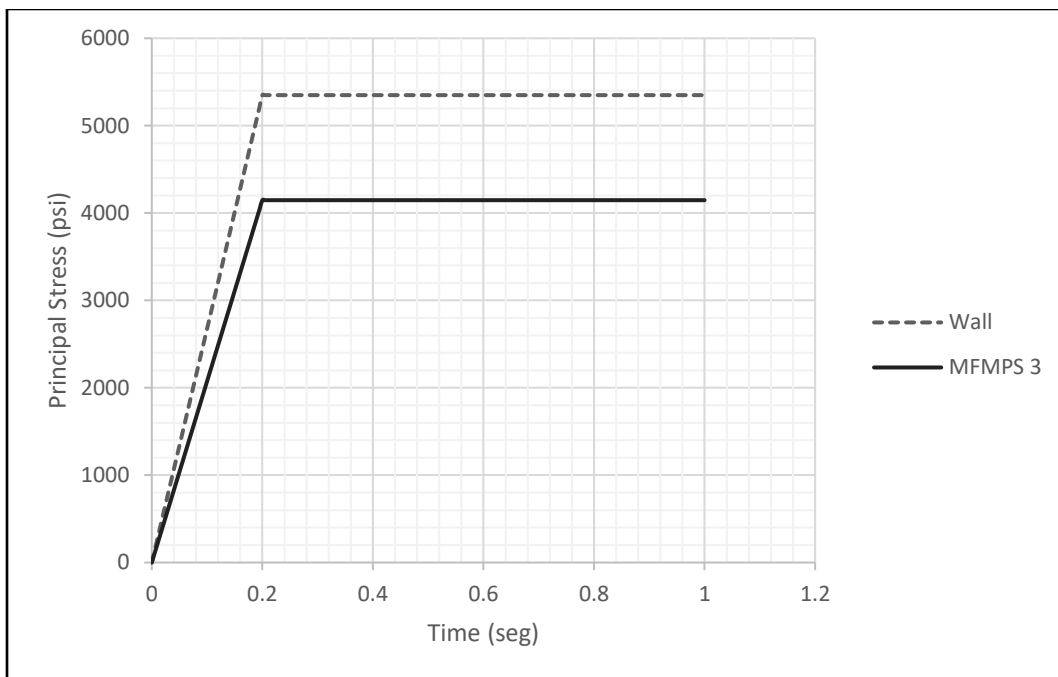


Figure 3.3.1c: Static stress evaluation of the wall against MFMPs 3

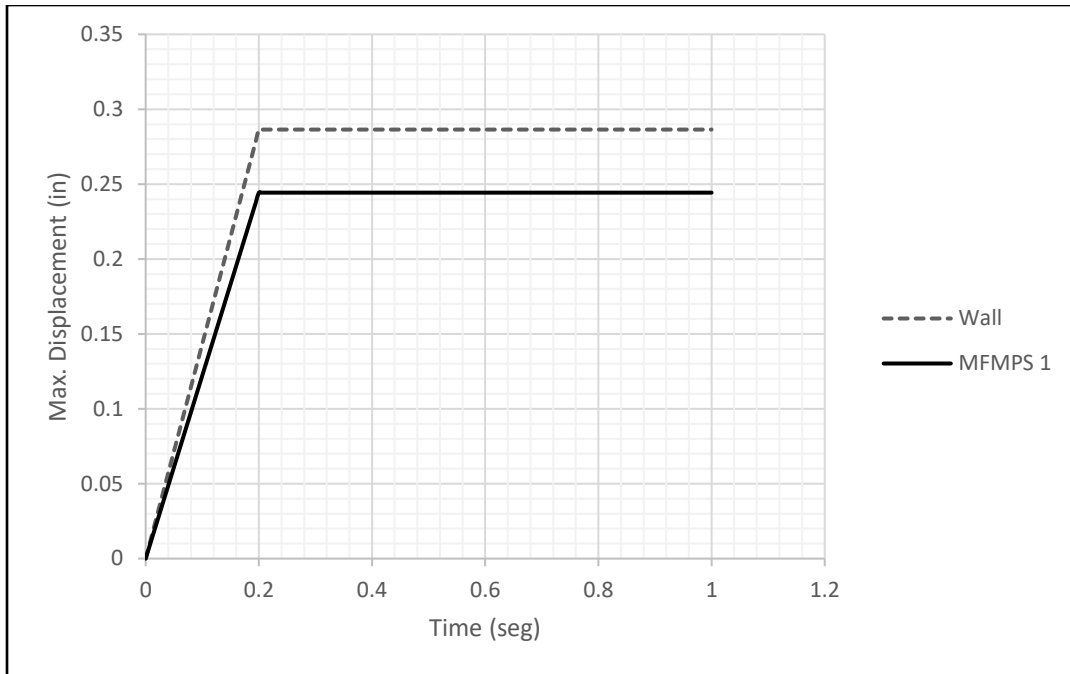


Figure 3.3.2a: Static change in displacement evaluation of the wall vs MFMPs 1

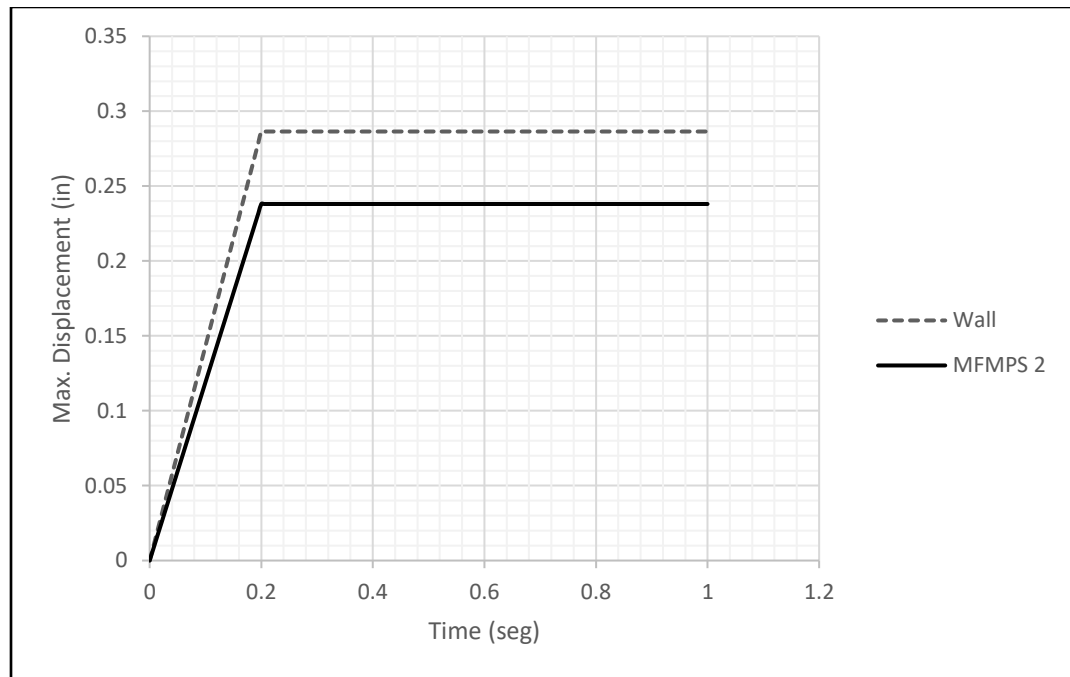


Figure 3.3.2b: Static change in displacement evaluation of the wall vs MFMPs 2

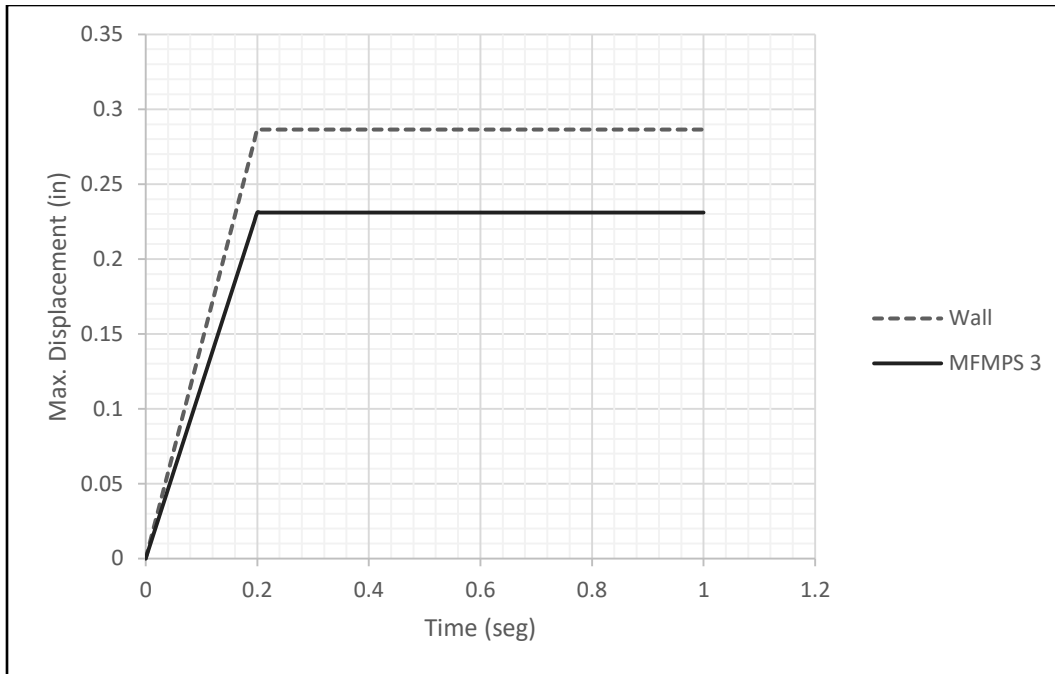


Figure 3.3.2c: Static change in displacement evaluation of the wall vs MFMP3

Table 3.3.1 shows how the MFMP3 reduce the stress and displacement according to the properties of each metallic foam as presented in Table 2.2.1.

It can be seen that the level of maximum response reduction obtained with the three MFMP3 configurations are comparable, although the third option gives better results. In addition, it can be observed that the level of reduction is slightly higher for the stresses than for the displacements.

Table 3.3.1: Reduction in displacements and stresses achieved by the MFMP3 for the static pressure load

Model #	U_{\max} (in)	σ_{\max} (psi)	U % reduction	σ % reduction
MFMP3 1 + Wall	0.2443	4431.620	14.708	17.155
MFMP3 2 + Wall	0.2380	4296.830	16.896	19.675
MFMP3 3 + Wall	0.2310	4147.270	19.342	22.471
Wall	0.2864	5349.290	-	-

Figure 3.3.3 shows an isometric and profile view of the deformed wall at the instant of maximum deformation. Figure 3.3.4 presents similar views but for the principal maximum stresses on the wall. The color code used to present the results in both figures illustrates that the points selected to monitor the response are those where the maximum values occur, namely at the center of the wall for the displacement and at the middle of the top edge for the stresses.

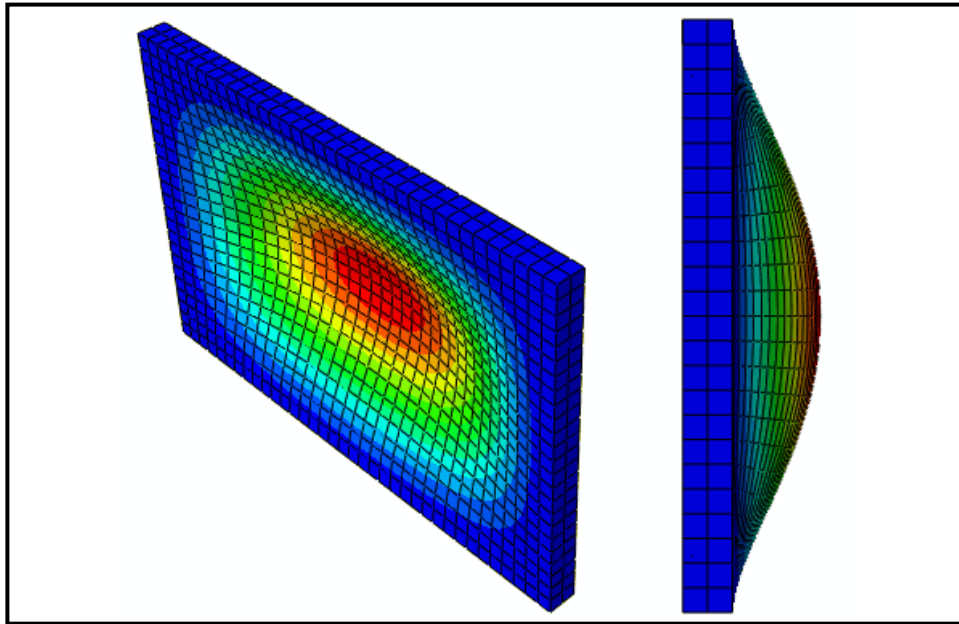


Figure 3.3.3: Isometric and profile view from Abaqus 6.14-4 of the displacements in the wall due to the static loading

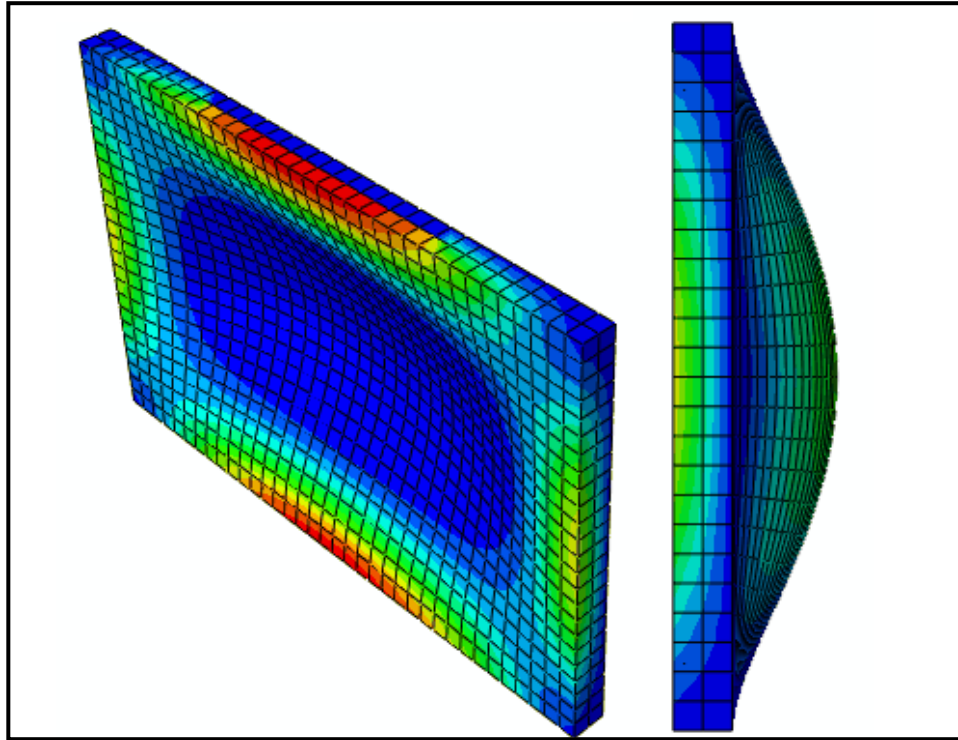


Figure 3.3.4: Isometric and profile view from Abaqus 6.14-4 of the normal stresses in the wall due to the static loading.

3.4 – Dynamic pressure load analysis and results

As mentioned before, the dynamic load selected to represent the pressure generated by an explosion has a symmetric triangular form. The duration of the load is smaller than the natural period of the structure, i.e. the clamped wall. To carry out this type of dynamic analysis, Abaqus recommends to use an explicit dynamic integration method to obtain better results.

The so called “explicit dynamics” methodology used by Abaqus is a mathematical algorithm for the integration of the equations of motion in time. It is particularly useful and efficient to solve problems involving high speed dynamics (i.e., short duration loads, such as the pressure due to explosions). The reason for the name is that the unknown response values are obtained from information already known.

Figures 3.4.1a through 3.4.1c display the variation in time of the normal stress at the most critical point in the concrete wall for the structure retrofitted with the three MFMPs. On each figure the response of the bare wall is also included for easy comparison. Figures 3.4.2a through 3.4.2c shows the displacement time histories at the point of maximum response calculated with the wall furnished with each of the MFMPs configurations. It can be noticed that the system retrofitted with the metallic foams returns more rapidly to equilibrium due to their higher damping capacity.

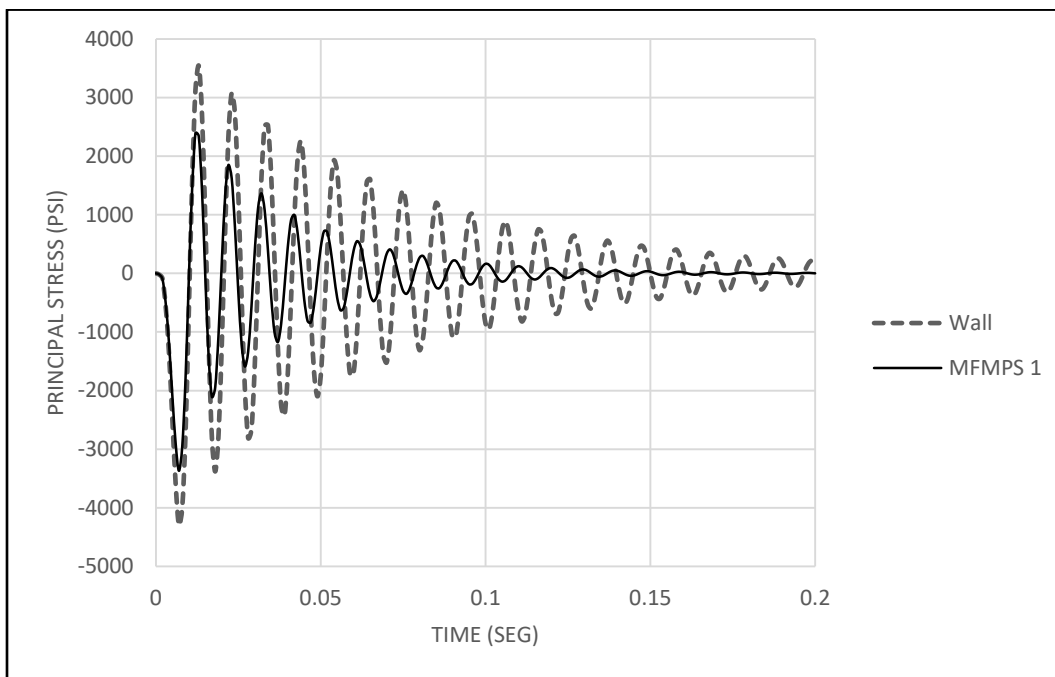


Figure 3.4.1a: Dynamic stress evaluation of the wall with MFMPs 1

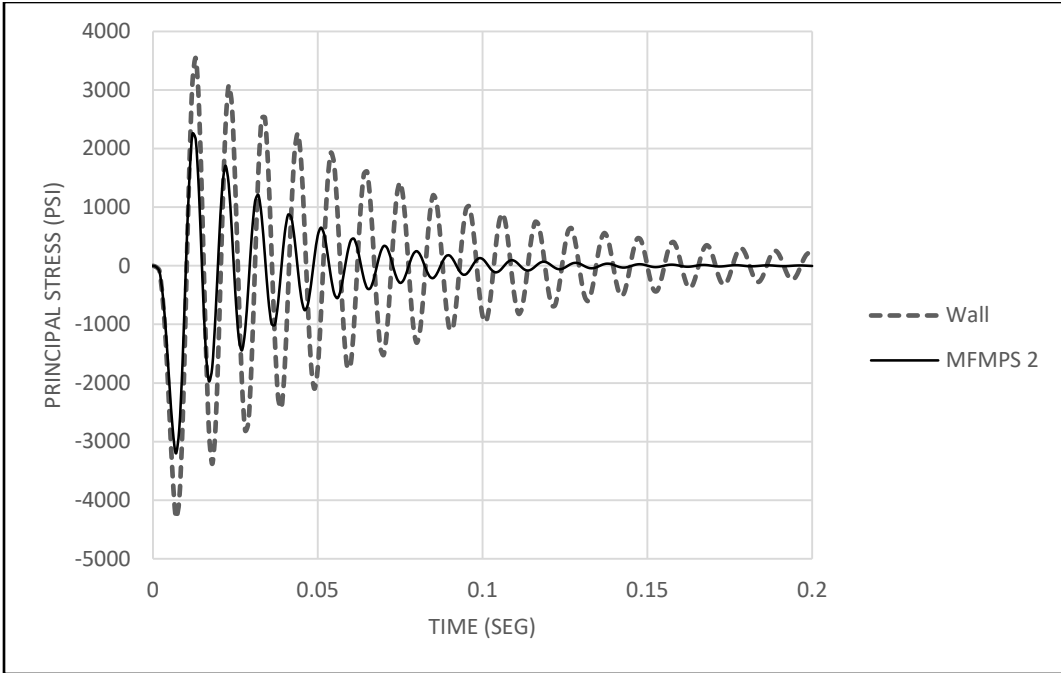


Figure 3.4.1b: Dynamic stress evaluation of the wall against MFMPs 2

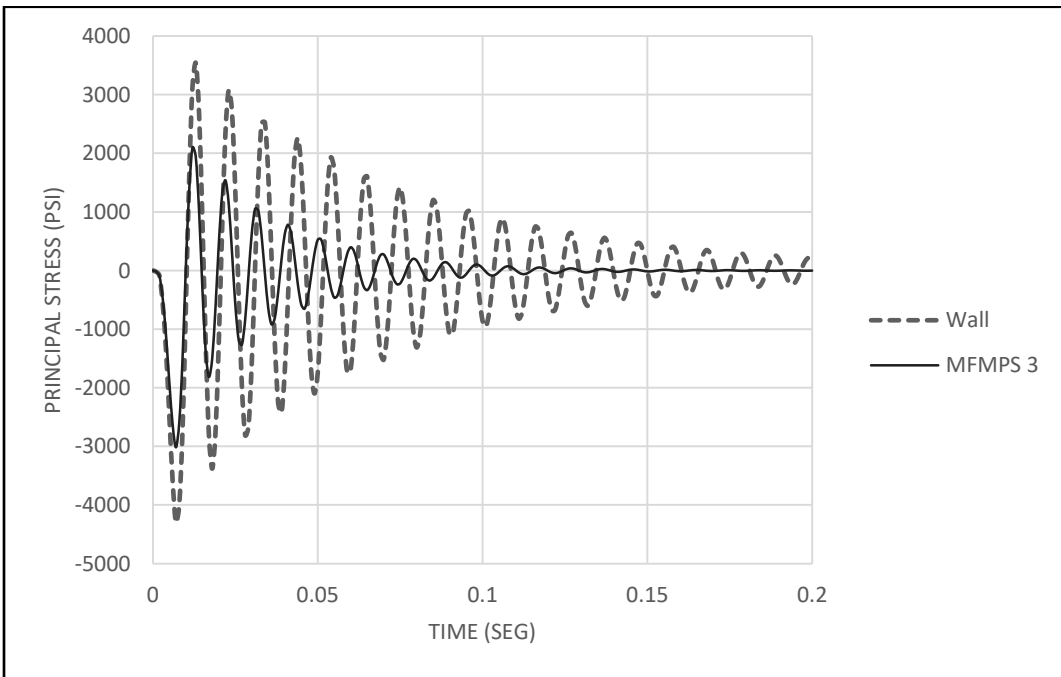


Figure 3.4.1c – Dynamic stress evaluation of the wall against MFMPs 3

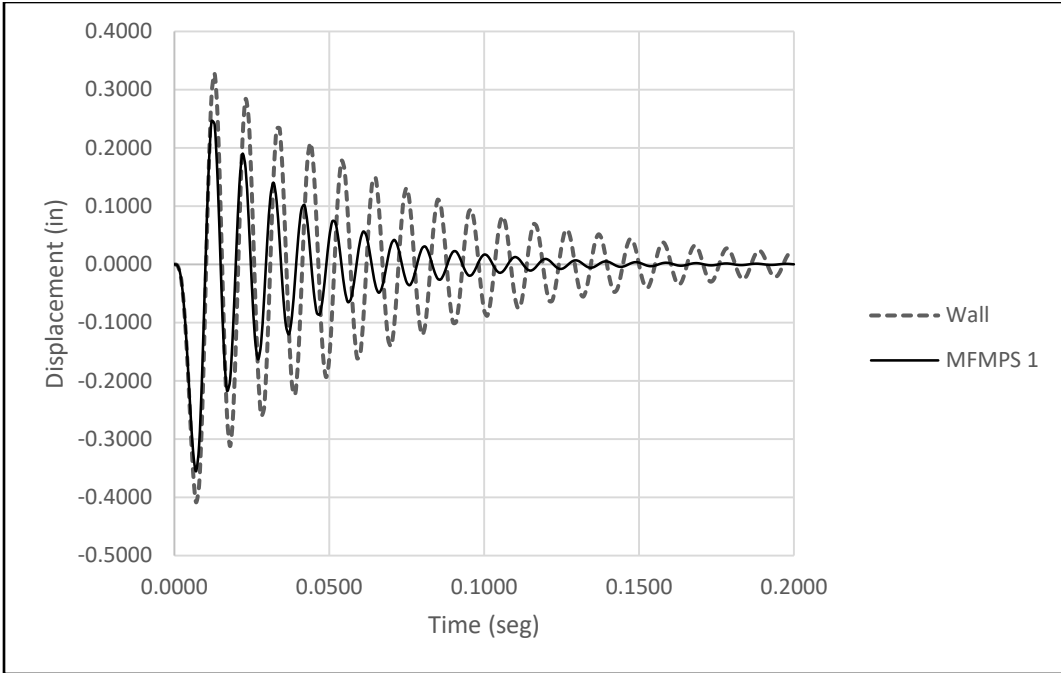


Figure 3.4.2a: Dynamic change in displacement of the wall with MFMPs 1

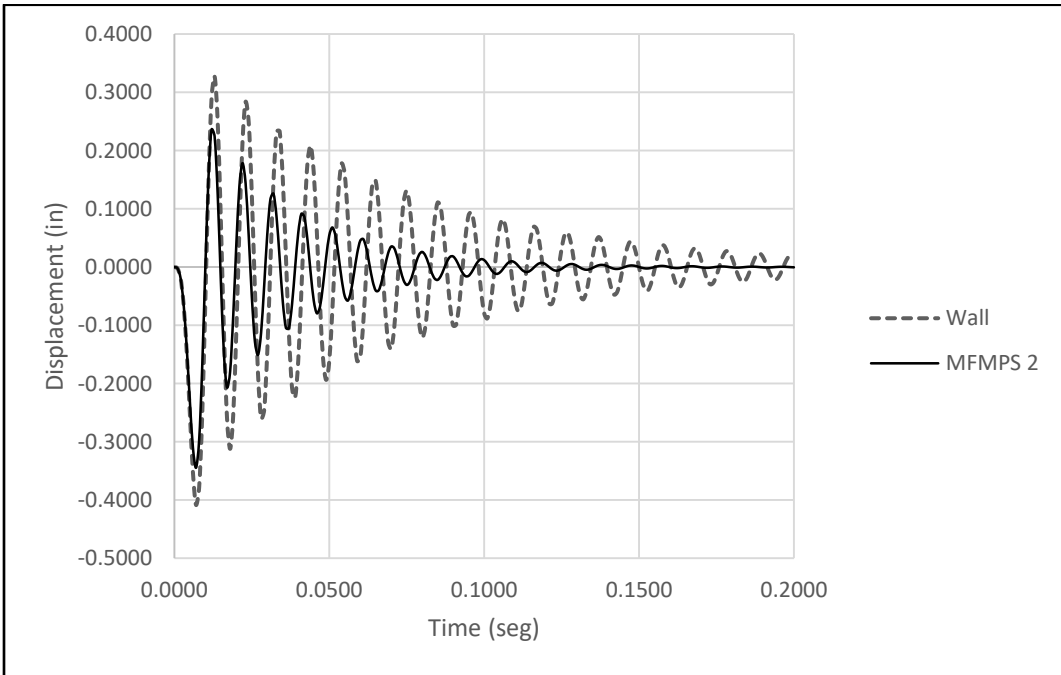


Figure 3.4.2b: Dynamic change in displacement evaluation of the wall vs MFMPs 2

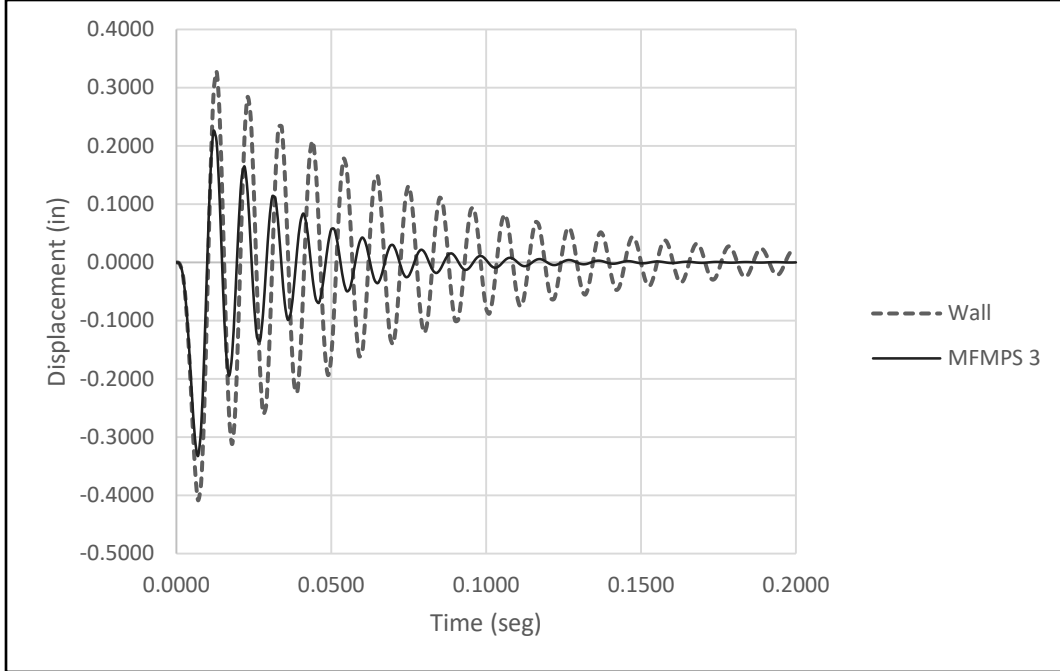


Figure 3.4.2c: Dynamic change in displacement evaluation of the wall vs MFMP3

The maximum absolute values of the diverse response quantities shown in the six previous figures were retrieved and they are presented in *Table 3.4.1*. In addition, the response reduction achieved by the three MFMP3 configurations is displayed in the same table. The reduction in percent was calculated with the following expression:

$$Reduction \% = \frac{|R_W - R_{MFMP3}|}{R_W} \times 100\% \quad (3.4)$$

where R_W is the peak value of the response of the bare wall and R_{MFMP3} is the same quantity but for the wall with one of the metallic foams assembly.

Table 3.4.1: Reduction in displacements and stresses achieved by the MFMPs for the impulsive pressure load

Model #	Umax (in)	σ_{max} (psi)	U % reduction	σ % reduction
MFMPs 1 +Wall	0.3554	3369.130	12.963	21.649
MFMPs 2 +Wall	0.3445	3201.500	15.631	25.548
MFMPs3 +Wall	0.3324	3016.280	18.586	29.855
Wall	0.4083	4300.070	-	-

The maximum principal stresses at the instant of maximum deformation is presented in a contour plot in *Figure 3.4.3*. The warmer colors indicate where the maximum stresses occur: at the bottom and top boundaries of the plate. The way the wall was deformed at the instant of maximum deformation is illustrated in *Figure 3.4.4* which shows an isometric and a profile view of the deformed structure.

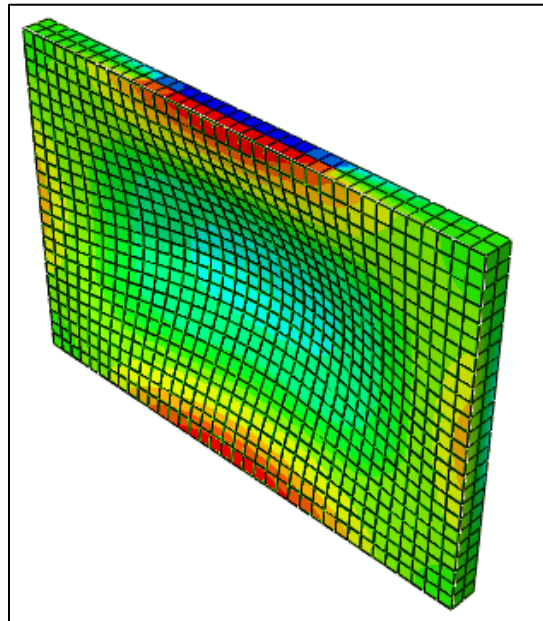


Figure 3.4.3: Isometric and profile view from Abaqus 6.14-4 of the normal stresses in the wall due to the dynamic loading.

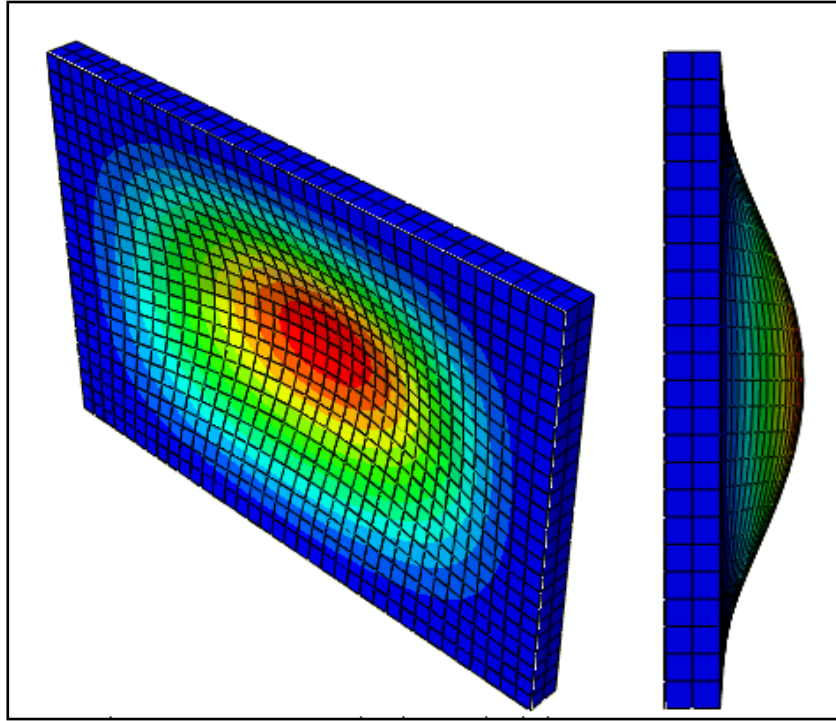
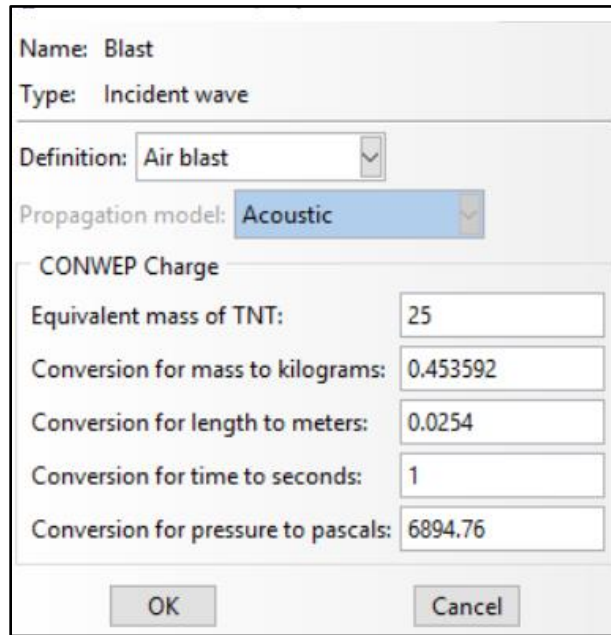


Figure 3.4.4: Isometric and profile view from Abaqus 6.14-4 of the displacements in the wall due to the dynamic loading.

3.5 – CONWEP analysis and results

Conventional weapons analysis, better known as CONWEP, is a subroutine in Abaqus that allows the user to apply an explosive load like the one shown in *Figure 3.2.3* to the external surface of a structure, in this case, the front face of the RC wall. CONWEP takes into consideration an explosive standoff distance, a TNT mass equivalent and four conversion factors which are: mass to kilograms, length to meters, time to seconds and pressure to Pascals. In other words, if the units being used to calculate the response of the wall are those of the fps (or Imperial) system, four constants must be input to the program to convert the current units to those of the SI used by CONWEP. *Figure 3.5.1* shows the input window in Abaqus with the information required by CONWEP. In this case the type of load is regarded as an incident wave: contrary to the triangularly shaped dynamic pressure used in the previous dynamic analyses which was uniformly and simultaneously applied over the surface, CONWEP will

generate a pressure wave that in theory will not reach the full surface at the same time and with the same intensity. Other information required by CONWEP is the load definition and propagation model; they are also shown in *Figure 3.5.1*.



The image shows a software dialog box for defining a blast. The fields are as follows:

Name:	Blast
Type:	Incident wave
Definition:	Air blast
Propagation model:	Acoustic
<input type="checkbox"/> CONWEP Charge	
Equivalent mass of TNT:	25
Conversion for mass to kilograms:	0.453592
Conversion for length to meters:	0.0254
Conversion for time to seconds:	1
Conversion for pressure to pascals:	6894.76

Buttons: OK, Cancel

Figure 3.5.1: Typical definition and parameters required by CONWEP.

3.5.1 – Explosive standoff distance considerations

The standoff distance is the distance measured from the center of the explosive charge to the surface that is being analyzed. According to Appendix B section B-1 of the document *UFC-4-010-1* (a DoD minimum antiterrorism standards for buildings), the most effective way to mitigate and create a cost-effective solution is regulating the standoff distance by keeping the explosive as far away as possible from the structure. In order to make this possible, an integrated design of the structural complex must be considered. Factors so as building design, landscaping, parking, access roads and other features can be used to maintain the so called Vehicles Borne Improvised Explosive Device (VBIED) far from any major structure (UFC 4-010-01, 2012). An example for controlling the standoff distance for existing

building will be a control of roadways access as well as controlling parking areas whenever is possible. Therefore a minimum standoff distance must be determined. This minimum distance is the smallest permissible distance allowed for a building in order to comply with the standards established by the DoD (UFC 4-010-01, 2012). *Figure 3.5.1* shows a diagram of some of the points of interest considered for the determination of the standoff distance.

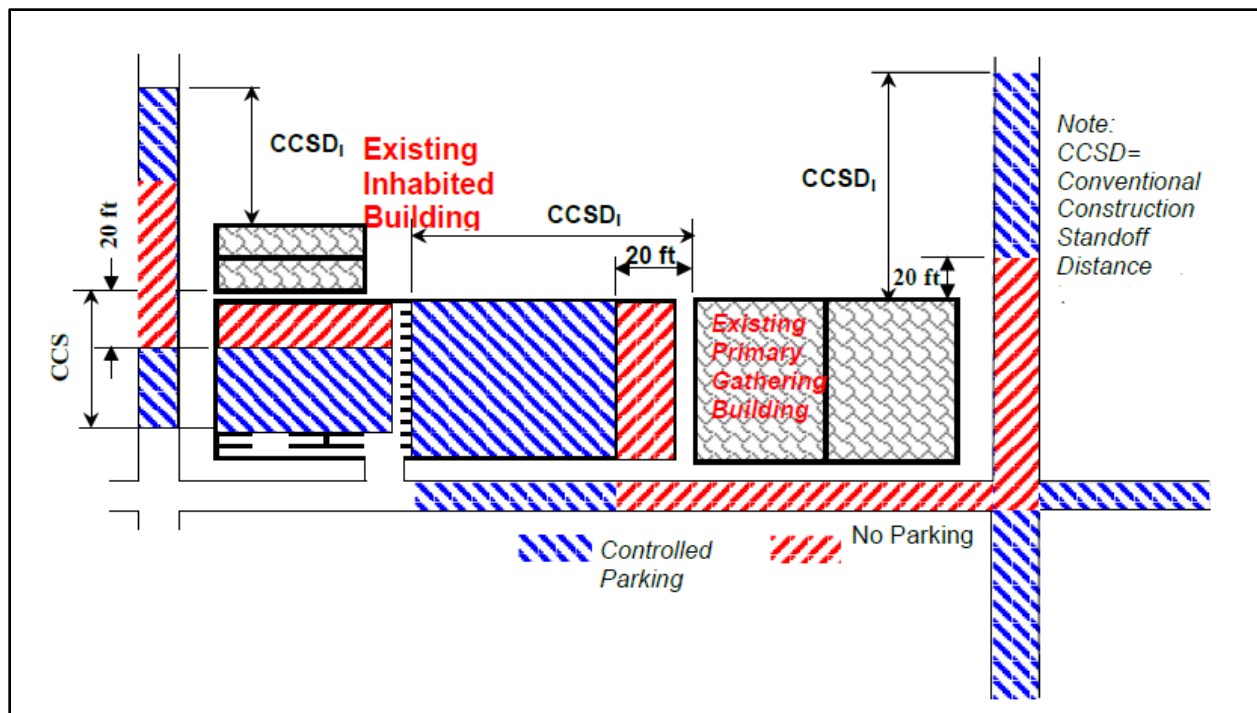


Figure 3.5.1: Parking and roadway control for existing buildings with no perimeter control, Source (UFC 4-010-01, 2012)

Three standoff distances of 10 ft, 20 ft and 30 ft were selected in order to investigate how they affect the performance of the MFMPs. Each of these distances is associated to a given amount of explosive: 100 lb, 200 lb, and 300 lb, respectively. Similar to the case of the static load and the triangular dynamic load, the magnitude of the pressure applied was selected to surpass the yielding point, even though the analysis presented here is a linear one. The magnitude of the pressure wave

generated by the CONWEP subroutine was indirectly scaled by means of the increasing standoff distances.

To establish a standoff distance in Abaqus, a reference point (denoted as RP-1) must be used. This point is shown in *Figure 3.5.2*: the standoff distance is defined according to the X, Y and Z axes presented in the same figure.

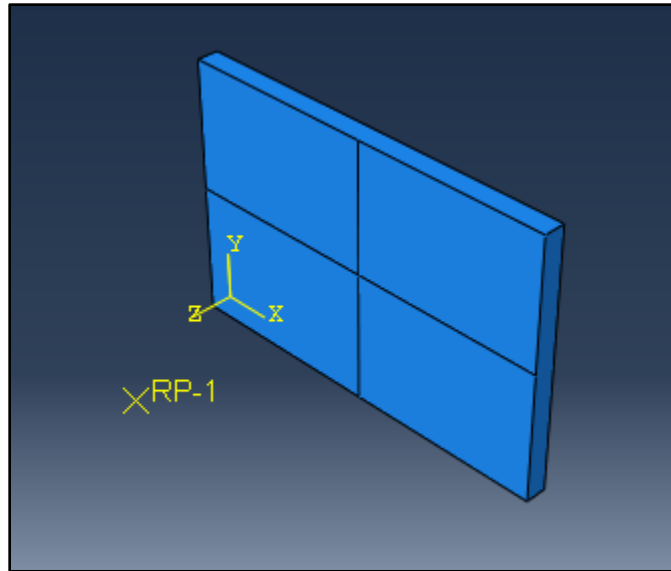


Figure 3.5.2: Standoff distance setup for CONWEP analysis in Abaqus 6.14-4

3.5.2 – CONWEP results

Contrary to the static or dynamic load cases, which were a uniform distributed long over the front wall or MFMPs surface, CONWEP load is an incident wave meaning that the load is not uniformly applied over the surface. *Figures 3.5.3a, 3.5.3b, 3.5.3c* present the variation in time of the normal stresses and displacements at the uncovered wall and the wall fitted with the three configurations of MFMPs when the explosive is 10 ft away from the structure. *Figures 3.5.4a, 3.5.4b, 3.5.4c* display

similar results but for a standoff distance of 20 ft and finally *Figures 3.5.5a, 3.5.5b, 3.5.5c* show the response time histories for the 30 ft standoff distance.

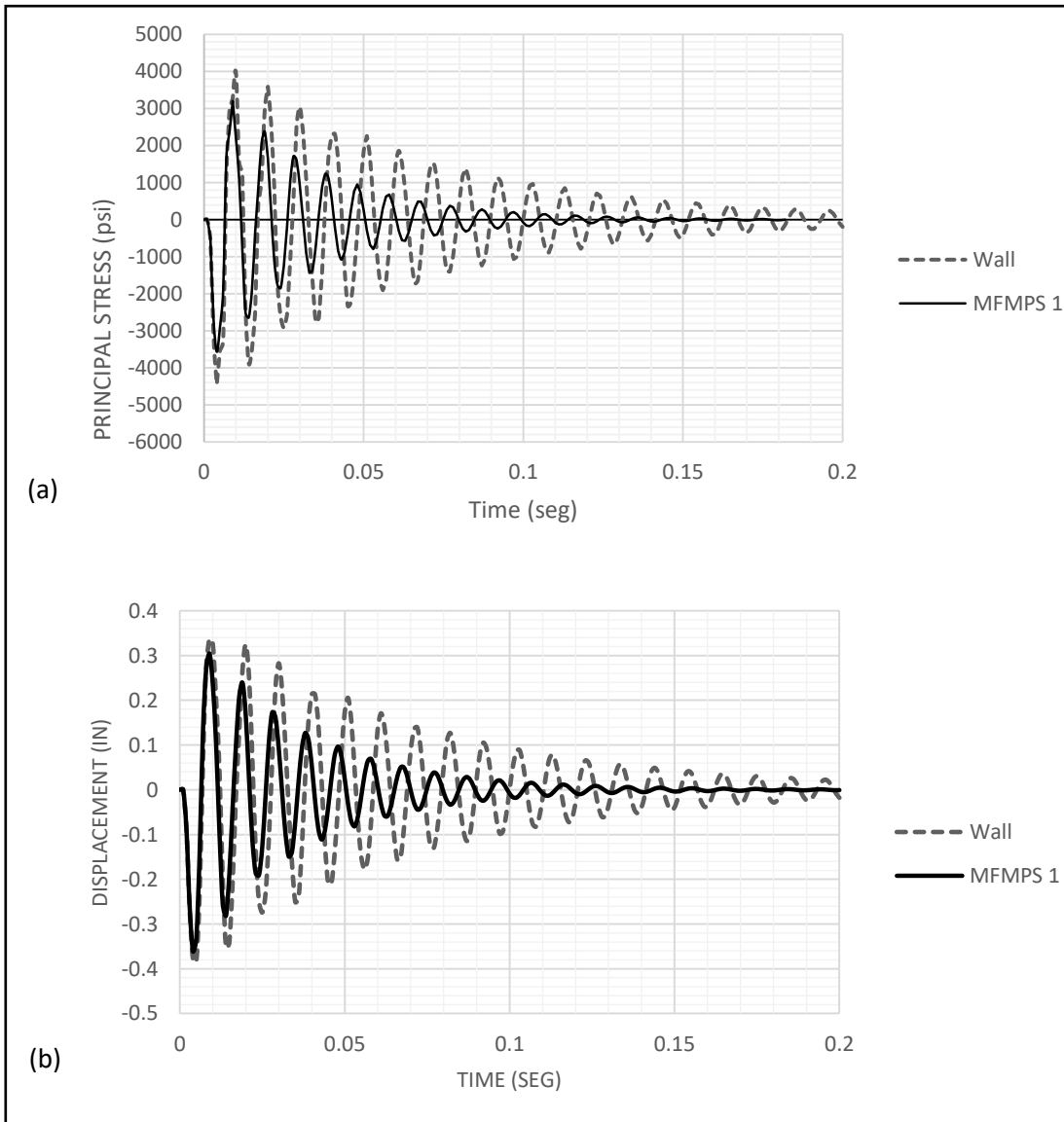


Figure 3.5.3a : Time response of the bare wall and wall with MFMPS 1 due to CONWEP load for a standoff distance of 10 ft and 100 lb of TNT: (a) stress; (b) displacement.

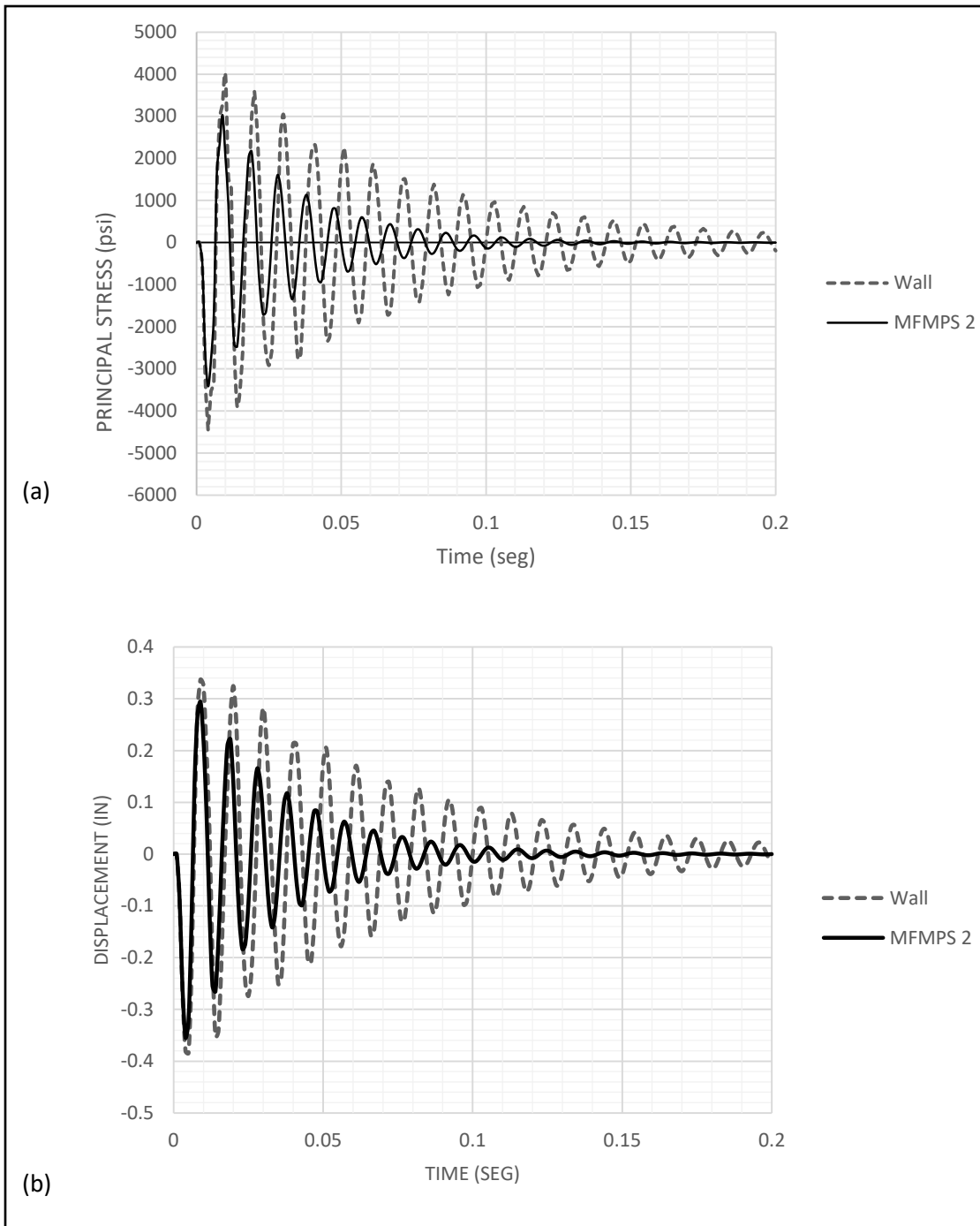


Figure 3.5.3b: Time response of the bare wall and wall with MFMPS 2 due to CONWEP load for a standoff distance of 10 ft and 100 lb of TNT: (a) stress; (b) displacement.

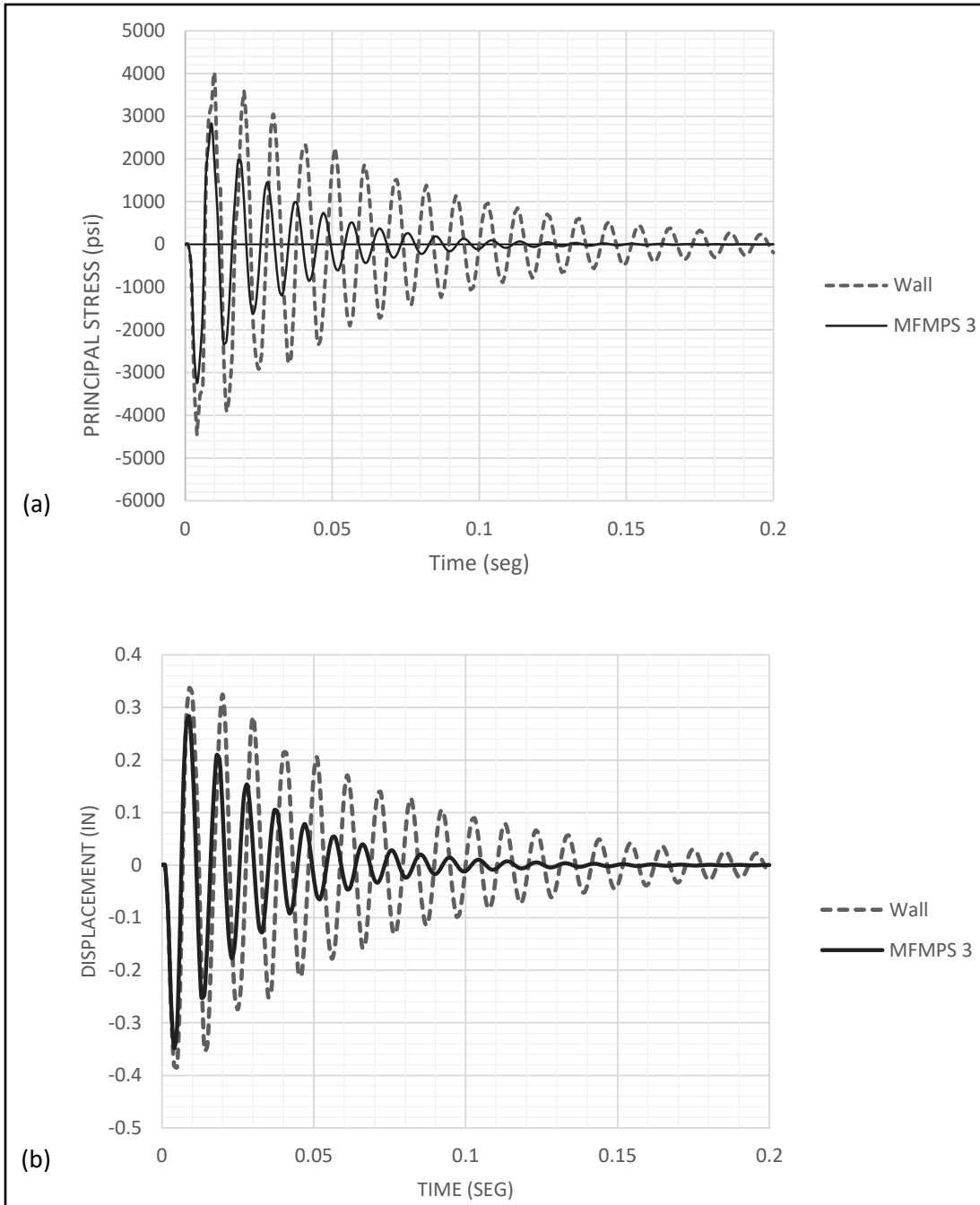


Figure 3.5.3c: Time response of the bare wall and wall with MFMPs 3 due to CONWEP load for a standoff distance of 10 ft and 100 lb of TNT: (a) stress; (b) displacement.

All the standoff distances values given by the DoD in UFC-4-010-01 in Appendix B are greater than 10 ft. The reason for running a case with this standoff distance is to have a critical case for comparing against more conservative ones.

For the second standoff distance case, 20ft is common value presented along in *Table 3.5.1* which is a copy of Table B-1 of the UFC-4-010-01 of the Department of Defense of the U.S. that take in consideration building category, the level of protection, explosive weight, and others.

Table 3.5.1: Standoff distances for new and existing buildings (UFC 4-010-01, 2012)

Distance to:	Building Category	Standoff Distances				
		Applicable Level of Protection	Conventional Construction Standoff Distance		Minimum Standoff Distance ⁽²⁾	Applicable Explosive Weight ⁽³⁾
			Load Bearing Walls ⁽¹⁾	Non-Load Bearing Walls ⁽¹⁾		
Controlled Perimeter or Parking and Roadways without a Controlled Perimeter	Billeting and High Occupancy Family Housing	Low	A	C	20 ft (6 m)	I
	Primary Gathering Building	Low	A	C	20 ft (6 m)	I
	Inhabited Building	Very Low	B	D	20 ft (6 m)	I
Parking and Roadways within a Controlled Perimeter	Billeting and High Occupancy Family Housing	Low	E	G	13 ft (4 m)	II
	Primary Gathering Building	Low	E	G	13 ft (4 m)	II
	Inhabited Building	Very Low	F	H	13 ft 1\ (4 m) /1/	II
Trash Containers	Billeting and High Occupancy Family Housing	Low	E	G	13 ft (4 m)	II
	Primary Gathering Building	Low	E	G	13 ft (4 m)	II
	Inhabited Building	Very Low	F	H	13 ft 1\ (4 m) /1/	II

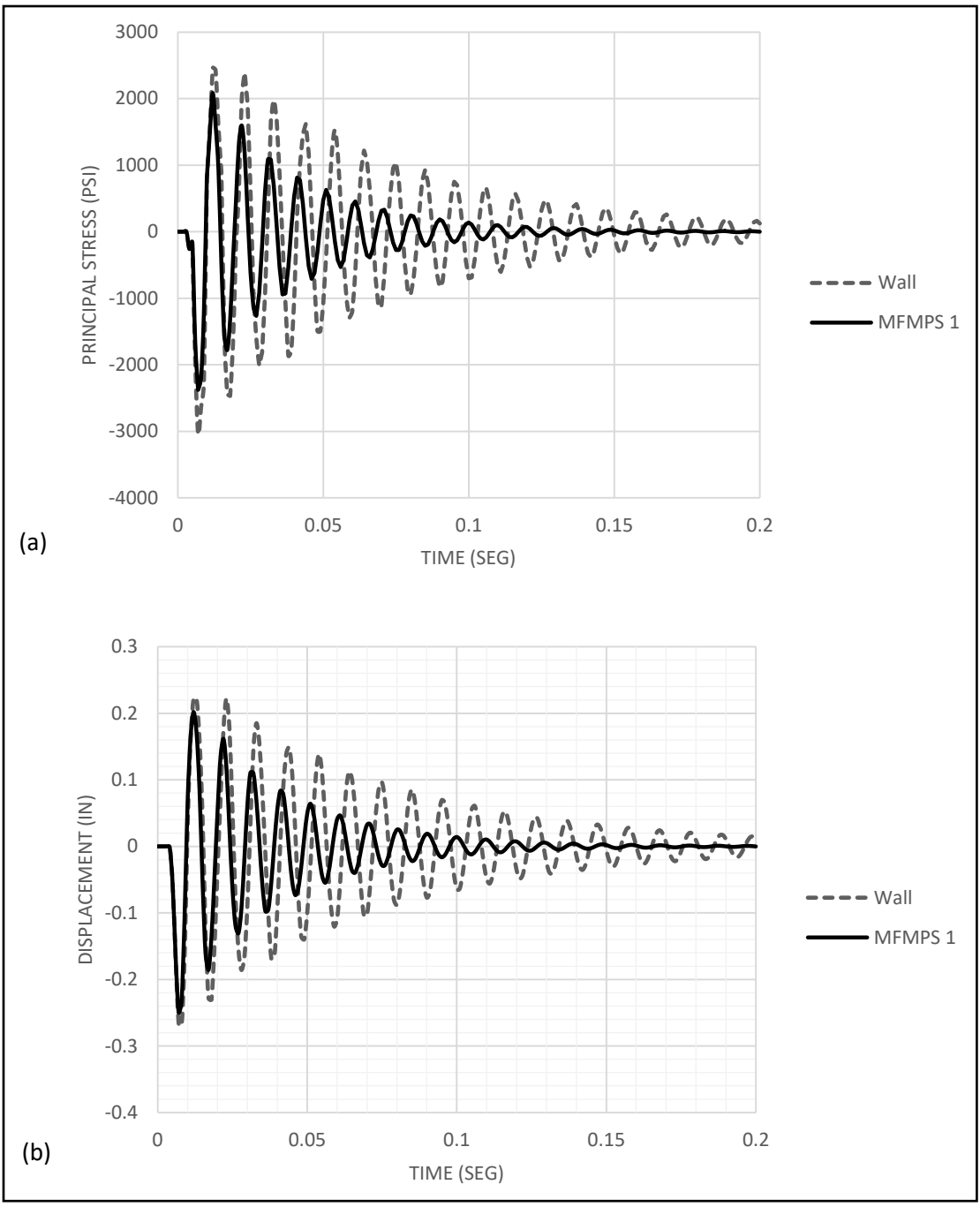


Figure 3.5.4a: Time response of the bare wall and wall with MFMPs 1 due to CONWEP load for a standoff distance of 20 ft and 200 lb of TNT: (a) stress; (b) displacement.

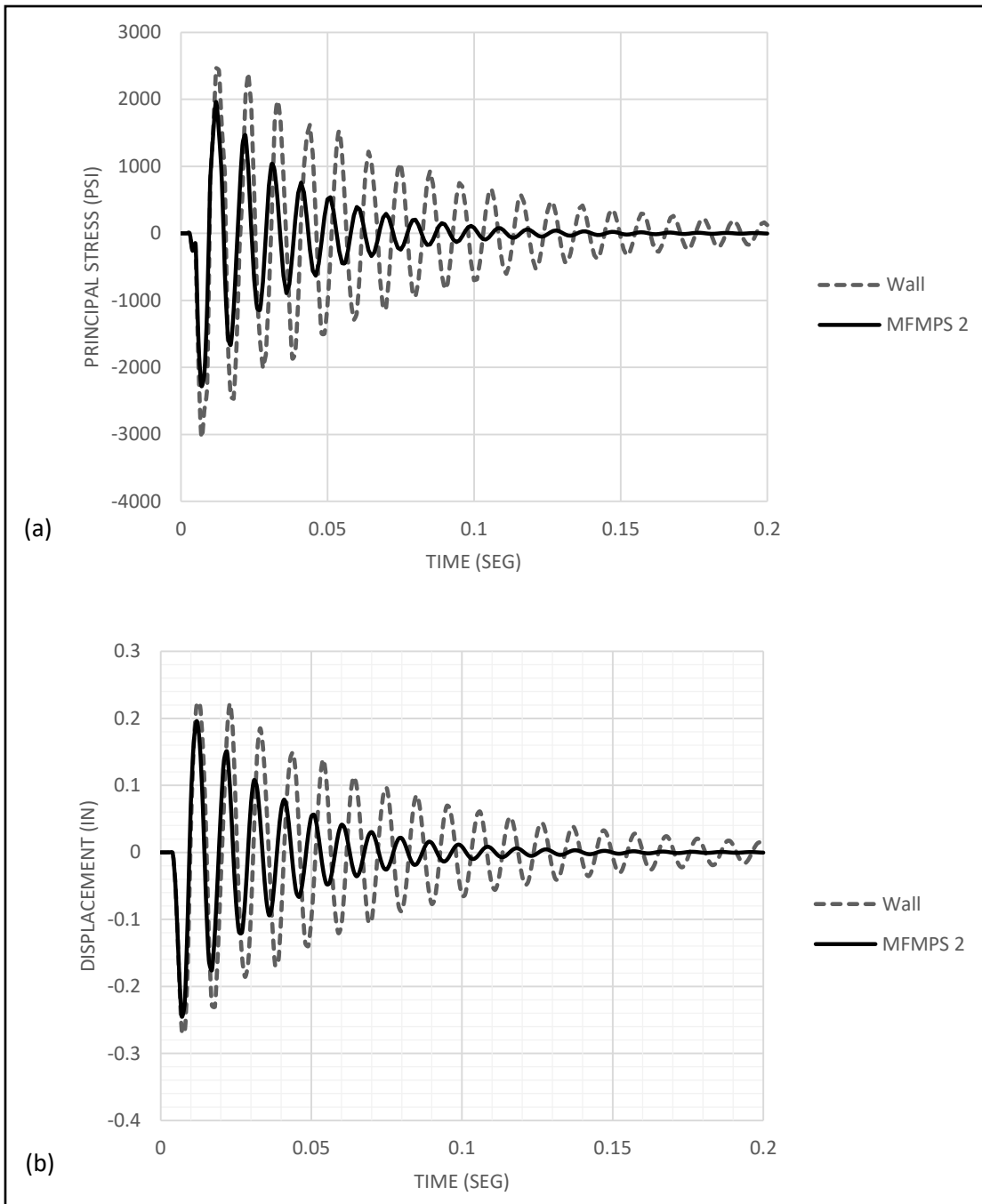


Figure 3.5.4b: Time response of the bare wall and wall with MFMPs 2 due to CONWEP load for a standoff distance of 20 ft and 200 lb of TNT: (a) stress; (b) displacement.

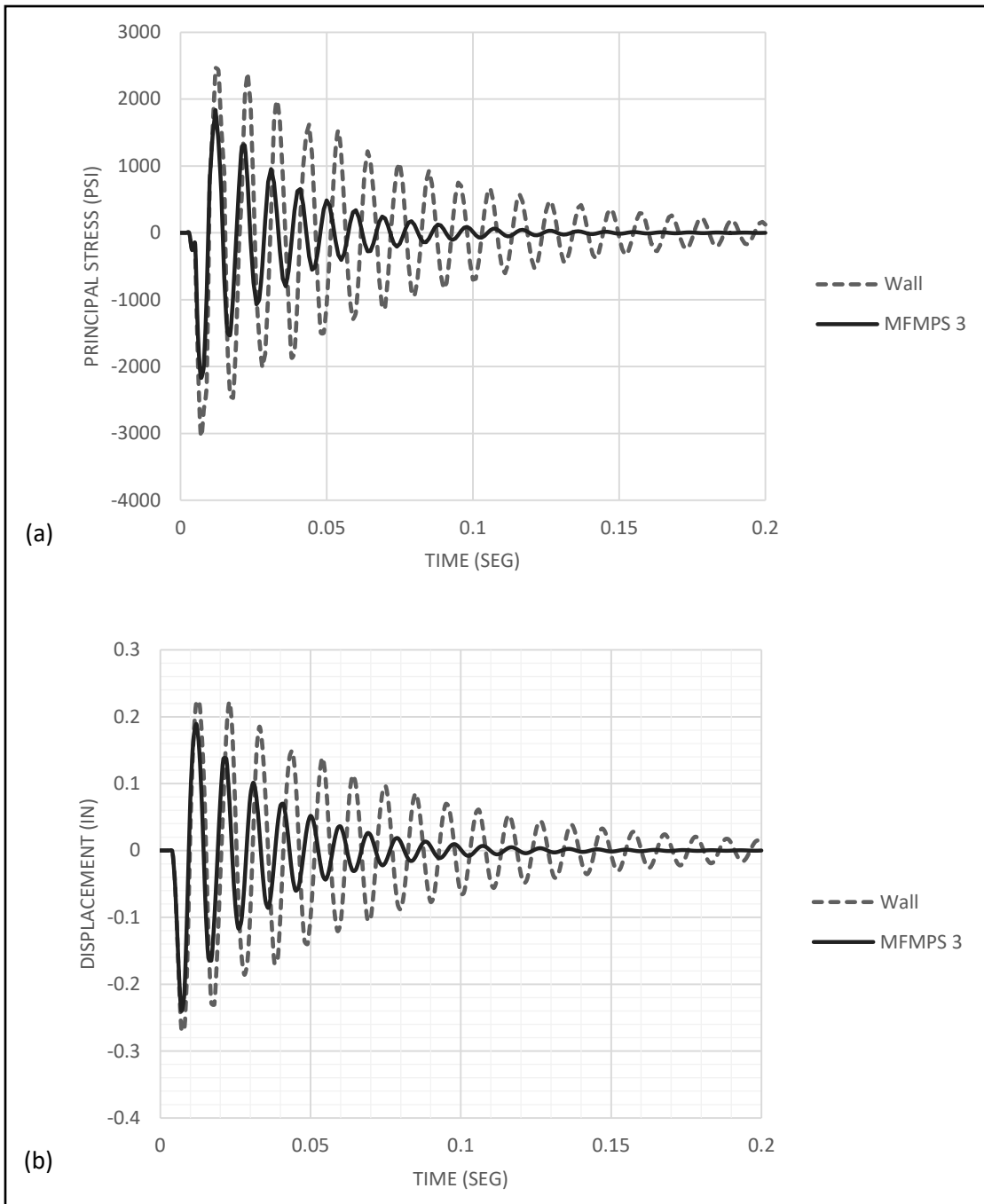


Figure 3.5.4c: Time response of the bare wall and wall with MFMPs 3 due to CONWEP load for a standoff distance of 20 ft and 200 lb of TNT: (a) stress; (b) displacement.

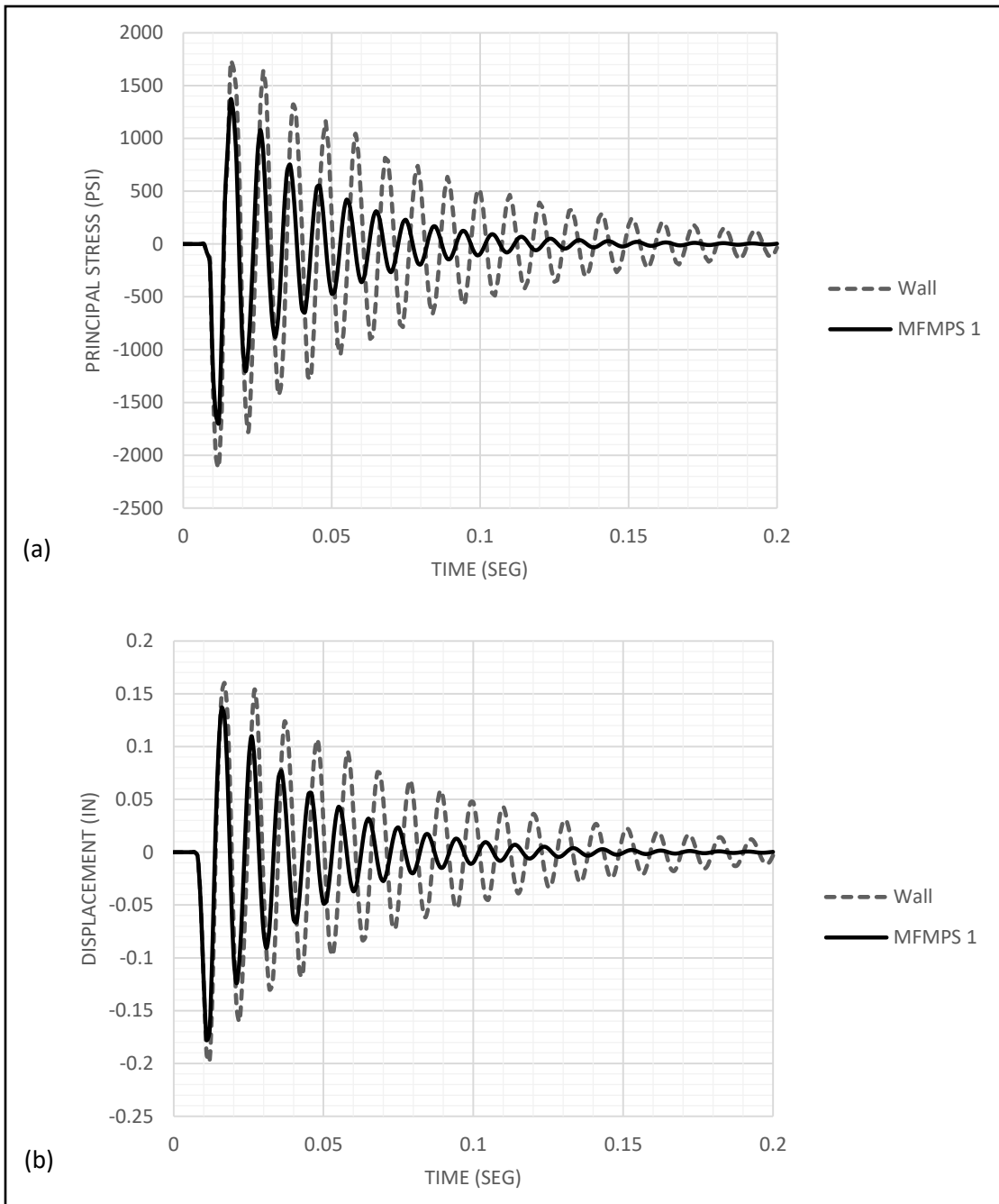


Figure 3.5.5a: Time response of the bare wall and wall with MFMPS 1 due to CONWEP load for a standoff distance of 30 ft and 300 lb of TNT: (a) stress; (b) displacement.

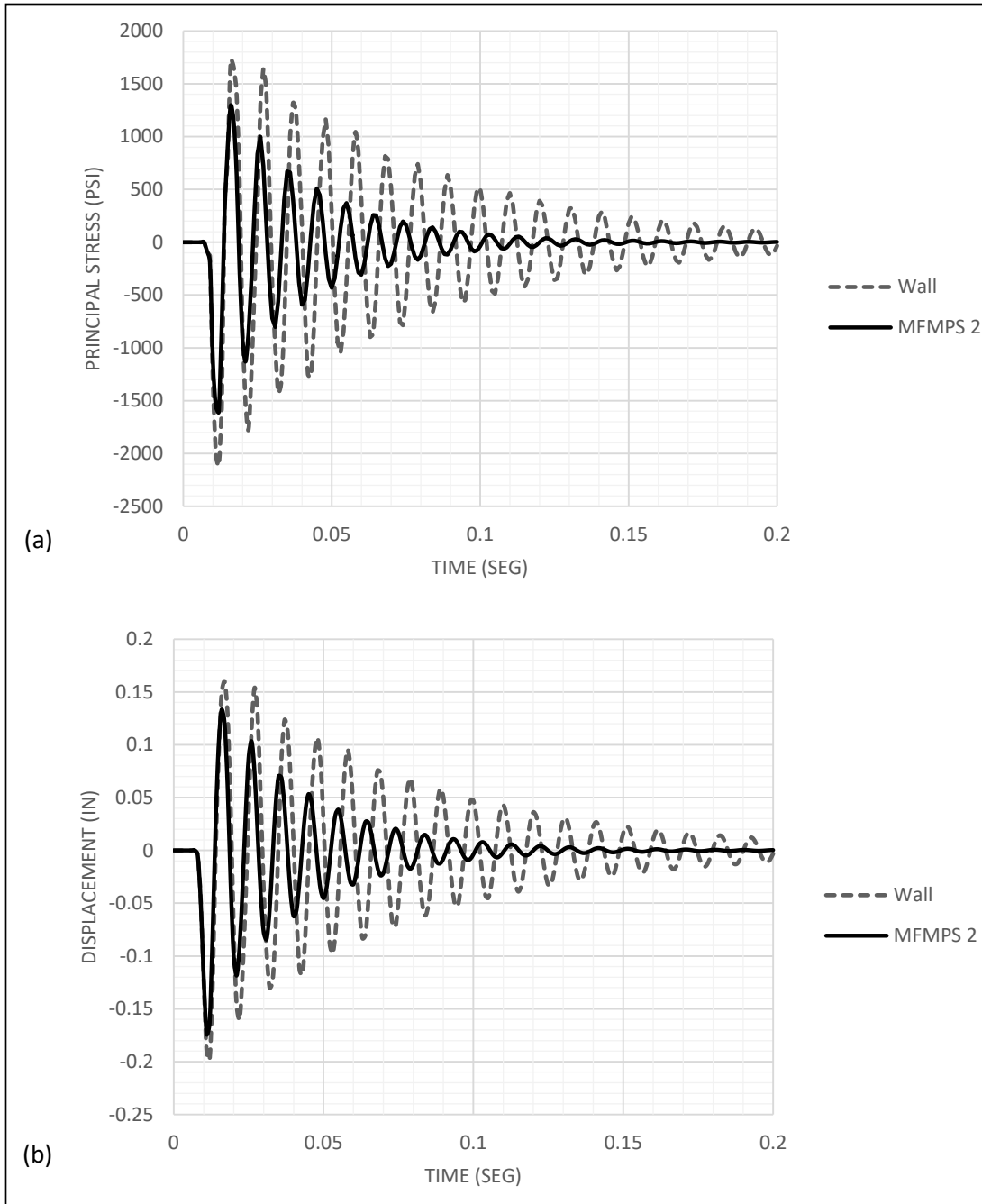


Figure 3.5.5b: Time response of the bare wall and wall with MFMPS 2 due to CONWEP load for a standoff distance of 30 ft and 300 lb of TNT: (a) stress; (b) displacement.

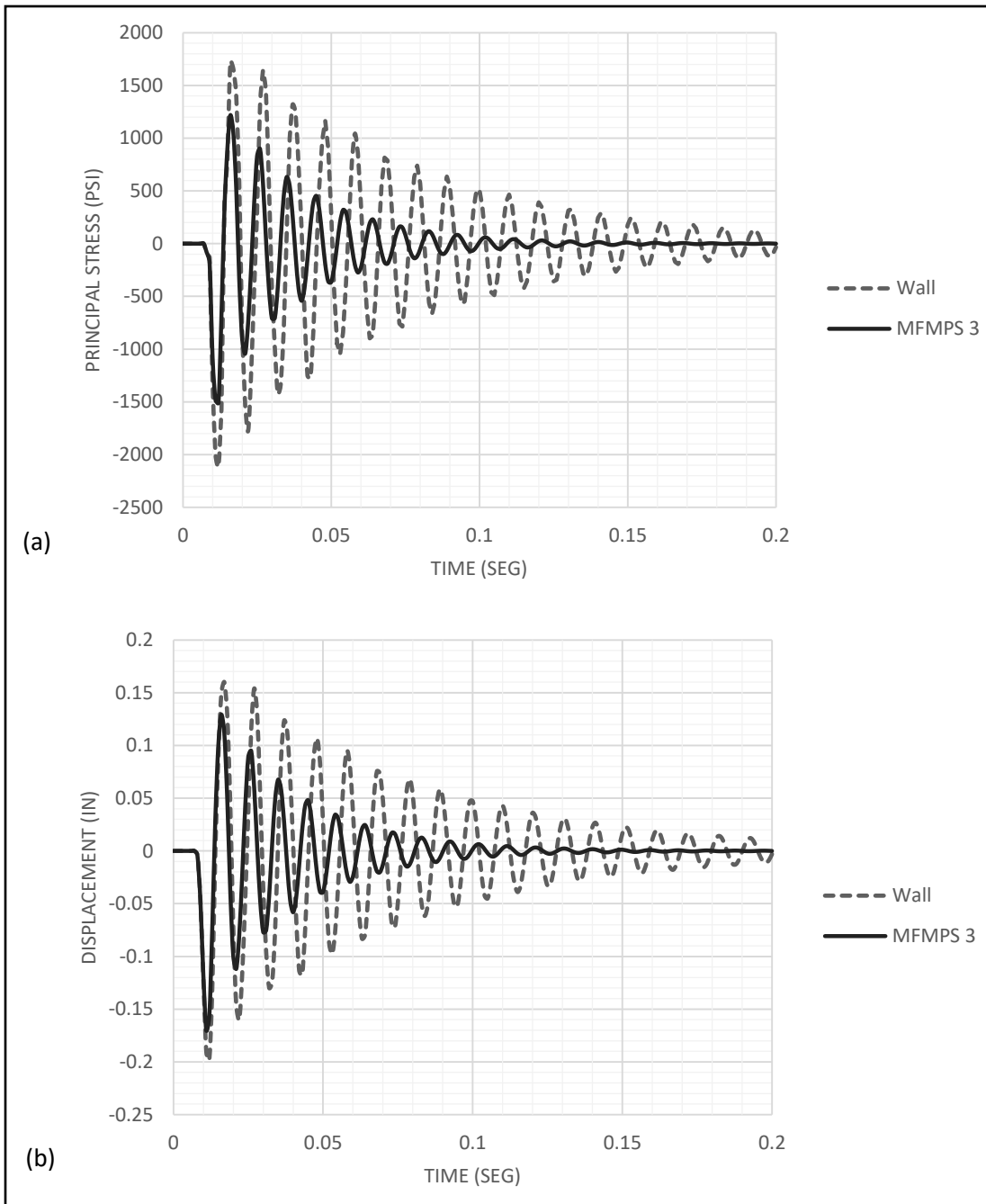


Figure 3.5.5c: Time response of the bare wall and wall with MFMPs 3 due to CONWEP load for a standoff distance of 30 ft and 300 lb of TNT: (a) stress; (b) displacement.

The maximum absolute values of the displacements and normal stresses from the twelve time histories in *Figures 3.5.4 a-c* and *3.5.5 a-c* were retrieved and they are presented in *Tables 3.5.2, 3.5.3* and *3.5.4*. Each table corresponds to a different standoff distance and amount of explosive. The percent improvement in the response attained by the three configurations were calculated with EQ 3.4 and they are displayed in the last two columns of the tables.

Table 3.5.2: Reduction in displacements and stresses achieved by the MFMPS due to the CONWEP load for a standoff distance of 10 ft and 100 lb of TNT.

Model #	U_{\max} (in)	σ_{\max} (psi)	U % reduction	σ % reduction
MFMPS 1 +Wall	0.3612	3565.420	5.966	19.890
MFMPS 2 +Wall	0.3549	3412.270	7.621	23.331
MFMPS3 +Wall	0.3481	3246.650	9.375	27.053
Wall	0.3841	4450.680	-	-

Table 3.5.3: Reduction in displacements and stresses achieved by the MFMPS due to the CONWEP load for a standoff distance of 20 ft and 200 lb of TNT.

Model #	U_{\max} (in)	σ_{\max} (psi)	U % reduction	σ % reduction
MFMPS 1 +Wall	0.2495	2377.500	7.333	21.528
MFMPS 2 +Wall	0.2448	2276.630	9.078	24.857
MFMPS3 +Wall	0.2396	2165.980	11.001	28.510
Wall	0.2692	3029.750	-	-

Table 3.5.4: Reduction in displacements and stresses achieved by the MFMPS due to the CONWEP load for a standoff distance of 30 ft and 300 lb of TNT.

Model #	U_{\max} (in)	σ_{\max} (psi)	U % reduction	σ % reduction
MFMPS 1 +Wall	0.1776	1690.870	10.231	19.925
MFMPS 2 +Wall	0.1741	1605.210	11.980	23.981
MFMPS3 +Wall	0.1703	1509.190	13.935	28.529
Wall	0.1978	2111.600	-	-

It can be seen that the response reduction in the stresses are markedly higher than those for the displacements. In addition, although the performance of the three MFMPs are comparable, the option 3 comes out as the most promising one.

Chapter 4 – Nonlinear Static and Dynamic Analysis of the Wall with the Metallic Foam Multilayer Protection System (MFMPS)

4.1 – Introduction

Nonlinear analysis has been increasing its popularity in the past decades not only because of today's software's computational capacities but also the research and development of new engineering materials. For example, the increase in the resistance of concrete mixtures that surpasses its typical limits made relevant knowing its behavior after passing the failure point all the way to its breaking point. Contrary to linear dynamic analyses, a nonlinear approach can assess the capacity of the material and the structures as a whole more realistically. This is so because for the case of linear analysis, the amount of simplifying assumptions is much greater than for nonlinear cases. While the linear approach considers that the materials can deform infinitely, the nonlinear method uses the failure points of each material due to its inherently mechanical capabilities. However, the fact that to perform a nonlinear dynamic analysis more information is needed about the materials, sections, and other data about the structure makes its application more difficult. Nevertheless, especially to assess as accurately as possible the blast resistant capacity of a structure, it is important to carry out a nonlinear dynamic analysis and this the objective of this chapter.

The models in this chapters use the same parameters, variables and load cases presented in Chapter 3 for the linear elastic analysis of the metallic foams and RC wall system but now their nonlinear behavior is taken into account. To verify the ability of the *Metallic Foam Multilayer Protection Systems* (MFMPS) to protect a structure against explosive loads, it is imperative to simulate the nonlinear behavior because the intensity of this type of loading can be very high in real cases.

Two numerical validations were performed on the Abaqus nonlinear model and they are presented in this chapter. By simulating a pushover analysis (a nonlinear static analysis) the stress-strain constitutive relationship defined in Abaqus with default parameters was obtained and compared with a well-accepted engineering curve. Another pushover analysis was carried out to validate a simplifying assumption dealing with the stress-strain curve adopted for the composite (concrete + steel section). The results were compared with those computed from a more sophisticated but also complicated model that explicitly includes the steel reinforcement grid typically used in two way slabs.

4.2– Numerical validation of the concrete wall nonlinear behavior

To define the constitutive equation for the reinforced concrete in the model of the wall created in Abaqus the default parameters (explained later) are used. However, this requires to independently validate if an acceptable $\sigma - \varepsilon$ curve was adopted. Therefore, a stress-strain curve for concrete that is available in a widely used structural analysis program, namely SAP2000, was selected to perform the validation. *Figure 4.1* shows the engineering stress-strain curve for a typical concrete with f_c' of 4000 psi taken from the database of the computer program SAP2000. The values that conform the curve are presented in *Table 4.1*. A $\sigma - \varepsilon$ curve similar to the one shown in *Figure 4.1* will be obtained indirectly from a simulation performed in Abaqus as discussed in a following section. However, to compare the two constitutive relations, the SAP2000 curve needs to be converted as explained in the next section.

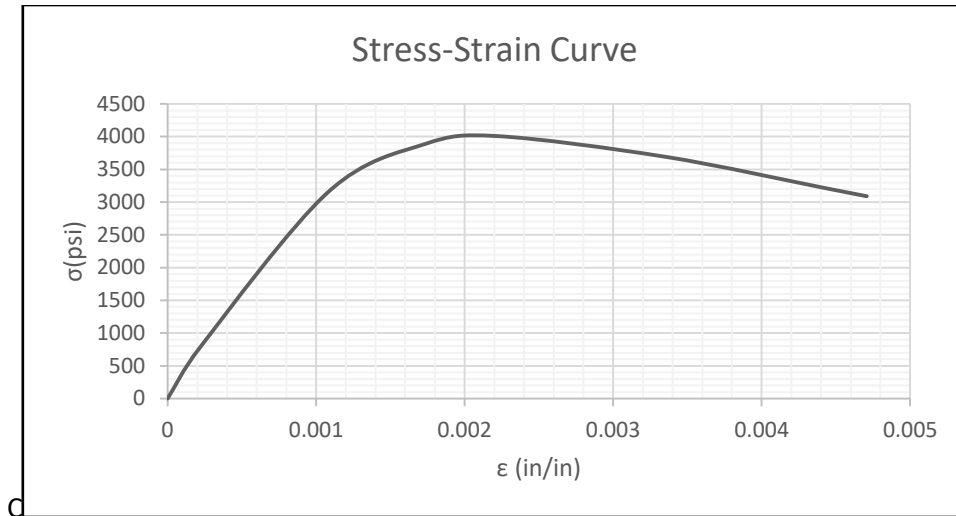


Figure 4.1 : Stress-strain curve for concrete with a capacity of 4000 psi, taken from SAP2000.

Table 4.1: Values of the stress-strain curve for concrete with $f_c' = 4000$ psi.

σ (psi)	ϵ (in/in)
0	0
792.08	0.000222
3153.11	0.001083
3884.42	0.001740
4000.00	0.002219
3680.91	0.003355
3200.00	0.004438
3075.28	0.004719

4.2.1 –Stresses and strains for constitutive relations used in Abaqus

To define their stress-strain curves, Abaqus (as well as other finite element programs) use the values known as “true stresses” and “true strains” instead of the more common engineering parameters. For the sake of completeness, a brief explanation of these concepts is presented next.

The engineering stress σ_{engrg} (also known as the nominal stress) is defined as the load applied in a tensile test P divided by the cross sectional area A_o of the specimen before any deformation took place, i.e.

$$\sigma_{engrg} = \frac{P}{A_o} \quad (4.1)$$

whereas the true stress σ_{true} is, by definition, the quotient between the applied load P and the actual area A at the instant when the load has its value P (i.e., A accounts for the reduction due to the “necking” of the deformed specimen):

$$\sigma_{true} = \frac{P}{A} \quad (4.2)$$

The engineering strain ε_{engrg} is the ratio between the total elongation of the specimen δ and its original length L_o (or more accurately, the gage length):

$$\varepsilon_{engrg} = \frac{\delta}{L_o} \quad (4.3)$$

The true strain ε_{true} , on the other hand, is obtained by adding successive small increments of the strain, which in turn are defined by dividing each increment ΔL by the corresponding value of L :

$$\varepsilon_{true} = \lim_{\Delta L \rightarrow 0} \sum \frac{\Delta L}{L} = \ln \left(\frac{L}{L_o} \right) \quad (4.4)$$

Because of the way it is defined in EQ (4.4), the true strain is sometimes referred to as the “logarithmic strain”. By equating the volume of the specimen before and after deformation one can also express the true strain as:

$$\varepsilon_{true} = \ln \left(\frac{A_o}{A} \right) \quad (4.5)$$

Using the definition of in EQ (4.4), one can write ε_{true} as:

$$\varepsilon_{true} = \ln\left(\frac{L}{L_o}\right) = \ln\left(\frac{L_o + \delta}{L_o}\right) = \ln\left(1 + \frac{\delta}{L_o}\right) \quad (4.6)$$

And therefore, considering the definition of ε_{engrg} in EQ (4.3), the relationship between the two strains is:

$$\varepsilon_{true} = \ln(1 + \varepsilon_{engrg}) \quad (4.7)$$

A relationship between the two normal stresses can be obtained by first dividing EQ (4.1) and EQ (4.2):

$$\frac{\sigma_{true}}{\sigma_{engrg}} = \frac{A_o}{A} \quad (4.8)$$

and then equating EQ (4.5) and EQ (4.7) to obtain:

$$\ln\left(\frac{A_o}{A}\right) = \ln(1 + \varepsilon_{engrg}) \Rightarrow \frac{A_o}{A} = (1 + \varepsilon_{engrg}) \quad (4.9)$$

Substituting this result in EQ (4.8), the relationship between the two stresses becomes:

$$\sigma_{true} = \sigma_{engrg} (1 + \varepsilon_{engrg}) \quad (4.10)$$

In addition, Abaqus defines a true (or logarithmic) plastic strain as follows:

$$\varepsilon_{true_plastic} = \varepsilon_{true} - \varepsilon_{true_elastic} \quad (4.11)$$

where the true elastic strain $\varepsilon_{true_elastic}$ is defined as

$$\varepsilon_{true_elastic} = \frac{\sigma_{true}}{E} \quad (4.12)$$

and E is the Young's modulus of the material. Abaqus requires that material data for should be given in these true measures. Therefore, if the user has nominal stress-strain data obtained from a uniaxial test and the material is isotropic, they must be converted to true stress and logarithmic plastic strain using the formulation presented above.

The true stresses and strains as well as the true elastic and plastic strains are obtained from the engineering values using EQ (4.7), (4.10), (4.11) and (4.12). The results shown in *Table 4.2* were calculated based on the engineering values presented in *Table 4.1*.

Table 4.2: True stresses and strains calculated from the engineering values.

Engrg. stress (psi)	ϵ	True stress (psi)	True strain	True elastic strain	True plastic strain
0.00E+00	0.00E+00	0.00E+00	0.00E+00	0.00E+00	0.00E+00
7.92E+02	2.22E-04	7.92E+02	2.22E-04	2.22E-04	-7.39E-08
3.15E+03	1.08E-03	3.16E+03	1.08E-03	8.85E-04	1.98E-04
3.88E+03	1.74E-03	3.89E+03	1.74E-03	1.09E-03	6.48E-04
4.00E+03	2.22E-03	4.01E+03	2.22E-03	1.12E-03	1.09E-03
3.68E+03	3.36E-03	3.69E+03	3.35E-03	1.04E-03	2.31E-03
3.20E+03	4.44E-03	3.21E+03	4.43E-03	9.01E-04	3.53E-03
3.08E+03	4.72E-03	3.09E+03	4.71E-03	8.66E-04	3.84E-03

Abaqus/Explicit has two different constitutive models for the analysis of plain and reinforced concrete structures (Abaqus 6.12, 2012). They are the “*brittle cracking model*” and the “*concrete damaged plasticity model*”. Each model is designed to provide a general capability for modeling plain and reinforced concrete (as well as other similar quasi-brittle materials) in all types of structures. The brittle cracking model is intended for applications in which the concrete behavior is dominated by tensile cracking and compressive failure is not important. The model assumes elastic behavior when deformed in compression.

The other constitutive model for concrete, known as the concrete damaged plasticity is based on the assumption of scalar (isotropic) damaged elasticity in combination with isotropic tensile and compressive plasticity to represent the inelastic behavior of concrete. It is intended for applications in which the concrete is subjected to more arbitrary loading conditions, including cyclic and dynamic loading. The model takes into consideration the degradation of the elastic stiffness induced by plastic straining both in tension and compression.

A description of the concrete damaged plasticity model implemented in Abaqus is well beyond the scope of this thesis. It uses a sophisticated plastic model as described by Sammarco and Matamoros (2010). Five plastic parameters are required to completely define the damage plastic model. They are: the dilation angle (ψ), flow potential eccentricity (ϵ), ratio of initial equibiaxial compressive yield stress to initial uniaxial compressive yield stress (σ_{b0}/σ_{c0}), ratio of the second invariant on the tensile meridian (K_c) and the viscosity parameter (μ). The dilation angles vary from 0 to 35° (25° for this case) but for the other four factors there is a default value assigned to each of them. These default values, which were the ones adopted for the analysis, are displayed in *Figure 4.2a*.

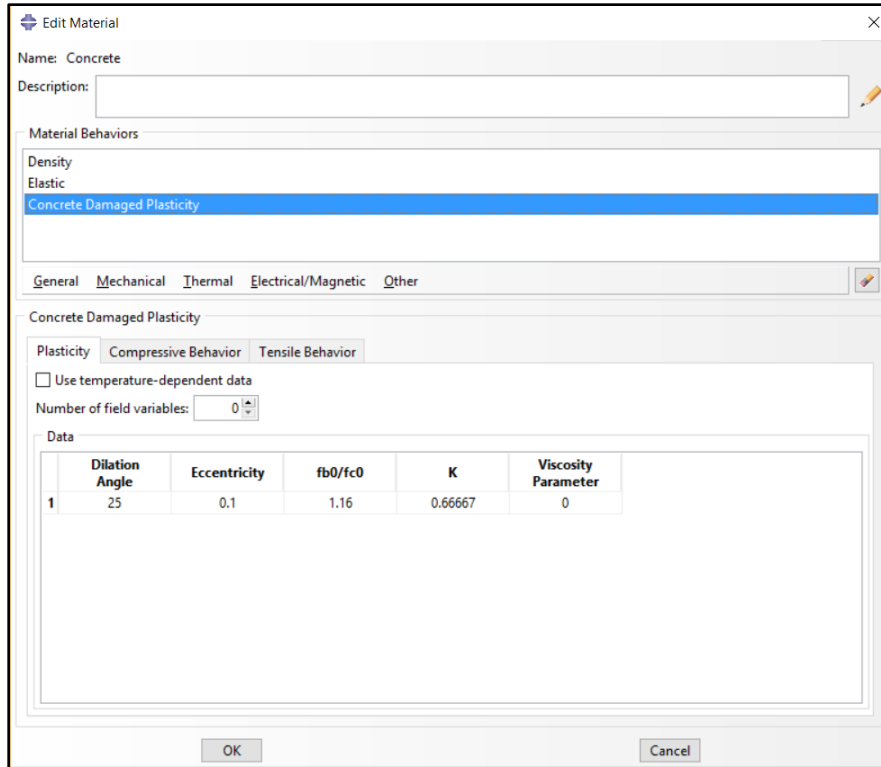


Figure 4.2a : Abaqus 6.14-4 input window for concrete damage plasticity parameters.

The next step required by Abaqus to define the nonlinear constitutive equation for the concrete is to provide the true yielding stress and true plastic strain. The window to enter the compressive and tensile behavior properties is shown in *Figure 4.2b*. Note that the value assigned to the inelastic (or plastic) strain is zero because this is not the total plastic strain, i.e. it is rather defined according to equation (4.11). Even though the behavior of concrete is greater in compression than in tension, the same values for both were used to take into account the benefits of having reinforcement in the concrete wall.

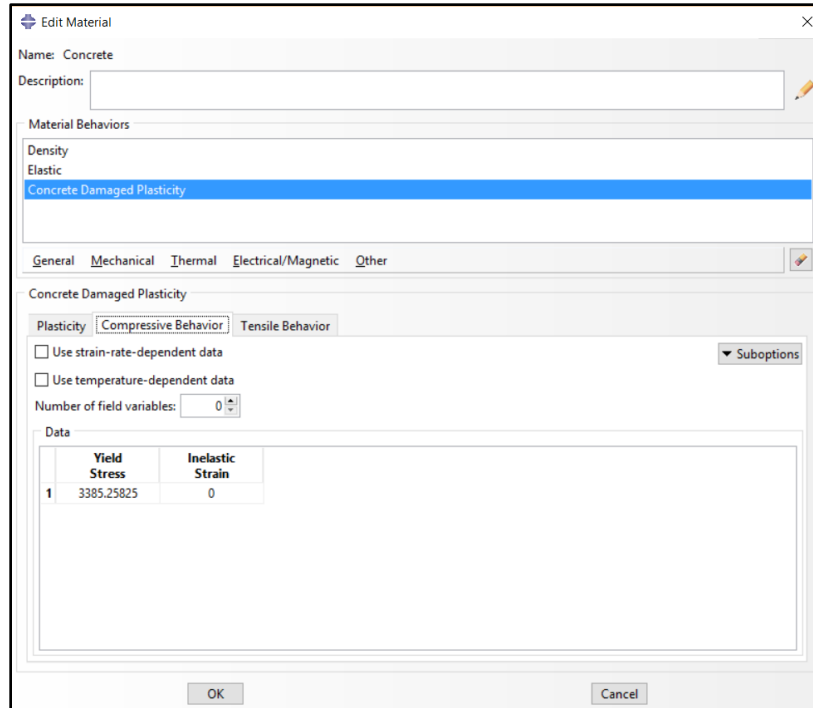


Figure 4.2b: Information about compressive and tensile behavior of the concrete material in Abaqus 6.14-4.

4.2.2 – Pushover analysis to validate the constitutive relations

When a stress-strain curve is developed for any material, a load is applied to a specimen of the material increasing its value in small increments with the purpose of creating enough points to define the σ - ϵ curve. A pushover analysis works in a similar way. When performing a pushover analysis in a building structure, a single load is applied at the top of the building or a distributed load with a selected pattern is applied along its height. This concept can be extended to other structures such as a column or a wall clamped at its bottom. By slowly increasing the value of the load applied at the free end of the structure just like in a real laboratory test, a stress-strain curve can be obtained from this process. A uniformly distributed load was applied at the free end of a cantilever model of the concrete wall as shown in *Figure 4.3*. Abaqus defines the force as a surface traction (i.e. in units of stresses); its value was increased up to a 100 psi in small increments. For a wall thickness of 10 inches, the uniformly

distributed force is 1 kip/inch. It should be mentioned that in other computer programs more specifically oriented towards civil engineering structures (such as SAP2000), the pushover analysis is done automatically; in Abaqus it required to implement the process herein described.

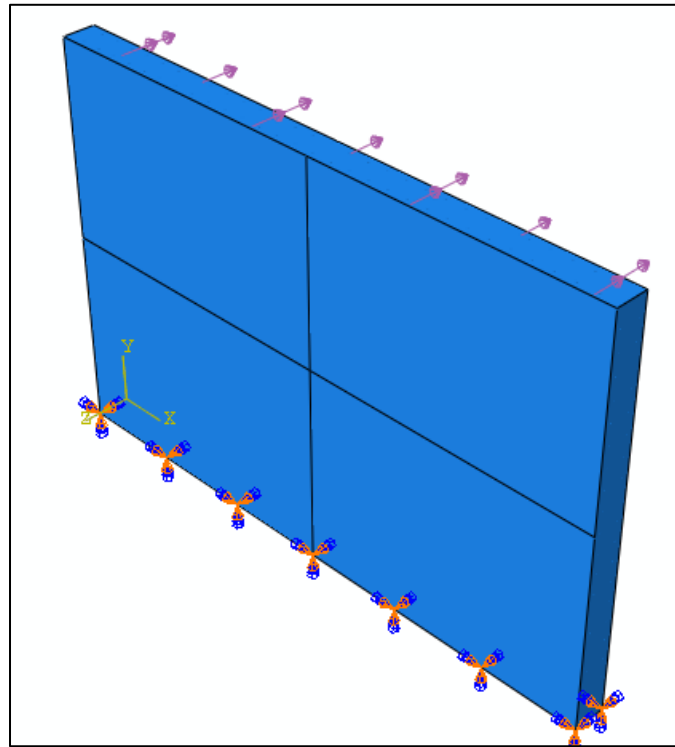


Figure 4.3: Pushover load of 1 kip/inch applied to the wall in Abaqus.

From the output provided by Abaqus as a result of the simulated pushover analysis, the bending stresses and strains at an element near the bottom of the wall and at the middle of the width were retrieved. The typical curve obtained from the SAP2000 library and the one calculated from the pushover analysis are compared in *Figure 4.4*.

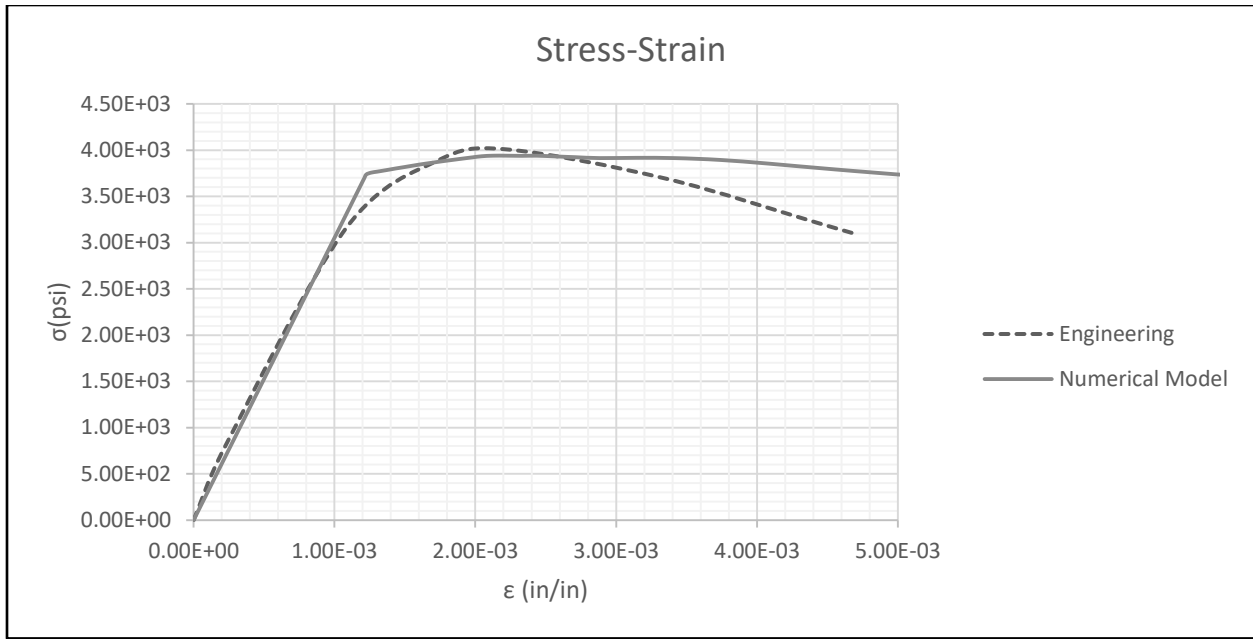


Figure 4.4: Comparison of stress-strain curves obtained from the pushover simulation and engineering data from SAP2000.

Examining Figure 4.4 it is evident that even though the two curves are not the same, they follow a similar pattern. Both initially increase in a linear fashion with a slope equal to the modulus E and after reaching the yielding point, the curve from the engineering data has an approximate quadratic form whereas the stress-strain calculated with the pushover analysis remains approximately constant after yielding. The error at the yielding point is only 0.01%. It is reasonable to conclude that the constitutive equation defined in Abaqus for its concrete damaged plasticity model with the default values yields realistic results and it can be used for the subsequent nonlinear analyses.

4.2.3 – Concrete wall with and without explicit modeling of the reinforcement

It is well known that the main reason for adding steel reinforcement to a concrete structure is to give it confinement and increase the small tension capacity of the material. Taking this aspect into consideration, the numerical model of the RC wall was assumed to have the same capacity in both tension and compression. In order to validate this important assumption, a special numerical model of

the RC wall was developed in Abaqus in which the steel reinforcement was explicitly included. Two grids of steel A36 rebars #4 evenly spaced at 6 inches were embedded into the concrete wall. *Figure 4.5a* displays the detailed geometry of each of the grids. *Figure 4.5b* shows a 3-D view of one of the steel grids: the two grids are separated by 6 inches and are placed 2 inches away from the external faces of the wall.

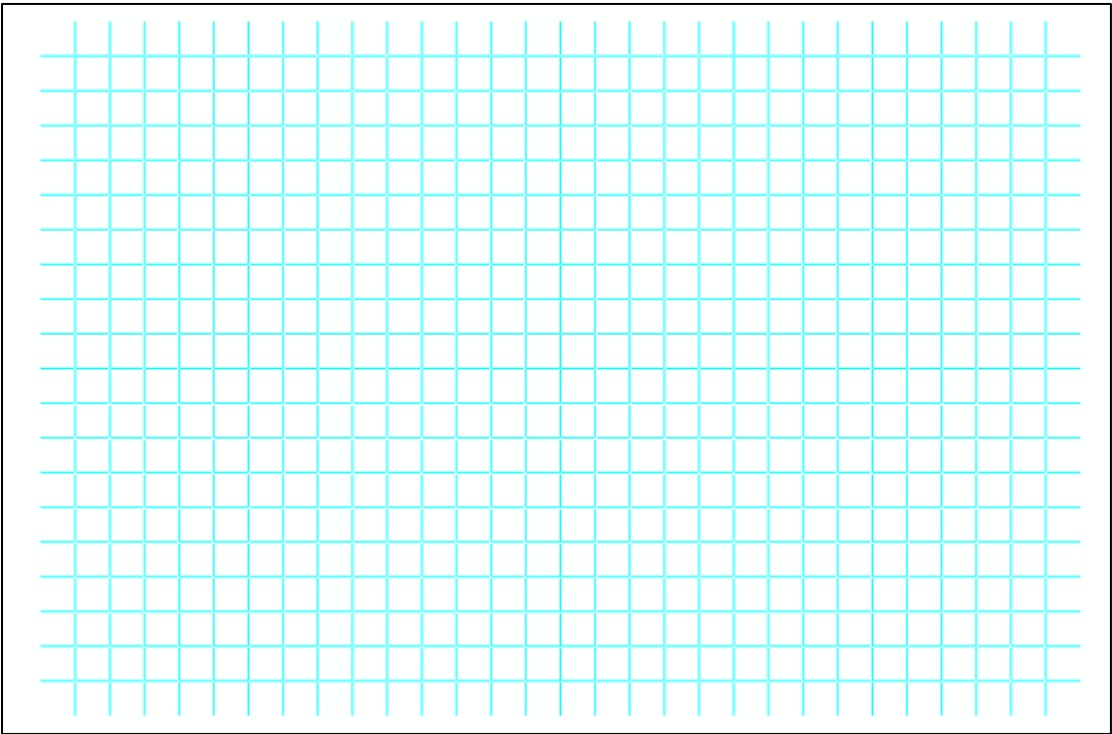


Figure 4.5a: Configuration of the A36 #4@6” reinforcement grid.

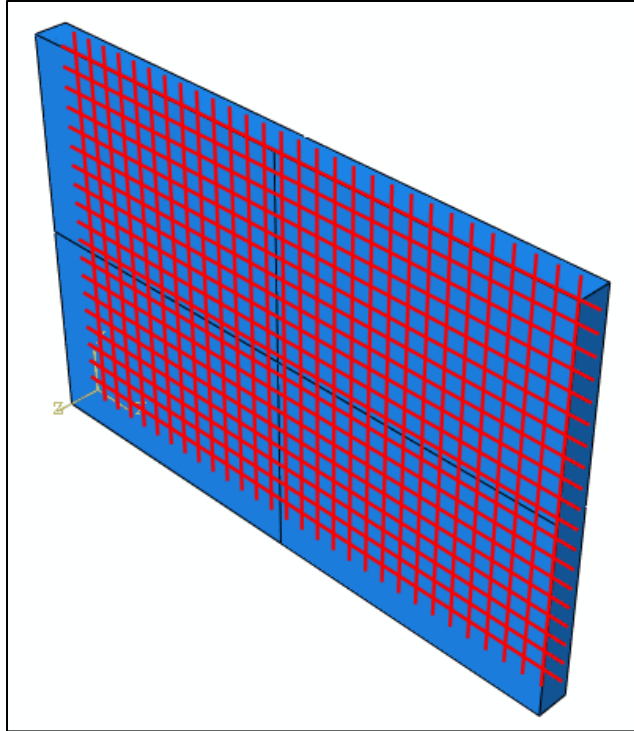


Figure 4.5b: Steel reinforcement mesh embedded on the concrete wall

Following the procedure described in Section 4.2.2 and applying a distributed load at the top of the wall (as illustrated in *Figure 4.3*) the simulation of a pushover analysis was carried out using two different models to account for the reinforced concrete. In one of the finite element models of the RC wall, a concrete material with the same capacity in tension and compression was used to compensate for the lack of reinforcement in the model. The other model had a tension capacity of 10% of its compression capacity but it had two embedded A36 steel reinforcement grids to increase its resistance in tension; this case simulates the way how RC walls are constructed in real life. As it was done in the previous simulation of the pushover in Section 4.2.2, the bending stresses and strains at an element at the bottom of the wall were recovered from the Abaqus output. They were used to prepare one of the two graphs shown in *Figure 4.6* The other curve in *Figure 4.6* was obtained with the simplified model that used the assumption that the constitutive relationship is equal in tension than in compression.

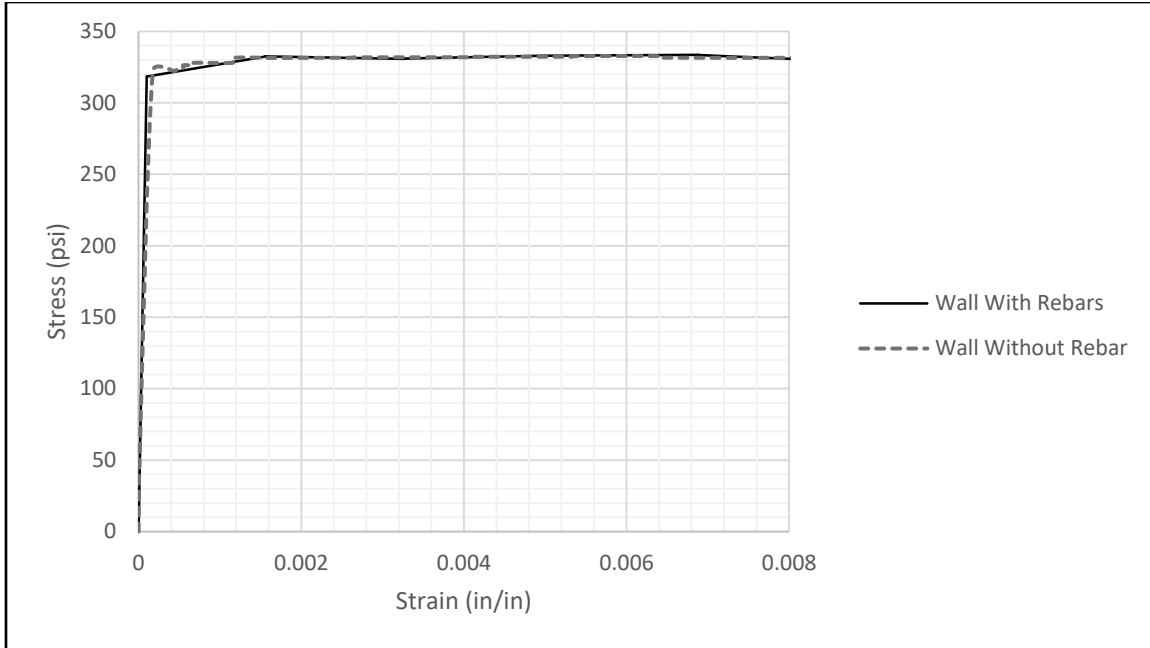


Figure 4.6: Stress-strain curves obtained from the pushover analyses for the models of the wall with and without reinforcement grids.

After evaluating the two curves displayed in *Figure 4.6* and obtained with both models, it is fair to conclude that the simplification done by assigning to the concrete of the wall the same capacity in tension as in compression is validated and it can be used for the rest of the nonlinear analyses. This assumption has two benefits: it can significantly reduce the computational time required to run the numerous nonlinear dynamic analyses, and it can help to avoid converge problems that showed up when the model with the embedded steel grid was used for time history analyses.

It must be pointed out that the numerical validation described was made exclusively for the concrete wall and not for the MFMPS. This is so because the reinforced concrete of the wall is a composite material formed with two materials with different properties. On the other hand, the aluminum alloy in the restraining plates can be regarded as a homogenous material with the same capacity in tension and in compression. Regarding the aluminum metallic foams, because it is a relatively new material that it is still under development, the amount of data of the properties is not

profuse. In spite of that, since the matrix of the foam is metallic, it is reasonable to think that its mechanical properties in compression and tension should be similar. Nevertheless, this is a topic that requires further investigation as the development of these materials continues and more data becomes available.

4.3 – Nonlinear response due to a static pressure

Even though the pressure generated by a blast is a quintessential dynamic load, examining the nonlinear response of the RC wall to a static pressure can provide a first insight into the behavior of the protection system due to impulse loads. In addition of providing a better grasp of the problem, it also serves as a comparison between the linear analysis (Chapter 3) and the nonlinear analysis. *Figure 4.7* illustrates the static pressure that was applied to the nonlinear models of the bare RC wall and the wall with the proposed metallic foam layers. To simulate a static load application, the pressure was increased until it reached its final value of 140 psi after 0.2 seconds. Because this final time is much higher than the fundamental natural period of the wall, it can be considered as a slowly applied load.

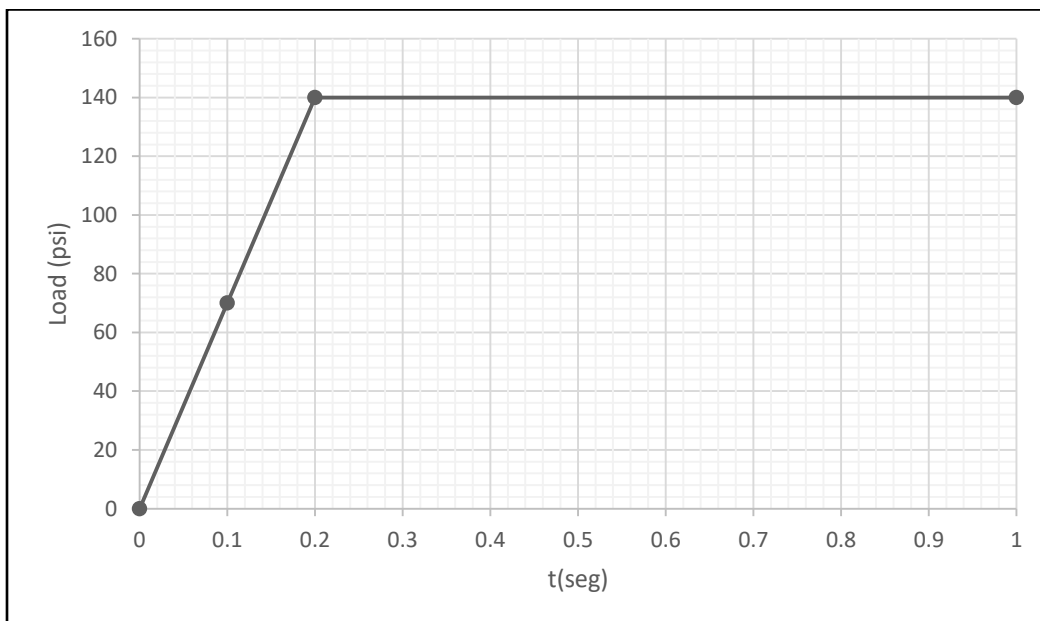


Figure 4.7: Static pressure application.

The same parameters used for the analysis presented in Chapter 3 were applied to calculate the displacement at the center of the wall and the bending stress at the middle of the top edge. The maximum stresses are presented in Figures 4.8a through 4.8c. The maximum displacements are shown in Figures 4.9a through 4.9.

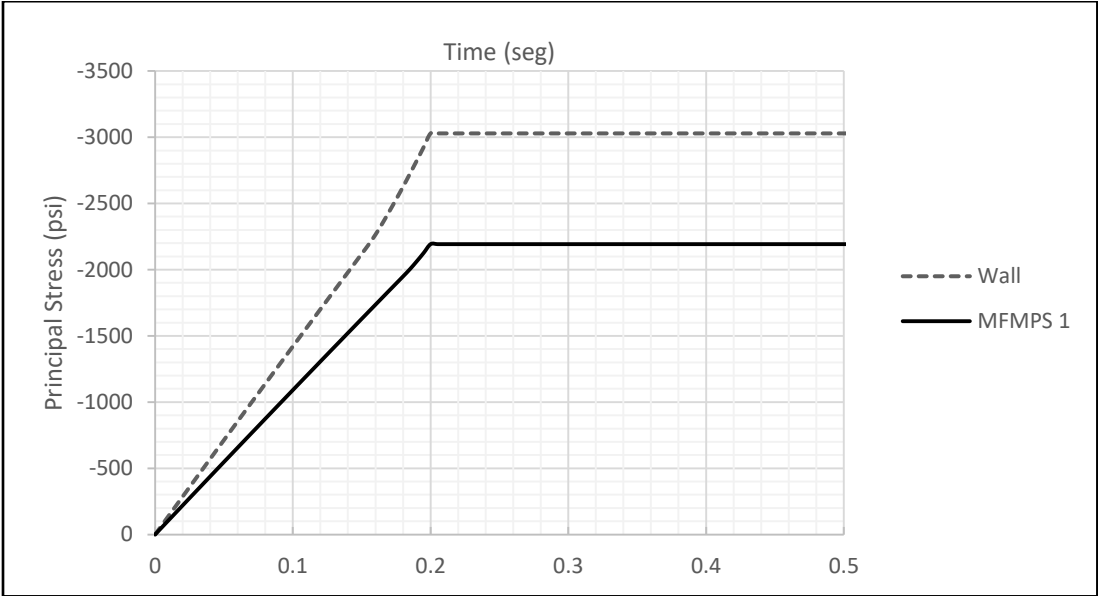


Figure 4.8a: Nonlinear static stresses in the wall with MFMPs 1 and bare wall.

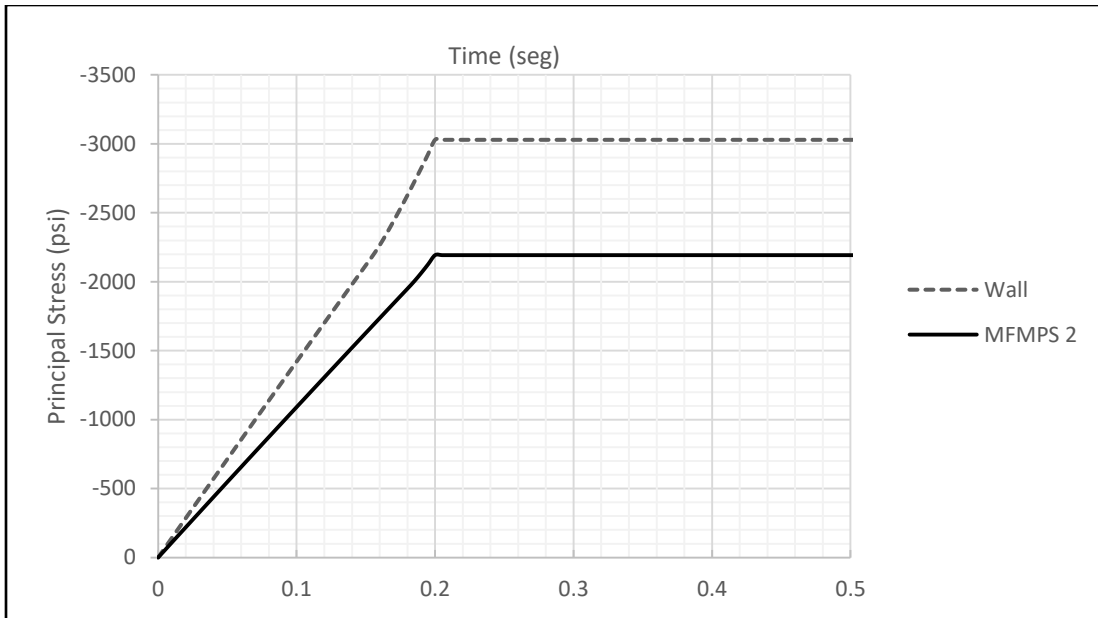


Figure 4.8b: Nonlinear static stresses in the wall with MFMPS 2 and bare wall.

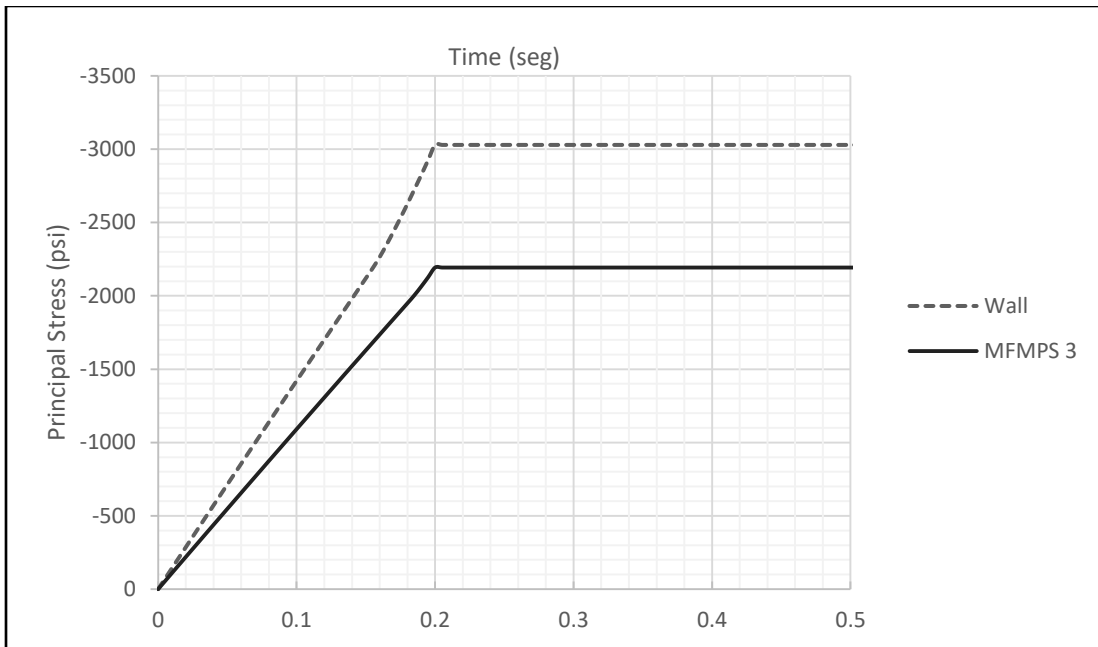


Figure 4.8c: Nonlinear static stresses in the wall with MFMPS 3 and bare wall.

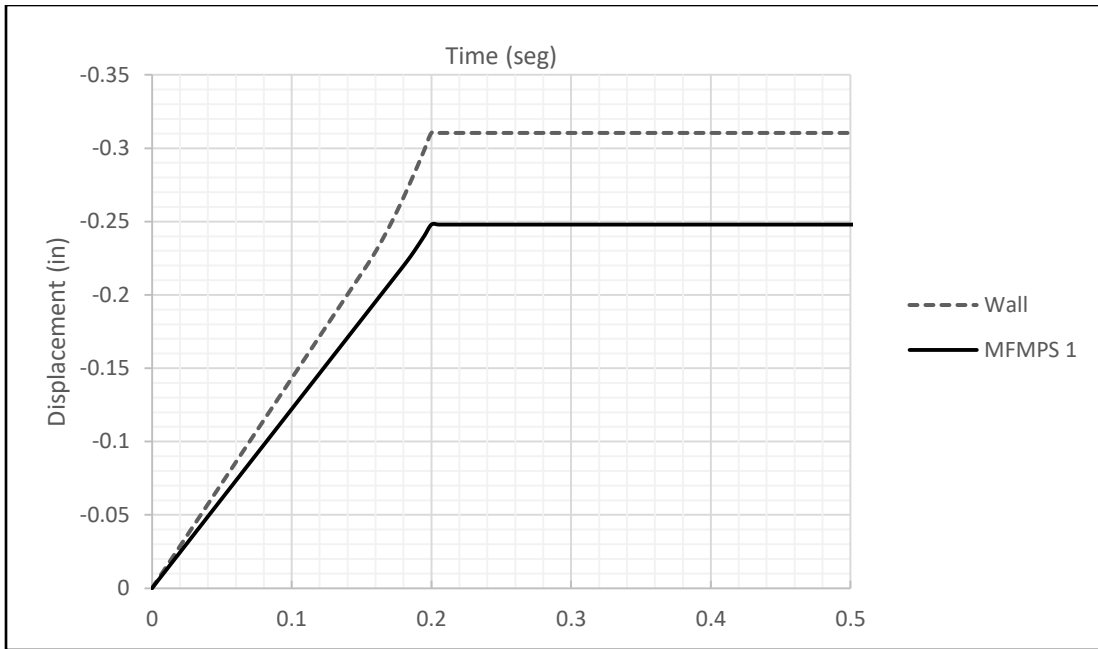


Figure 4.9a: Nonlinear static displacement in the wall with MFMPs 1 and bare wall.

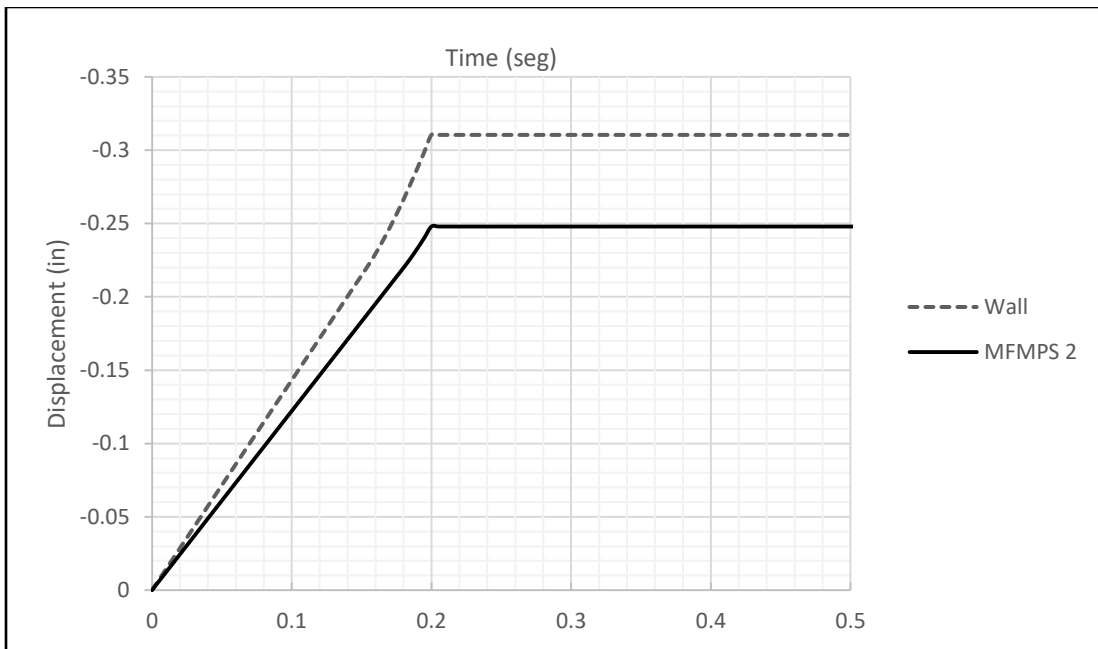


Figure 4.9b: Nonlinear static displacement in the wall with MFMPs 2 and bare wall.

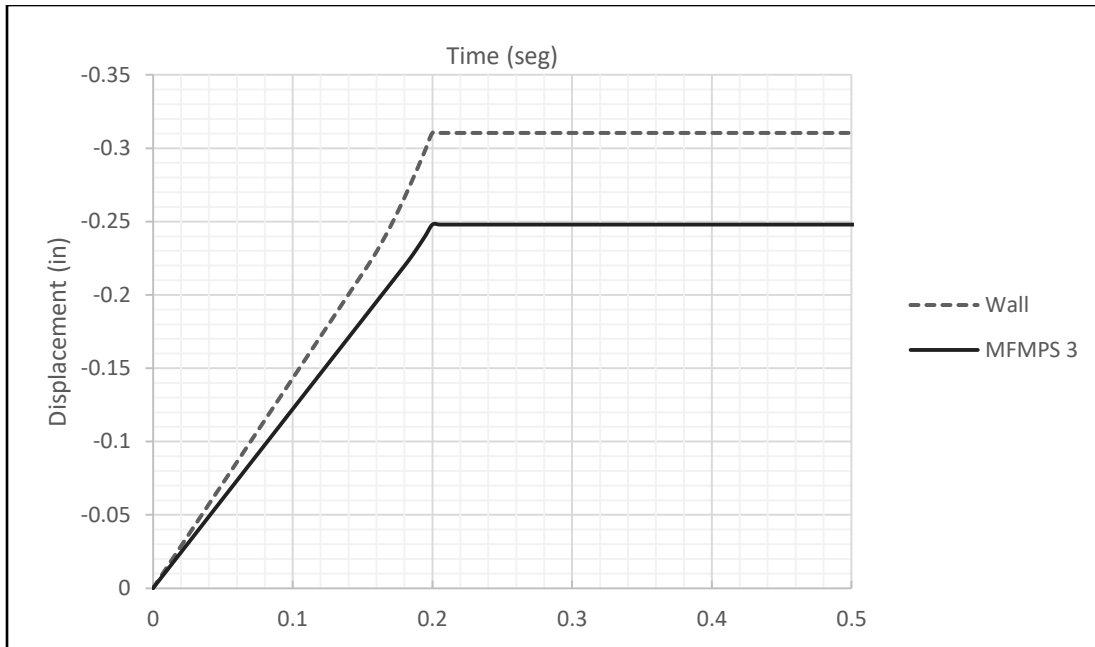


Figure 4.9c: Nonlinear static displacement in the wall with MFMPS 3 and bare wall.

The maximum values of the stresses and displacements for each MFMPS-wall system and for the bare wall are shown in Table 4.3.

Table 4.3: Displacements and stresses in the wall with and without MFMPS for the nonlinear static load case.

Model	Max. displ. (in)	Max. stress (psi)	U % reduction	σ % reduction
MFMPS 1 + Wall	0.248	2192.790	20.127	27.608
MFMPS 2 + Wall	0.248	2192.790	20.127	27.608
MFMPS3 + Wall	0.248	2192.790	20.127	27.608
Wall	0.310	3029.030	-	-

4.4 – Nonlinear response due to the impulsive pressure

The ability to accurately predict the response of RC structure to blast-induced pressure loads is vital to develop retrofitting techniques or other nonstructural protective measures. However, this problem poses a challenge because for a realistic simulation it is necessary to let the material move into the nonlinear range. Even for a relatively simple model such as the reinforced concrete wall clamped on

all sides considered in this project, the amount of time to run the analyses was considerable. Because of the very short duration and high intensity nature of the dynamic pressure caused by an explosion, a very small time step is required.

When it is intended to take into account the nonlinear behavior of the structure the problem is compounded. The Abaqus/Explicit version is used in this project because it is appropriate to solve nonlinear high-speed dynamic problems that can be extremely costly to analyze using implicit programs such as Abaqus/Standard (Abaqus 6.12, 2012). However, to capture accurately the time variation of the stresses on the wall, very small time increments are required because stress waves are associated with the highest frequencies of the system. Abaqus/Explicit uses a central difference scheme to integrate the equations of motion explicitly through time, using the displacements and velocities at one increment to calculate these kinematic variables at the next increment. The central difference method integrates constant accelerations exactly and thus to produce accurate results, the time increments must be very small so that the accelerations are nearly constant during an increment.

This sections presents the dynamic response of the RC wall strengthened by the protection system when the load applied to simulate the effect of an explosion is the triangular pulse shown in *Figure 4.10*. This is the same load that was applied in the preceding chapter to calculate the linear response of the system. Because the dynamic pressure has a simple shape, the user can vary its two parameters (intensity and duration) to gain a better understanding of the performance of the metallic foams when both the protected structure and the protection system have an inelastic behavior.

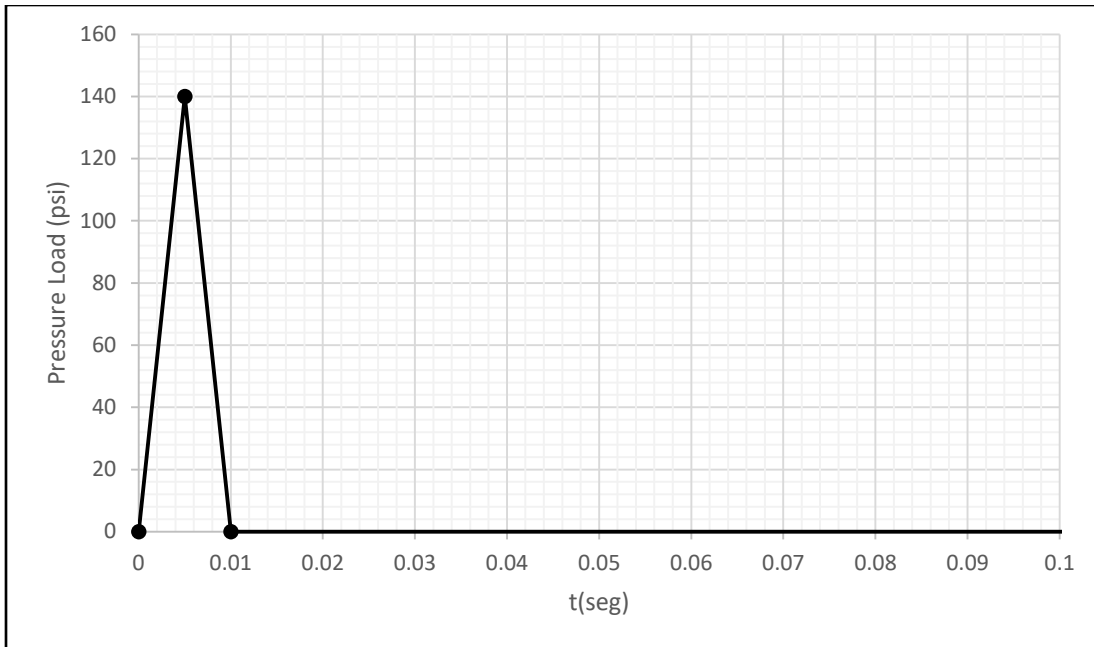


Figure 4.10: Dynamic pressure load for nonlinear analyses.

Figures 4.11a through 4.11c display the variation with time of the bending stresses at the most critical location for the original RC wall and the wall retrofitted with one of the metallic foam layers. *Figures 4.12a through 4.12c* shows the time history of the displacements at the middle of the wall without and with the MFMPs.

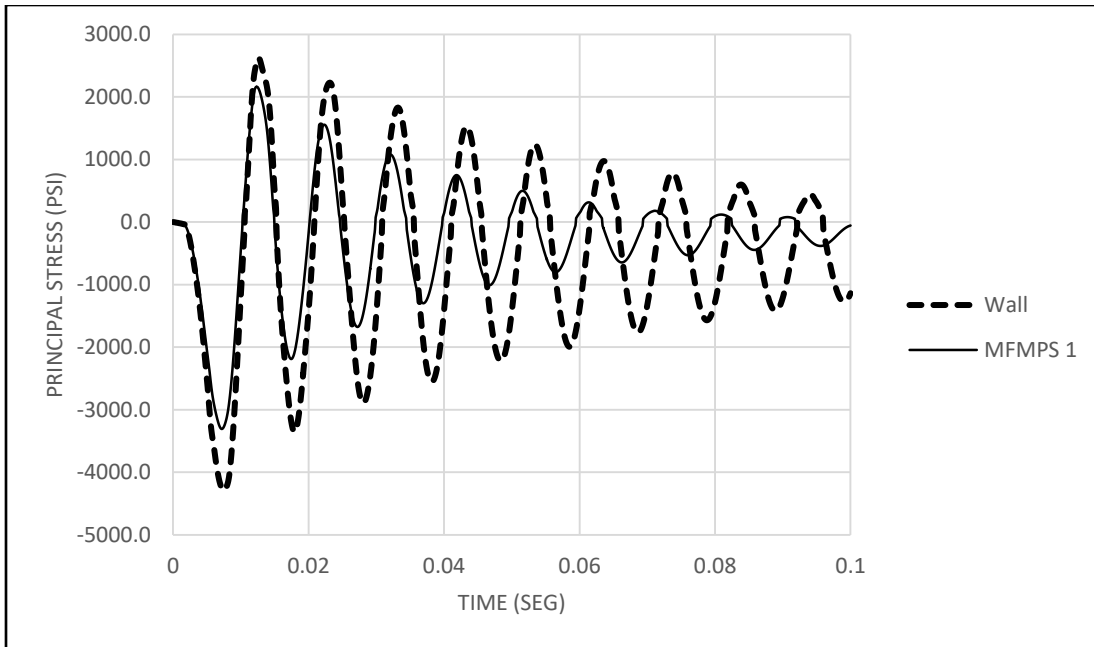


Figure 4.11a: Nonlinear stress time histories in the RC wall with and without the MFMPs 1.

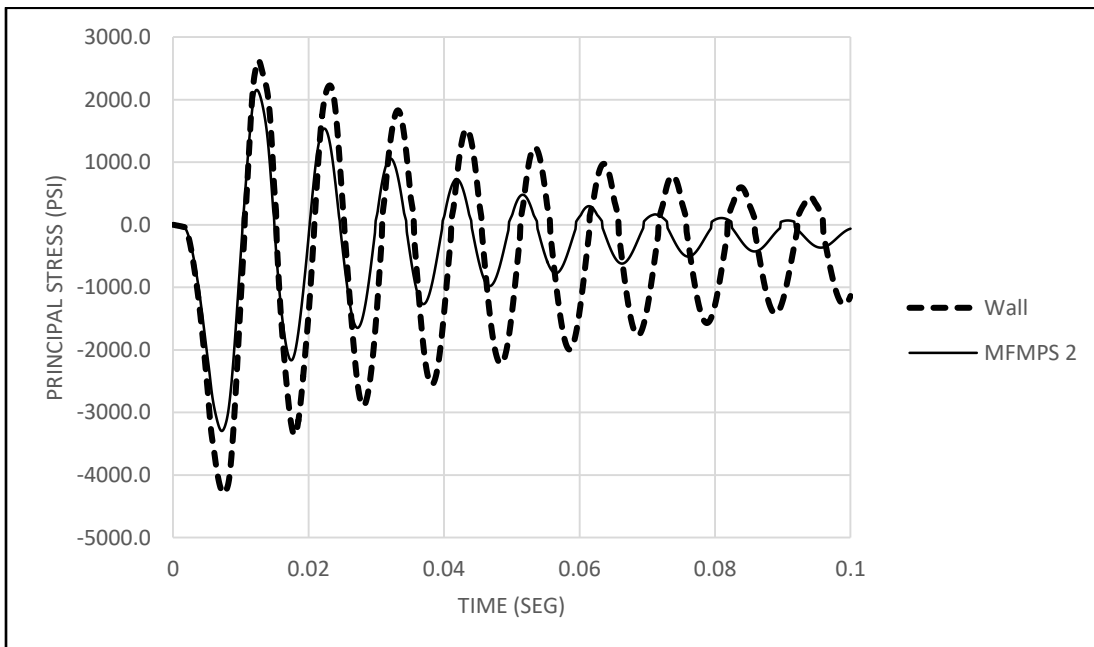


Figure 4.11b: Nonlinear stress time histories in the RC wall with and without the MFMPs 2.

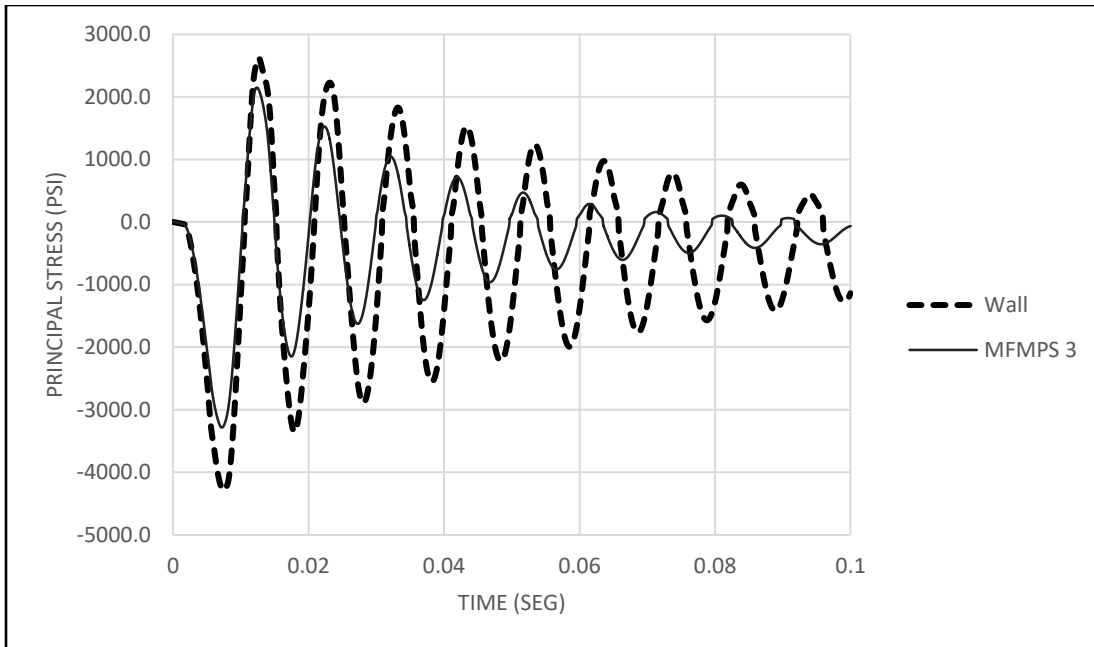


Figure 4.11c: Nonlinear stress time histories in the RC wall with and without the MFMP3.

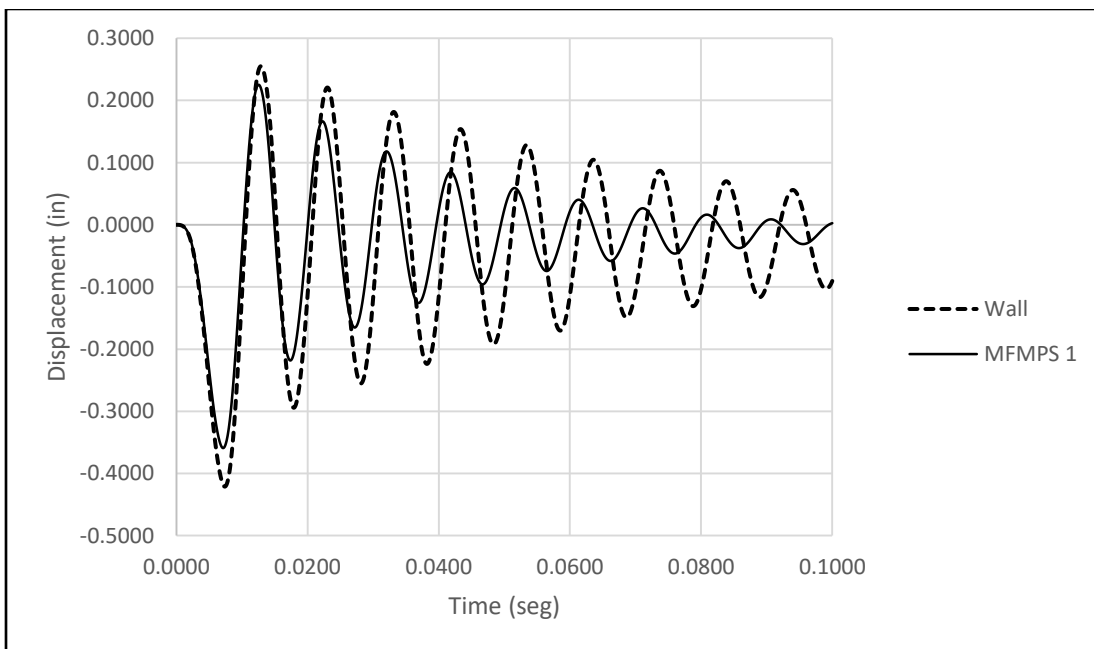


Figure 4.12a: Nonlinear displacement time histories in the RC wall with and without the MFMP1.

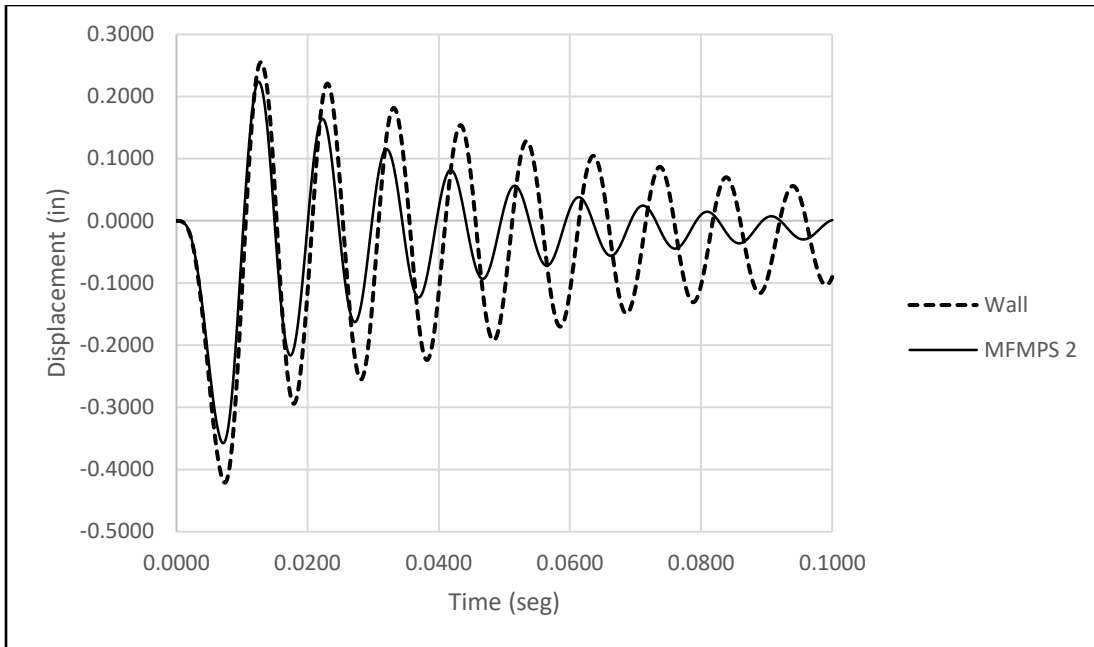


Figure 4.12b: Nonlinear displacement time histories in the RC wall with and without the MFMPs 2.

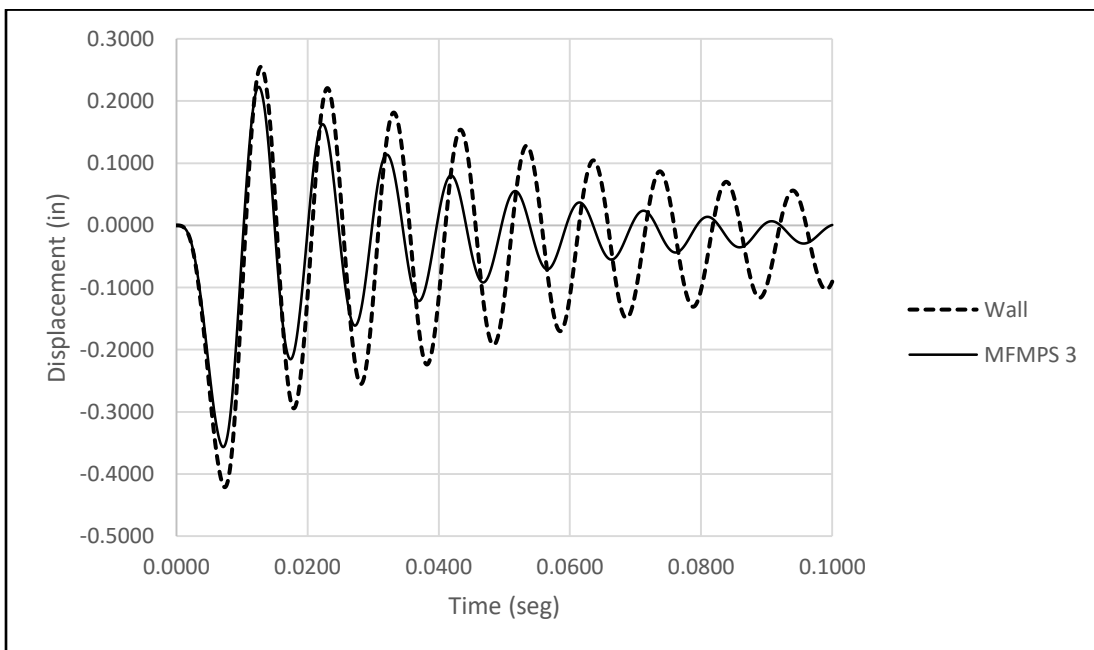


Figure 4.12c: Nonlinear displacement time histories in the RC wall with and without the MFMPs 3.

The peak response quantities were retrieved from each of the eight time histories presented in the previous figures (two responses corresponding to each of the three walls with MFMPs plus two for the bare wall). They are presented in *Table 4.4* where in addition, the last two columns display the reduction in percent that the protective systems were able to achieve.

Table 4.4: Peak displacements and stresses for the triangular load case and nonlinear analysis.

Model	Max. displ. (in)	Max. stress (psi)	U % difference	σ % difference
MFMPs 1 + Wall	0.359	3306.400	14.728	22.943
MFMPs 2 + Wall	0.358	3294.790	16.280	26.262
MFMPs3 + Wall	0.356	3284.240	16.623	26.577
Wall	0.421	4290.850	-	-

Examining the results in the table it can be inferred that the three metallic foam systems practically were able to reduce the maximum responses at the same degree. The reduction attained, however, is higher for the bending stresses than for the displacements (approximately 26% versus 16%).

4.5 – Nonlinear response due to the CONWEP generated load

CONWEP is a procedure based on an empirical model whose objective is to define the shockwave and associated pressure acting on a structure due to an external blasting. It can simulate the effect of explosions due to hemispherical charges on the ground or spherical charges in the air (LeBlanc et al., 2005). It is regarded as an empirical procedure because the fluid between the charge and the structure is not included in the model but rather the shockwave is defined based on experimental data. The CONWEP procedure is implemented in a subroutine of Abaqus. The shape and duration of the dynamic pressure generated by CONWEP of Abaqus are relatively similar to the loading used in the previous section and shown in *Figure 4.10*. However, there are several differences that makes the

analysis with CONWEP more realistic. First, when using CONWEP the pressure is not applied uniformly throughout the external surface of the wall surface like the dynamic pressure previously considered. CONWEP, on the contrary, simulates the propagation of a spherical shock wave and thus the pressure is not be applied simultaneously and uniformly over the surface of the structure. Moreover, the intensity of the pressure and the way it is applied on the structure is affected by the standoff distance. In the case of the dynamic pressure with a triangular shape, the amplitude (140 psi) was selected somehow arbitrarily so that it would be high enough to drive the system into the nonlinear range. In CONWEP the pressure wave is generated at a selected distance of the structural system and the amplitude felt by the structure decreases as it is further away from the explosion point. Moreover, the amplitude is also a function of the amount of the detonating product. To describe the energy released by an explosion it is customary to use the so called TNT equivalent units (for instance, a kilogram of TNT is equivalent to 4.184 Mega Joules).

For the analyses conducted in this section three amounts of explosives were used: 100, 200 and 300 pounds of TNT equivalent. In each case the standoff distance was increased, beginning with 10 ft for the first amount, 20 ft for the 200 lb and 30 ft for the third case.

Figures 4.13a through 4.13c present the stresses and displacements on the bare wall and on the wall with one the MFMPs configuration when the explosion takes place at a standoff distance of 10 ft and for a TNT equivalent weight of 100 lb. For all cases the figure identified as *4.13a* corresponds to the MFMPs1 system, *Figures 4.13b* are for the MFMPs 2 and *Figures 4.13c* display the results for the MFMPs 3 configuration. *Figures 4.14a through 4.14c* show stress and displacement time histories but for an explosion with a standoff distance of 20 ft and 200 lb of explosives (in TNT equivalent units).

Finally *Figures 4.15a through 4.15c* display the time variation of the stress and displacement due to the detonation of 300 lb of TNT equivalent at a distance of 30 ft from the structure.

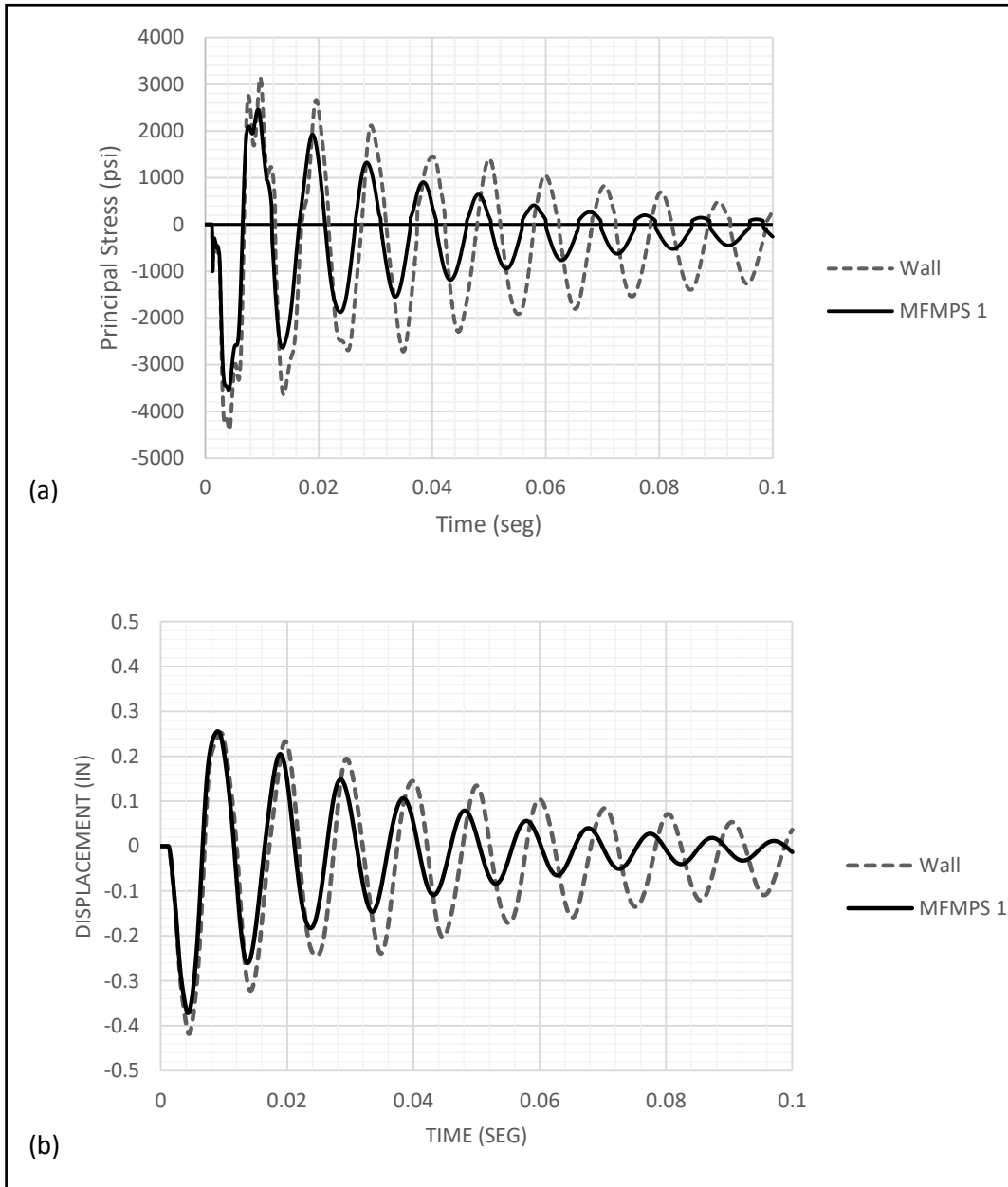


Figure 4.13a: Nonlinear stress and displacement time histories for the wall-MFMPs 1 system for a standoff distance of 10 ft and a 100 lb equivalent TNT : (a) stress; (b) displacement.

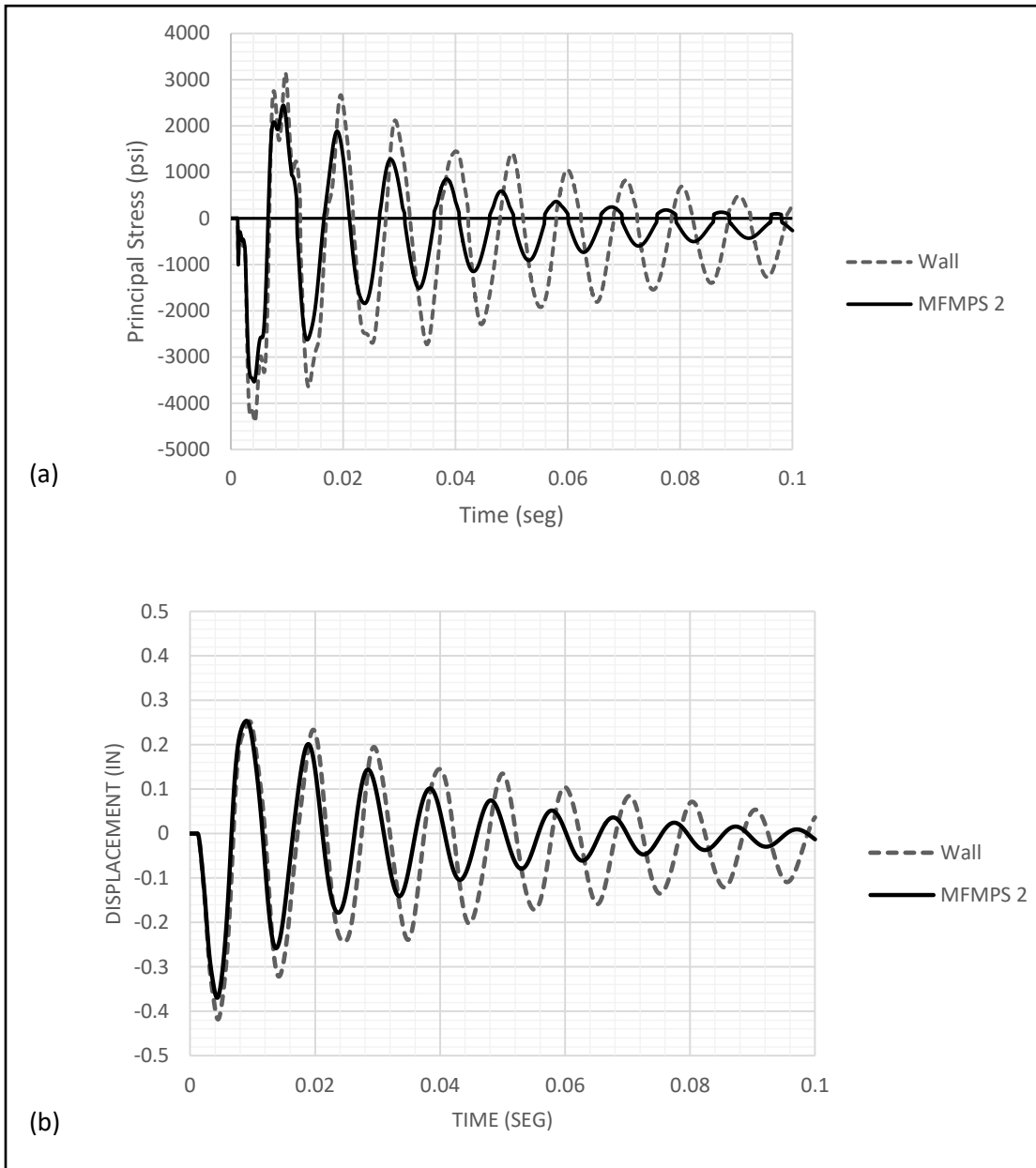


Figure 4.13b: Nonlinear stress and displacement time histories for the wall-MFMPS 2 system for a standoff distance of 10 ft and a 100 lb equivalent TNT : (a) stress; (b) displacement.

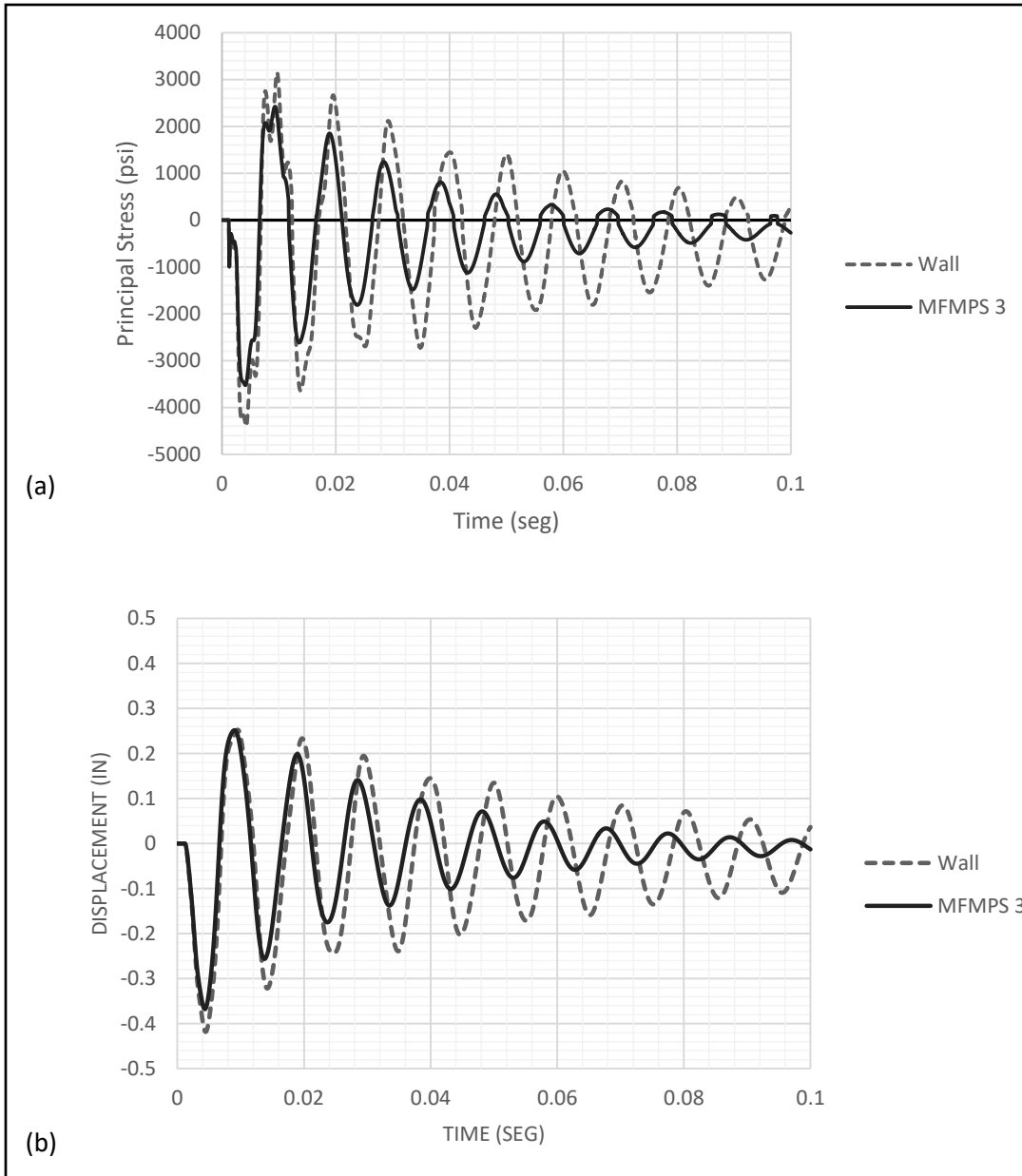


Figure 4.13c: Nonlinear stress and displacement time histories for the wall-MFMPS 3 system for a standoff distance of 10 ft and a 100 lb equivalent TNT: (a) stress; (b) displacement.

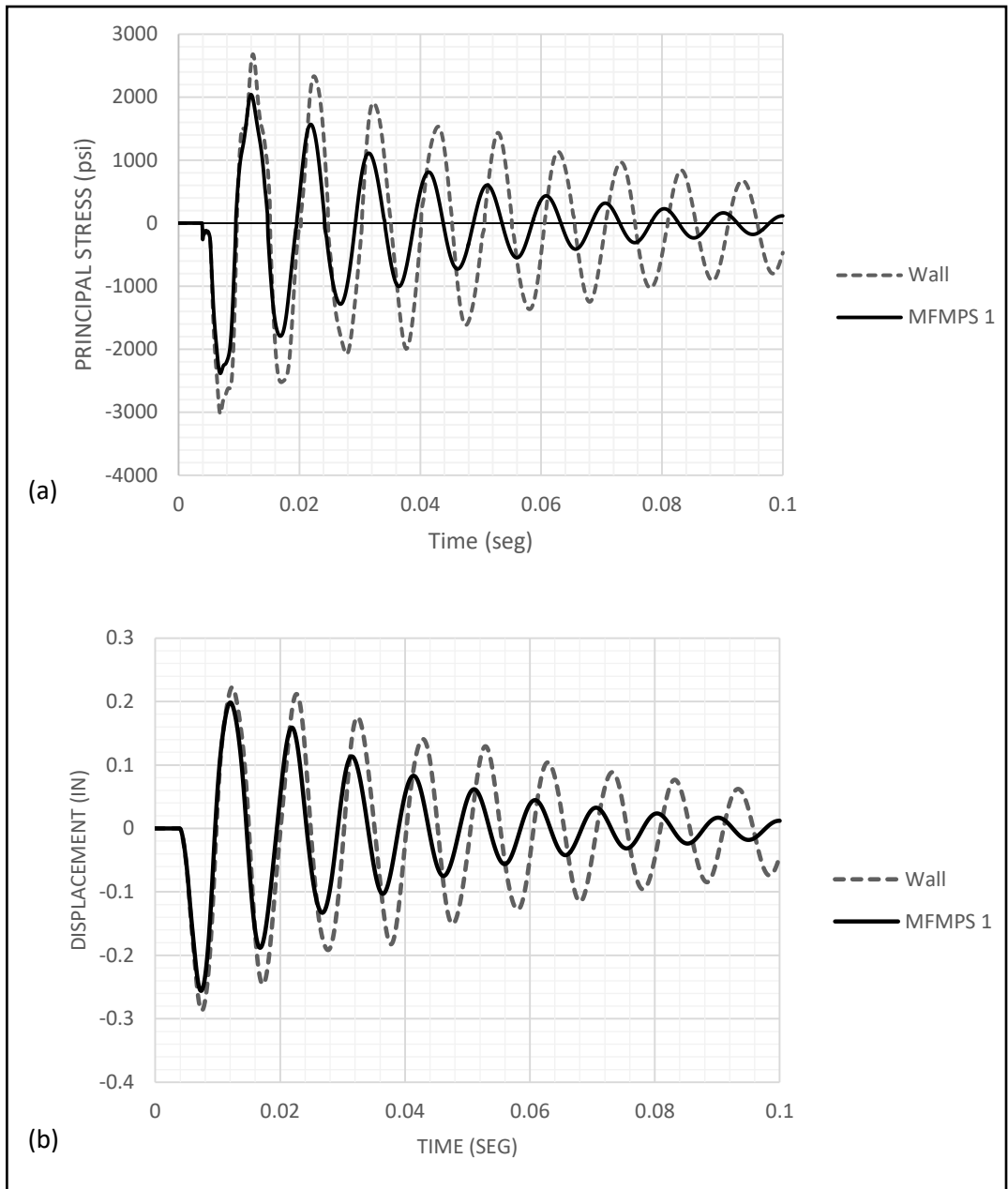


Figure 4.14a: Nonlinear stress and displacement time histories for the wall-MFMPS 1 system for a standoff distance of 20 ft and a 200 lb equivalent TNT : (a) stress; (b) displacement.

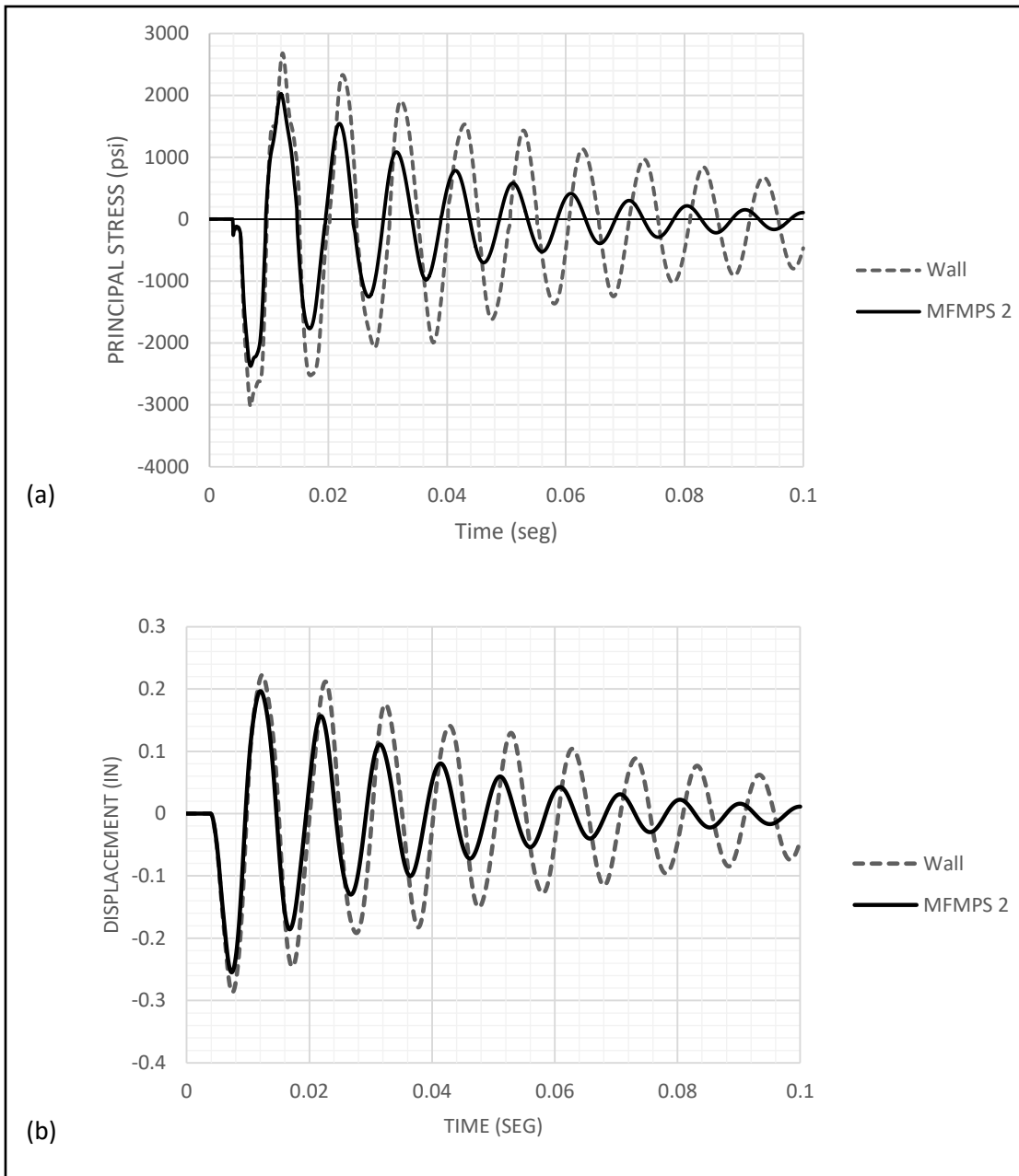


Figure 4.14b: Nonlinear stress and displacement time histories for the wall-MFMPS 2 system for a standoff distance of 20 ft and a 200 lb equivalent TNT : (a) stress; (b) displacement.

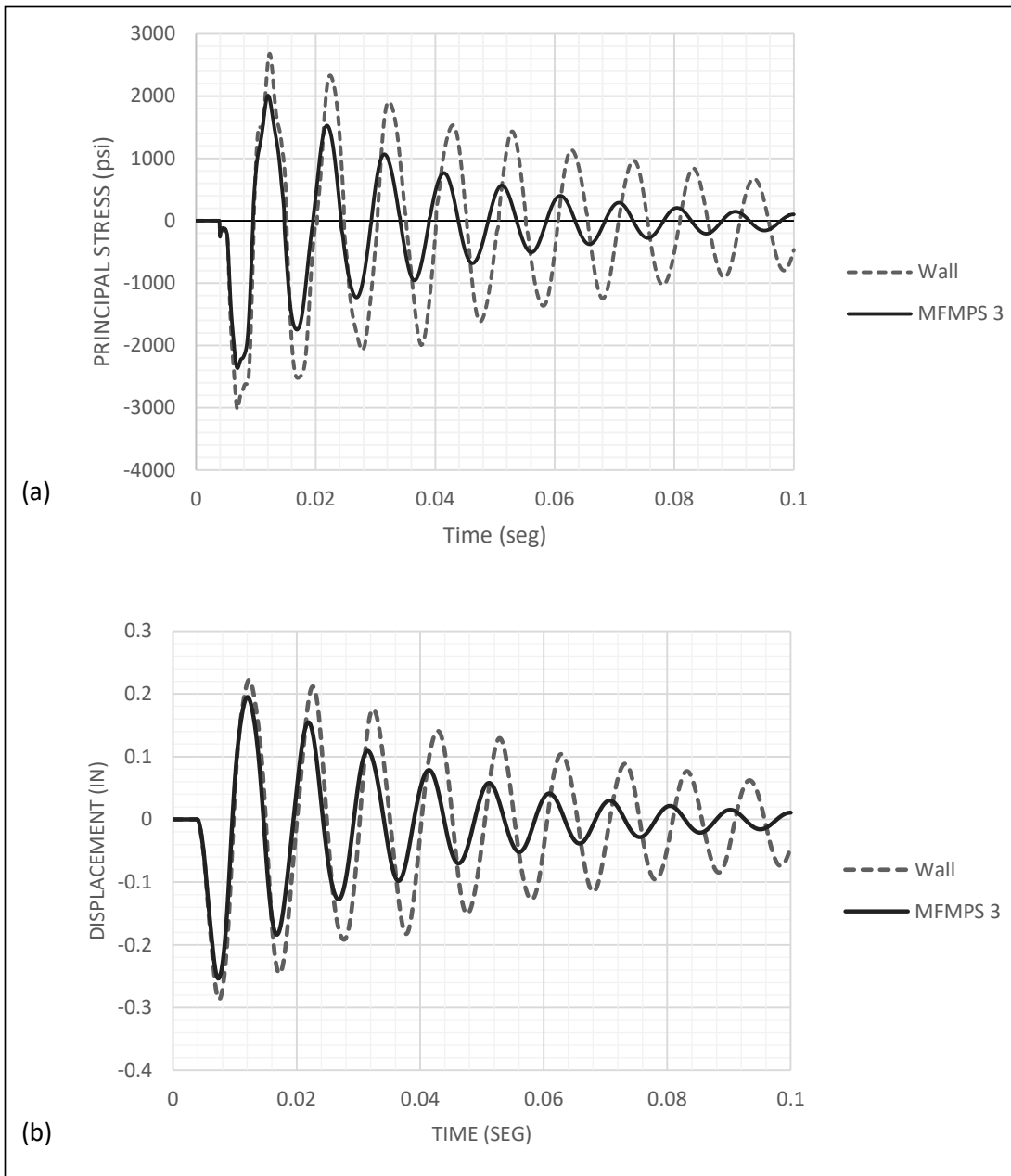


Figure 4.14c: Nonlinear stress and displacement time histories for the wall-MFMPS 3 system for a standoff distance of 20 ft and a 200 lb equivalent TNT : (a) stress; (b) displacement.

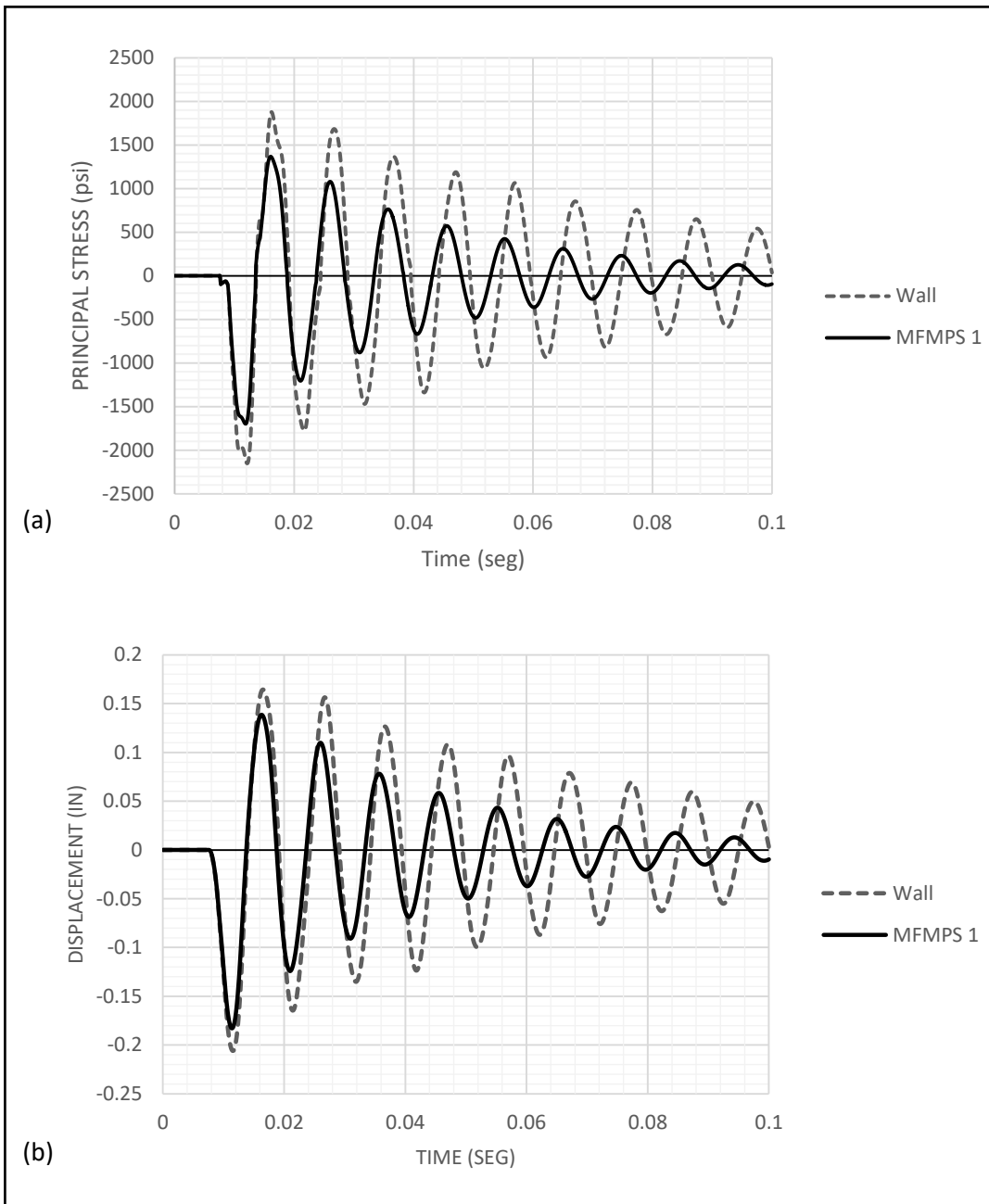


Figure 4.15a: Nonlinear stress and displacement time histories for the wall-MFMPS 1 system for a standoff distance of 30 ft and a 300 lb equivalent TNT : (a) stress; (b) displacement.

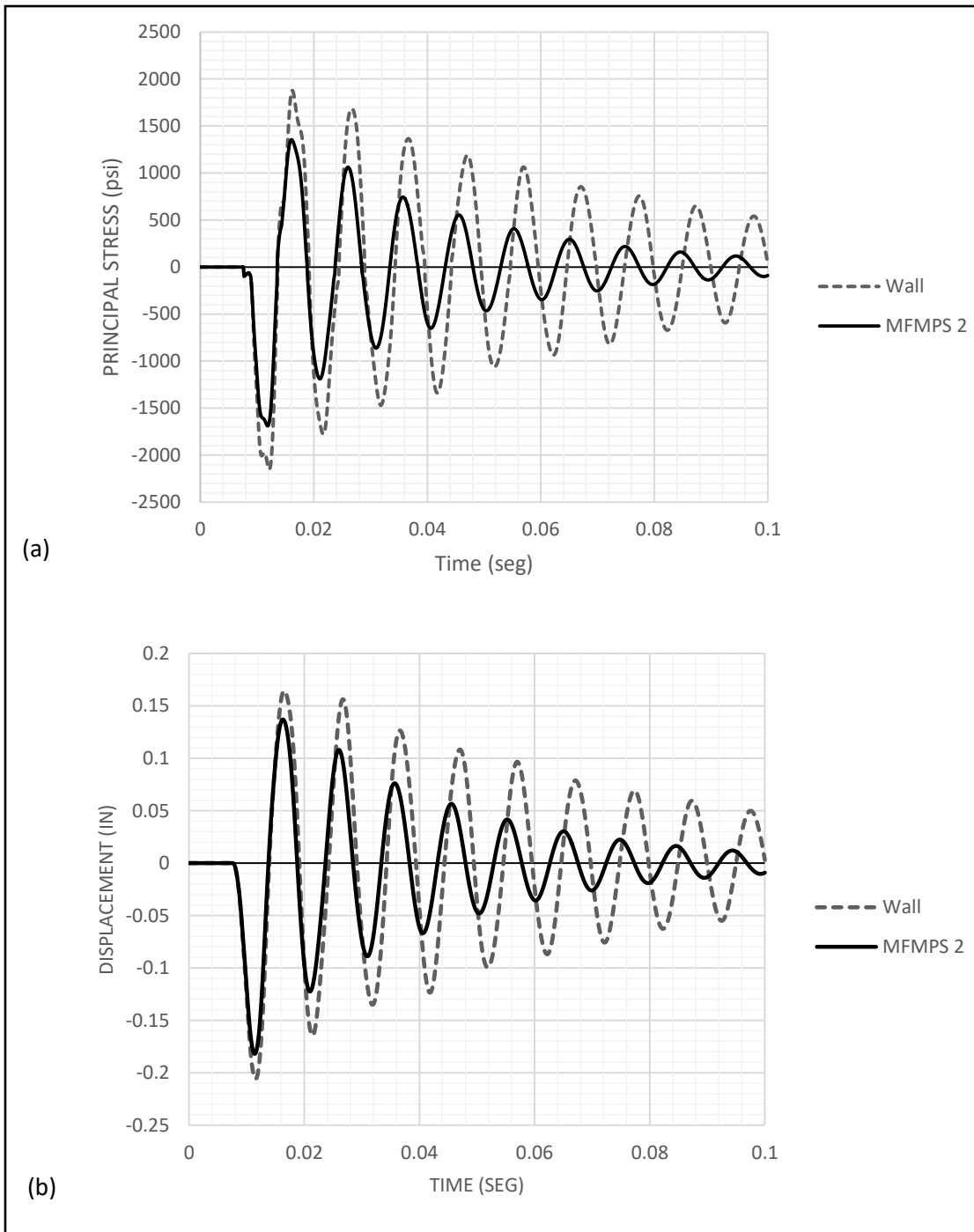


Figure 4.15b: Nonlinear stress and displacement time histories for the wall-MFMPS 2 system for a standoff distance of 30 ft and a 300 lb equivalent TNT : (a) stress; (b) displacement.

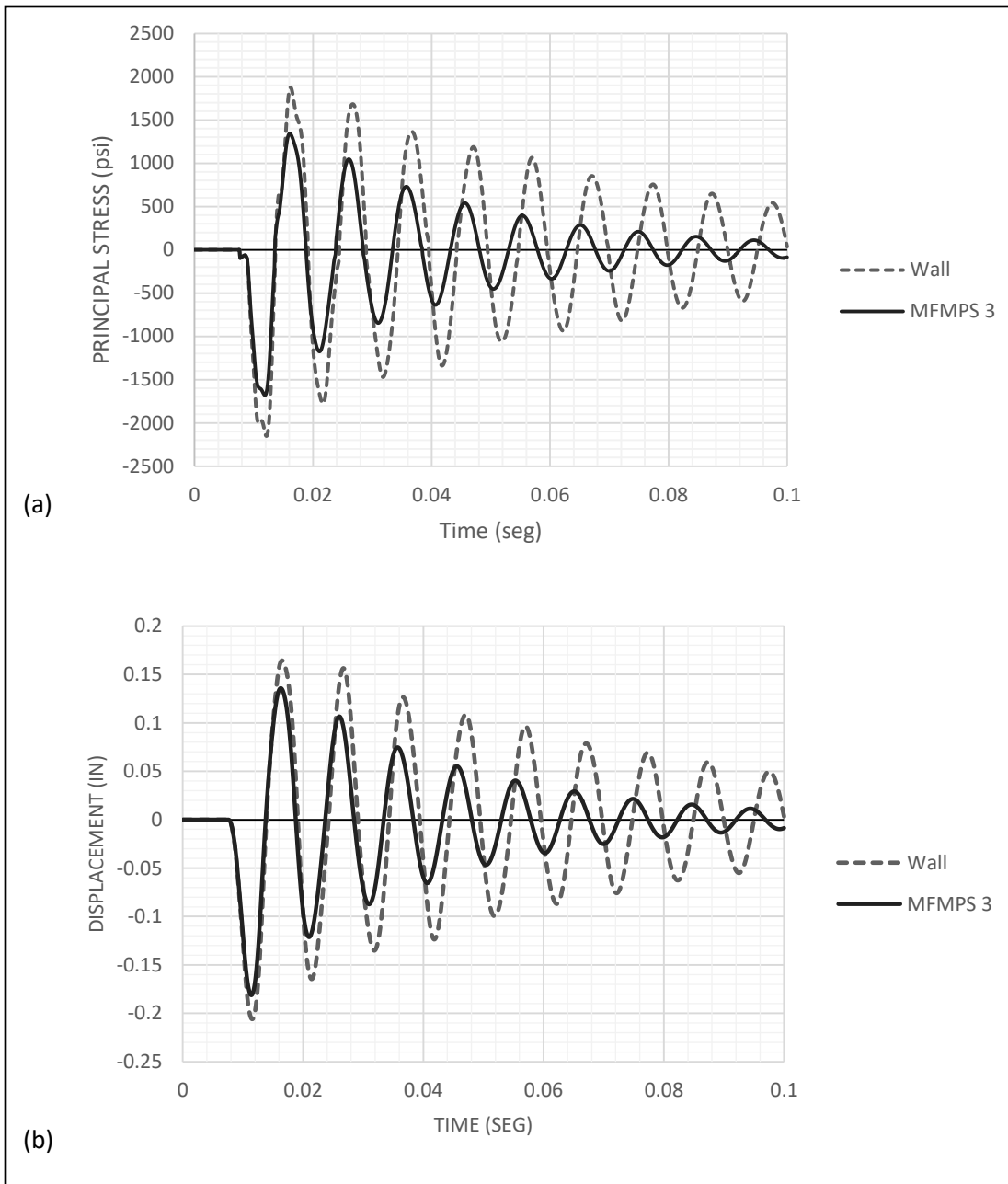


Figure 4.15c: Nonlinear stress and displacement time histories for the wall-MFMPS 3 system for a standoff distance of 30 ft and a 300 lb equivalent TNT : (a) stress; (b) displacement.

Based on the information provided in the preceding figures, three tables were prepared to display the peak displacements and stresses; each table compares the response reduction achieved with the three proposed layers of metallic foams. Table 4.5 contains the data due to the explosion of a 100 lb charge (of equivalent TNT) at a distance of 10 ft. Table 4.6 displays similar results but for 200 lb of explosives

at a 20 ft standoff distance. Finally, *Table 4.7* shows the peak response data for the 300 lb charge applied 30 ft away from the structure.

Table 4.5: Nonlinear peak displacements and stresses in the MFMPs 1 + Wall system due to a CONWEP generated load for 100 lb of explosives at a 10 ft standoff distance.

Model	Max. displ. (in)	Max. stress (psi)	U % reduction	σ % reduction
MFMPs 1 + Wall	0.372	3545.860	11.011	19.426
MFMPs 2 + Wall	0.370	3535.530	11.556	19.660
MFMPs 3 + Wall	0.368	3525.630	12.024	19.885
Wall	0.418	4400.73	-	-

Table 4.6: Nonlinear peak displacements and stresses in the MFMPs + Wall systems due to a CONWEP generated load for 200 lb of explosives at a 20 ft standoff distance.

Model	Max. displ. (in)	Max. stress (psi)	U % reduction	σ % reduction
MFMPs 1 + Wall	0.256	2386.35	10.731	21.192
MFMPs 2 + Wall	0.255	2377.24	11.160	21.492
MFMPs 3 + Wall	0.254	2369.20	11.568	21.758
Wall	0.287	3028.04	-	-

Table 4.7: Nonlinear peak displacements and stresses in the MFMPs + Wall systems due to a CONWEP generated load for 300 lb of explosives at a 30 ft standoff distance.

Model	Max. displ. (in)	Max. stress (psi)	U % reduction	σ % reduction
MFMPs 1 + Wall	0.1829	1698.21	11.180	21.063
MFMPs 2 + Wall	0.1820	1688.98	11.586	21.492
MFMPs 3 + Wall	0.1812	1680.06	11.982	21.907
Wall	0.2059	2151.36	-	-

Observing the three tables, the following conclusions can be drawn. The three MFMPs were able to accomplish a similar level of response reduction: on average it is 11% for the peak displacements and 20% for the maximum stresses, depending on the amount of explosives and standoff distances considered. The first case (100 lb of explosives at 10 ft) is the most severe event. Among the three

alternatives, the third one (MFMP3 3) produces the highest response reduction, albeit by a small difference.

Chapter 5 – Results Summary, Conclusions and Recommendations

5.1- Summary

The primary purpose of the work presented was to evaluate the effectiveness of a multilayered protective system for blast mitigation. Due to its energy absorption capacity, tensile strength, and relatively high damping properties the metallic foams can be a useful material for protective purposes. A brief overview of previous research works that corroborate the attributes of these systems as a blast protection technique was discussed (i.e. Wu et al., 2011; Wu and Sheikh, 2012b). If it is used for retrofitting applications, its lightweight avoids adding extra loads that have to be supported by the existing wall and other structural elements. Based on the promising properties of metallic foams for blast mitigation, a multilayered protective system consisting of two layers constrained by two thin aluminum sheets was proposed. The proposed configuration is shown in *Figure 5.1*. The system is identified with the acronym MFMPs, for Metallic Foam Multilayered Protective System.

To assess the performance of the proposed system numerical models of the MFMPs and a RC wall were created in the finite element program Abaqus. This is one of the most powerful and versatile programs currently available that can deal with a large variety of loads, materials and multiphysics phenomena, in particular with problems involving high speed loads and nonlinear response.

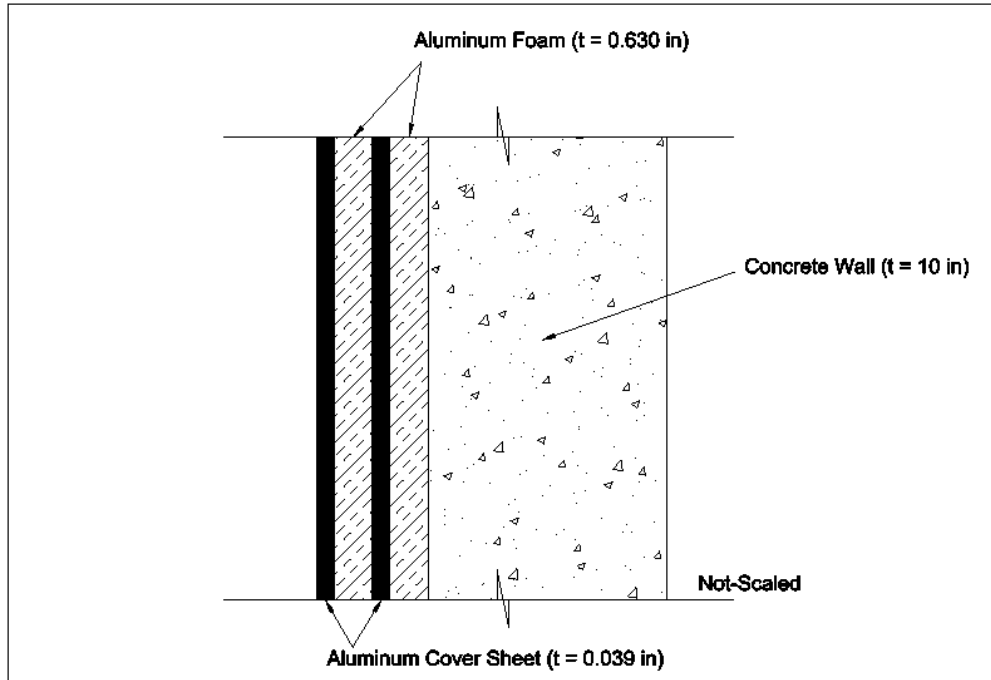


Figure 5.1: Metallic Foam Multilayer Protective System (MFMPs) configuration.

Three different MFMPs were considered in the analysis changing the properties of the metallic foam using commercialize standards, (IFAM, 2010), these values are presented in *Table 5.1*.

Table 5.1: Geometry of the structure and mechanical properties of the materials.

Material	Width (in)	Height (in)	Thickness (in)	Unit weight (lb s ² / in ⁴)	E (ksi)	Poisson's ratio	Compressive yield strength (psi)
Concrete	180.0	120.0	10.000	0.083	3605	0.180	4000.00
Aluminum foam (FoamA)	180.0	120.0	0.630	0.018	5076	0.334	2016.02
Aluminum foam (FoamB)	180.0	120.0	0.630	0.022	7106	0.334	2726.71
Aluminum foam (FoamC)	180.0	120.0	0.630	0.025	9572	0.334	3524.42
Metallic sheet (Al)	180.0	120.0	0.039	0.097	10200	0.334	40000.00

The model created in Abaqus was validated in three ways. First, to check the correct application of the boundary conditions, material properties, geometry, etc., the maximum displacement due to a

uniform static pressure was compared in Chapter 2 with those calculated from formulas from the Theory of Plates.

In Chapter 4 two additional validations were carried out. The nonlinear constitutive relation for the concrete was defined using the default parameters available in Abaqus to establish the concrete plasticity model. Therefore, the resulting σ - ε curve was determined indirectly via a simulated pushover analysis of a RC wall in cantilever. The curve obtained was compared with a typical σ - ε curve for 4,000 psi concrete available in the structural analysis program SAP2000.

The next validation involved a simplification used to model the nonlinear constitutive relation of the reinforced concrete. It was assumed that the resistance of the concrete section with steel reinforcement was the same in tension and compression. To validate this assumption, a finite element model of the concrete wall with steel reinforcement in the form of two embedded grids was created. The simplified and the detailed models were subjected to a simulated pushover test and two σ - ε curves were obtained and compared.

After the successful validations three load cases were considered: a uniform static pressure, a uniform dynamic pressure with a triangular time variation and a CONWEP-generated blast pressure. The last one is a subroutine inside Abaqus that simulates an explosive event taking into consideration the weight of explosives (in equivalent TNT units) and the distance between the blast and the structure. For the CONWEP analysis three standoff distances (10, 20 and 30 ft) were considered, each with an associated amount of explosives (100, 200 and 300 lb, respectively). Two kinds of analyses were performed: a linear elastic (Chapter 3) and an inelastic non-linear analysis (Chapter 4). The response quantities selected for comparison were the normal displacements (at the center of the plate and normal to its surface) and the peak bending stresses (at the middle of the top support).

5.2 – Final results

The variation with time of each response quantity for the three loading conditions and four structural configurations (three MFMPs plus the bare RC wall) were presented in graphical form in Chapters 3 and 4. The level of reduction compared to the response of the bare wall are presented next in tabular form. *Tables 5.2 through 5.6* display the reduction in percent achieved with each MFMP configuration and for the linear and nonlinear analyses. The differences in percent between the reduction obtained for the linear and nonlinear responses is also included in the tables.

Table 5.2: Response reduction achieved for the static pressure and for linear and nonlinear analyses (140 psi).

Model	U %			σ %		
	Linear Analysis	Non-Linear Analysis	Difference	Linear Analysis	Non-Linear Analysis	Difference
MFMPs 1 + Wall	14.708	20.127	5.419	17.155	27.608	10.453
MFMPs 2 + Wall	16.896	20.127	3.232	19.675	27.608	7.933
MFMPs 3 + Wall	19.342	20.127	0.786	22.471	27.608	5.137

Table 5.3: Response reduction achieved for the triangular dynamic pressure and for linear and nonlinear analyses (140 psi).

Model	U %			σ %		
	Linear Analysis	Non-Linear Analysis	Difference	Linear Analysis	Non-Linear Analysis	Difference
MFMPs 1 + Wall	12.963	14.728	1.765	21.649	22.943	1.294
MFMPs 2 + Wall	15.631	16.280	0.649	25.548	26.262	0.714
MFMPs 3 + Wall	18.586	16.623	1.963	29.855	26.577	3.278

Table 5.4: Response reduction achieved for the CONWEP loading and for linear and nonlinear analyses (100 lb of TNT and a 10 ft standoff distance).

Model	U %			σ %		
	Linear Analysis	Non-Linear Analysis	Difference	Linear Analysis	Non-Linear Analysis	Difference
MFMPs 1 + Wall	5.966	11.011	5.045	19.890	19.426	0.465
MFMPs 2 + Wall	7.621	11.556	3.935	23.331	19.660	3.671
MFMPs 3 + Wall	9.375	12.024	2.649	27.053	19.885	7.167

Table 5.5: Response reduction achieved for the CONWEP loading and for linear and nonlinear analyses (200 lb of TNT and a 20 ft standoff distance).

Model	U %			σ %		
	Linear Analysis	Non-Linear Analysis	Difference	Linear Analysis	Non-Linear Analysis	Difference
MFMPs 1 + Wall	7.333	10.731	3.398	21.528	21.192	0.337
MFMPs 2 + Wall	9.078	11.160	2.082	24.857	21.492	3.365
MFMPs 3 + Wall	11.001	11.568	0.566	28.510	21.758	6.752

Table 5.6: Response reduction achieved for the CONWEP loading and for linear and nonlinear analyses (300 lb of TNT and a 30 ft standoff distance).

Model	U %			σ %		
	Linear Analysis	Non-Linear Analysis	Difference	Linear Analysis	Non-Linear Analysis	Difference
MFMPs 1 + Wall	10.231	11.180	0.950	19.925	21.063	1.139
MFMPs 2 + Wall	11.980	11.586	0.394	23.981	21.492	2.489
MFMPs 3 + Wall	13.935	11.982	1.953	28.529	21.907	6.622

5.3 – Conclusions

Examining the results of the numerical simulations it is readily apparent that the system of metallic foams and constraining plates were able to reduce the response of the RC wall to the three different loading conditions (static pressure, impulsive triangular pressure and CONWEP generated pressure wave). The level of the response reduction that each of the different systems of metallic foams was able to attain is similar. The maximum bending stresses were reduced more than the displacements in all cases. As shown in the tables of Chapter 4, among the three CONWEP blast loads, the case where the explosion takes place closer to the structure (10 ft) is the most demanding one, even though the amount of explosive material is smaller (100 lb of TNT equivalent). The best reduction in the peak bending stress for this case was 19.8%.

Even though the three metallic foam systems (MFMPs 1, MFMPs 2 and MFMPs 3) had a comparable performance, the one with a higher density and elastic module (MFMPs 3) was the most promising of them in reducing the stresses and displacements generated by blast loads.

The final overall conclusion is that it is worth to study further the use of constrained layers of metallic foams as a retrofitting technique to increase the capacity of existing structures to resist the high-intensity short-duration pressures created by an explosion at the site. However, as mentioned in the final section, more comprehensive studies are needed; the work presented in this thesis should be regarded as a preliminary validation of the beneficial effects of this kind of protective systems.

5.4 – Recommendations for future work

An accurate simulation of the response of a reinforced concrete structures to blast loading is by itself a very challenging problem and thus it is still the object of research. The problem is compounded

when new materials such as metallic foams are included in the structural model. Therefore some simplifying assumptions were made throughout the thesis to calculate the nonlinear dynamic response. To further verify the attributes of the layers of metallic foams as a blast protecting device, it is necessary to perform additional, more comprehensive studies removing some of the assumptions used here.

For example, the metallic foams were modeled as a homogeneous and continuous material with equivalent properties when in reality they have voids such as in a conventional plastic foam. For a future study it is worth improving the modeling of the metallic foams by considering that it is not a homogenous body. Moreover, only aluminum foams were considered in the simulations carried out in this thesis. There are metallic foams whose matrices consist of other metals; it could prove valuable to consider some of them.

To simplify the numerical model and to reduce the associated computational time, a rectangular RC wall clamped on all sides was adopted in the thesis. Walls with more realistic support conditions should be considered, for instance a model of a 2-story building with walls surrounded by beams and columns.

The more accurate modeling of the reinforced concrete wall in the nonlinear regime is another topic for further studies. For instance, the use of steel grids embedded in the wall was used in this thesis to validate a simpler model of the RC wall by replacing the composite material by a homogeneous one. A nonlinear but static analysis was performed with the model of the wall with the steel grids. Although the steel grids better represent the actual wall construction, when the model with them was used to carry out nonlinear dynamic analyses some convergence problems arose.

Other aspects recommended to be studied in the future is the performance of the bonding agent of the MFMPs with the RC wall, adding another protective layer in the back of the wall, and examining the effect of adding more layers of metallic foams.

The final validation of the concept requires an experimental test. Ideally, to simulate the real life situations an actual explosive charge should be applied in front of a physical model of the RC wall. Because this experiment has many logistics problems and it can only be conducted in specialized federal labs and research centers, another alternative is the use of blast simulators to study the performance of the protective system.

Reference

- Abaqus/User's Guide. Abaqus User's Guide. Available at:
<http://130.149.89.49:2080/v6.13/books/usb/default.htm?startat=pt07ch34s04aus125.html>, 2013
- ACI, C. (2014). *Report for the Design of Concrete Structures for Blast Effects*. Farmington Hills, MI: American Concrete Institute.
- ASCE (2012). *Design of Blast-Resistant Buildings in Petrochemical Facilities*. Reston, VI: American Society of Civil Engineers.
- Dassault/Systemes. (2016). *History: From Digital Mock-Up to 3D Experience*. From Dassault Systemes: www.3ds.com
- Duarte, I., & Oliveira, M. (09 de March de 2012). Aluminum Alloy Foams: Production and Properties, Powder Metallurgy, Dr. Katsuyoshi Kondoh. InTech.
- IFAM, F. (2010). FOAMINAL, Properties Overview and Design Guideline. FOAMINAL.
- M.F. Ashby, A. E. (2000). *Metal Foams: A Design Guide*. Woburn, MA: Butterworth-Heinemann.
- Orton, S. L., Chiarito, V. P., Minor, J. K., & Coleman, T. G. (2014). Experimental Testing of CFRP-Strengthened Reinforced Concrete Slab Elements Loaded by Close-In Blast. *Journal of Structural Engineering*, 1-9.
- Raman, S., Ngo, T., Mendis, P., & Pham, T. (2012). Elastomeric Polymers for Retrofitting of Reinforced Concrete Structures against the Explosive Blast Effects. *Advances in Materials Science and Engineering*, 1-8.
- Sammarco, E., & Matamoros, A. (2010). Plasticity-Based Nonlinear Finite Element Analysis of Reinforced Concrete Columns with Inadequate Seismic Detailing. *Proceedings of the 9th U.S. National and 10th Canadian Conference on Earthquake Engineering*. Toronto.
- Suarez, L. E. (2008). *Soil and Foundation Dynamics*. Mayaguez: University Of Puerto Rico Mayaguez Campus.
- Timoshenko, S., & Woinowsky-Krieger, S. (1987). *Theory of Plates and Shells*. McGraw-Hill.

- UFC 4-010-01. (2012). *DoD Minimum Antiterrorism Standards for Buildings*. U.S. Army Corps of Engineers.
- USACE. (2005). *Convencional Wepon Effect Software*. USACE Engineering Research and Development Center.
- Wu, C. (2012a). Research development on protection of structures against blast loading at University of Adelaide. *Australian Journal of Structural Engineering*, 13(1), 97-108.
- Wu, C., & Sheikh, H. (2012b). A finite element modelling to investigate the mitigation of blast effects on reinforce concrete panel using foam cladding. *International Journal of Impact Engineering*, 24-33.
- Wu, C., Huang, L., & Oehlers, D. J. (2011). Blast Testing of Aluminum Foam-Protected Reinforced Concrete Slabs. *Journal of Performance of Constructed Facilities*, 25(5), 464-474.
- Ye, Z. Q., & Ma, G. W. (2007). Effects of Foam Claddings for Structure Protection against Blast Load. *Jornal of Engineering Mechanics*, 133 (1), 41-47.